Aus dem Institut für Physiologie
Direktor: Herr Prof. Dr. Andreas Deußen

The roles of soluble adenylate cyclase in cell cycle control of endothelial cells

D i s s e r t a t i o n s s c h r i f t

zur Erlangung des akademischen Grades
Doctor of Philosophy (Ph.D.)
vorgelegt
der Medizinischen Fakultät Carl Gustav Carus
der Technischen Universität Dresden

von

Master of Science
Warunya Woranush

aus Suphanburi, Thailand

Dresden 2019

1. Gutachter: Prof. Dr. rer. nat. Thomas Noll

2. Gutachter:

Tag der mündlichen Prüfung:

gez.: ----------

Vorsitzender der Promotionskommission

Printed with the support of the German Academic Exchange Service

List of abbreviations

6-BNZ-cAMP	N^6-Benzoyladenosine-3′,5′-cyclic monophosphate sodium salt
8-pcpt-2'-o-me-cAMP	8-(4-Chlorophenylthio)-2′-O-methyladenosine 3′,5′-cyclic monophosphate monosodium hydrate
ADCY10	Adenylate cyclase type 10
ADCY1-9	Adenylate cyclase type 1-9
ADCYs	Adenylate cyclases
AMP	Adenosine monophosphate
ANOVA	Analysis of variance
ATP	Adenosine triphosphate
BSA	Bovine serum albumin
CA	Carbonic anhydrase
Ca^{2+}	Calcium
CaM	Calmodulin
cAMP	3’,5’-cyclic adenosine monophosphate
CDKs	Cyclin-dependent kinases
CNGs	Cyclic nucleotide-gated ion channels
CO_2	Carbon dioxide
CREB	cAMP response element binding
ddH_2O	Deionized distilled water
DIFMUP	6,8-difluoro-4-methylumbelliferyl phosphates
DMSO	Dimethyl sulfoxide
DNA	Deoxyribonucleic acid
DTT	Dithiothreitol
EC_{50}	Half maximal effective concentration
ECL	Enhanced chemiluminescence
Epac	Exchange protein directly activated by cAMP
FACS	Fluorescence-activated cell sorting
FCS	Fetal calf serum
FITC	Fluorescein isothiocyanate
FSK	Forskolin
g	Unit of gravity
G_0 phase	Quiescent stage of cell cycle
G_1 phase	First gap of cell cycle

G_2 phase	Second gap of cell cycle
$G_i\alpha$	α subunits of the inhibitory family of G protein
GPCRs	G protein-coupled receptors
$G_s\alpha$	α subunit of a stimulatory G protein
h	Hours
H-89	Protein kinase A inhibitor
HCNs	Hyperpolarization-activated cyclic nucleotide-gated channels
HCO_3^-	Bicarbonate
HEPES	4-(2-hydroxyethyl)-1-piperazine ethane sulfonic acid
HRP	Horseradish peroxidase
HUVECs	Human umbilical vein endothelial cells
IBMX	3-isobutyl-1-methylxanthine
KH7	ADCY10 inhibitor
Km	Michaelis-Menten constant
M	Molar
M phase	Mitotic phase of cell cycle
MAPK	Mitogen-activated protein kinase
Mg^{2+}	Magnesium
min	Minutes
ml	Milliliter
mM	Milimolar
mmHg	Millimetre of mercury
MPF	Maturation-promoting factor
$NiCl_2$	Nickel chloride
nM	Nanomolar
nm	Nanometer
OA	Okadaic acid, PP2A inhibitor
p53	Tumor suppressor protein
PBS	Phosphate-buffered saline
PBST	Phosphate-buffered saline plus Tween 20
PCO_2	Partial pressure of carbon dioxide
PDEs	Phosphodiesterases
Pen/Strep	Penicillin/Streptomycin
PGEs	Prostaglandins
pH	Negative log of H^+ concentration
PI3K	Phosphoinositide-3-kinase

PKA	Protein kinase A
PKI	Protein kinase A inhibitor
PP1	Protein phosphatase 1
PP2A	Protein phosphatase 2A
PPase	Pyrophosphate
PPs	Protein phosphatases
PVDF	Polyvinylidene difluoride
PY	Pyronin Y
RNA	Ribonucleic acid
RT	Room temperature
S phase	Synthetic phase of cell cycle
sAC	Soluble adenylate cyclase
SDS	Sodium dodecyl sulfate
SDS-PAGE	Sodium dodecyl sulfate - polyacrylamide gel
SEM	Standard error of the mean
Ser	Serine
TBS	Tris-buffered saline
TBST	Tris-buffered saline plus Tween 20
Thr	Threonine
tmACs	Transmembrane adenylate cyclases
TRITC	Tetramethylrhodamine
TSH	Thyroid stimulating hormone
Vmax	Maximum velocity that enzyme catalyzed the reaction
X	Fold change
β-Ars	Beta-adrenergic receptors
µg	Microgram
µM	Micromolar

Contents

1. Introduction 1

1.1 3', 5'-cyclic adenosine monophosphate (cAMP) 1

1.2 Adenylate cyclases (ADCYs) isoforms 1

1.2.1 Adenylate cyclases 1-9 (ADCY1-9) 1

1.2.2 Adenylate cyclase type 10 3

1.3 Intracellular cAMP distribution 5

1.4 Effect of cAMP on cell proliferation 6

1.5 Cell proliferation and cell cycle 8

1.5.1 Interphase 8

1.5.2 Mitotic phase (M phase) 8

1.5.3 Cyclin-dependent kinases (CDKs) 10

1.5.4 Protein phosphatases (PPs) 10

1.5.5 Cell cycle checkpoints 11

1.6 cAMP in diseases and pathophysiology 11

2. Aims 13

3. Experimental design and methods 14

3.1 Isolation and culturing of HUVECs 14

3.1.1 Isolation of HUVECs 14

3.1.2 Culturing of HUVECs 15

3.2 Experimental designs 16

3.2.1. Experimental design for objective 1, 2, and 5 17

3.3 Methods 20

3.3.1 Cell proliferation assay 20

3.3.2 Fluorescence-activated cell sorting (FACS) analysis 21

3.3.3 Immunofluorescence 22

3.3.4 Protein analysis 24

3.3.5 PP2A activity assay 29

3.3.6 Data analysis 30

4. Results 31

4.1 Colocalization and translocation of ADCY10 and α-Tubulin during the cell cycle of HUVECs. 31

4.2 ADCY10 induces cell proliferation by modulating cell cycle progression of HUVECs..**Fehler! Textmarke nicht definiert.**

4.2 ADCY10 induces cell proliferation by modulating cell cycle progression of HUVECs 33

4.2.1 HCO_3^- promotes cell proliferation of HUVECs 33

4.2.2 Pharmacological inhibition of ADCY10 reduces cell proliferation of HUVECs 34

4.2.3 ADCY10 controls cyclin B1 content. 37

4.3 Epac and PKA control cell proliferation and cell cycle regulation 39

4.3.1 Epac modulates cell proliferation 39

4.3.2 PKA controls cell proliferation 42

4.3.3 Interaction of Epac and PKA modulates cell proliferation and cell cycle control 45

4.4 ADCY10 modulates regulatory kinases and phosphatases 48

4.4.1 ADCY10 affects WEE1 expression 48

4.4.2 ADCY10 mediates PP2A in cell proliferation and cell cycle control 50

4.5 ADCY10 induces classical pathways of cell proliferation 57

4.5.1 ADCY10 induces cell proliferation via MAPK pathway 58

4.5.2 ADCY10 has no effect on phosphorylation of GSK-3β or CREB signaling pathways. 61

4.6 ADCY10 and ADCY1-9 promote cell proliferation 62

5. Discussion 65

5.1 ADCY10 regulates HUVECs proliferation by controlling cell cycle progression 65

5.2 ADCY10 controls cell cycle progression via Epac and PKA 67

5.3 PP2A is a main downstream molecule of ADCY10 to regulate cell proliferation and cell cycle progression 68

5.4 ADCY10 induces cell proliferation via MAPK pathway 70

5.5 Activated-transmembrane type of ADCYs is the alternative source of cAMP when ADCY10

is deprived in cell proliferation. 71

5.6 Perspective of further studies 72

6. Conclusions 73

Summary 74

Zusammenfassung 76

References 79

Supplementary data for materials 856

Acknowledgements 89

Anlage 1 90

Anlage 2 91

List of Figures

1.	Cellular localization of adenylate cyclase isoforms (ADCYs).	3
2.	Cell cycle stages of a somatic cell.	9
3.	Diagram of the experimental design for objective 1, 2, and 5.	17
4.	Diagram of the experimental design for objective 3.	18
5.	Diagram of the experimental design for objective 4.	19
6.	FACS analysis enables the differentiation between cell cycle phases.	22
7.	Translocation of ADCY10 during cell division.	32
8.	Inhibition of ADCY10 activity suppresses cell proliferation.	34
9.	Inhibition of ADCY10 activity using 0 mM HCO_3^- delays cell cycle progression.	35
10.	Inhibition of ADCY10 activity using KH7 delays cell cycle progression.	36
11.	ADCY10 is necessary for cyclin B1 accumulation in HUVECs.	38
12.	Inhibition of Epac represses cell proliferation.	40
13.	Inhibition of Epac restricts cells in G_0/G_1.	41
14.	Inhibition of PKA using PKI induced cell proliferation.	43
15.	Inhibition of PKA using H-89 represses cell proliferation.	44
16.	PKA agonist partially increases cell proliferation under ADCY10 inhibition.	46
17.	PKA prohibits cell cycle arrest in G_2 under ADCY10 inhibition.	47
18.	ADCY10 induces an increase of WEE1 protein level independent of Epac and PKA.	49
19.	PP2A suppresses cell proliferation and induces cell accumulation in G_2/M phases.	51
20.	ADCY10 and PP2A change expression localization during the cell cycle.	52
21.	Inhibition of ADCY10 suppresses PP2A activity at 48 and 72 h.	54
22.	Inhibition of ADCY10 has no effect on PP2A content.	55
23.	ADCY10 regulates PP2A activity independently of Epac and PKA.	57
24.	Inhibition of either ADCY10 or Epac represses phosphorylation of MEK1/2.	59

25. Inhibition of either ADCY10 or Epac represses the phosphorylation of ERK1/2. 60

26. ADCY10 has no effect on phosphorylation of GSK-3β and CREB. 61

27. ADCY1-9 as well as ADCY10 promote cell proliferation. 63

28. ADCY1-9 as well as ADCY10 promote cell cycle progression from interphase to mitotic phase. 64

29. Cyclin B1/CDK1 auto-amplification loop. 69

30. Summary of the current study: ADCY10 induces cell proliferation pathways via Epac, PKA, and PP2A pathways. 71

31. The roles of soluble adenylate cyclase in cell cycle control of endothelial cells. 75

31. Die Signalwege der löslichen Adenylatcyclase während der Kontrolle des Zellzyklus von Endothelzellen. 78

List of Tables

1.	Controversial effect of cAMP on cell proliferation in different cell types.	7
2.	Preparation of diluted albumin (BSA) standards.	25
3.	Composition of SDS-gel.	26
4.	Reference standards for the RediPlate 96 Serine/Threonine Phosphatase Assay Kit.	30

1. Introduction

1.1 3', 5'-cyclic adenosine monophosphate (cAMP)

The 3', 5'-cyclic adenosine monophosphate (cAMP) is one of the first discovered secondary messengers. It was initially described more than half a century ago (Sutherland and Rall, 1958). A number of studies identified cAMP signaling cascades, which are involved in the regulation of cell homeostasis, metabolism, and cell growth on the cellular level as well as organ development and remodeling during embryogenesis on the tissue level (Della Fazia et al., 1997; Howe, 2004; Ichiki, 2006; Valsecchi et al., 2013; Almahariq et al., 2014). To date, there are four major cAMP effectors identified: 1. protein kinase A (PKA), 2. exchange proteins activated by cAMP (Epac), 3. cyclic nucleotide gate ion channels (CNGs and HCNs), and 4. phosphodiesterases (PDEs).

Likewise, cAMP also plays a role in many pathological conditions like cardiovascular diseases, diabetes, and cancer. Therefore, it is essential that the cAMP level is strictly regulated to maintain cellular and organ functions in all mammalian cells. Intracellular cAMP levels are modulated by two families of enzymes: 1. adenylate cyclases (ADCYs), which catalyze the conversion of adenosine triphosphate (ATP) to cAMP (Steer, 1975; Sadana and Dessauer, 2009) and 2. phosphodiesterases (PDEs), which hydrolyze cAMP to adenosine monophosphate (AMP) (Conti et al., 2014).

This thesis focuses on the roles of a specific type of ADCYs, namely adenylate cyclases type 10 or soluble adenylate cyclase (ADCY10, sAC), in cell proliferation and cell cycle regulation.

1.2 Adenylate cyclases (ADCYs) isoforms

1.2.1 Adenylate cyclases 1-9 (ADCY1-9)

There are six classes of nucleotidyl cyclases. Eukaryotic ADCYs are one type of nucleotidyl cyclases enzymes producing cAMP from ATP. Previous studies have characterized different isoforms of ADCYs in mammals (Defer et al., 2000; Hanoune and Defer, 2001; Sunahara, 2010). Human ADCYs belong to class III (Kamenetsky et al., 2006) which consists of a 5 stranded, antiparallel β-sheet of strand in the order β2-β3-β1-β4-β5 and 4 helices, α1-α4 (Sinha and Sprang, 2006). In addition, there are two types of adenylate cyclases. First, ADCY1-9, which are transmembrane adenylate cyclases (tmACs) and second, ADCY10, a soluble form of adenylate cyclase (Figure 1). Each isoform of ADCY1-9 contains six transmembrane spans within two hydrophobic domains and two cytoplasmic domains resulting in a pseudo-

symmetrical protein (Figure 1). The catalytic sites (C1 and C2) only reside in cytoplasmic domains. To stimulate the catalytic activity, both C1 and C2 domains are required (Defer et al., 2000; Hanoune and Defer, 2001; Kleinboelting et al., 2014). The α subunit of a stimulatory G protein ($G_s\alpha$) activates all nine tmACs. $G_s\alpha$ activates ADCY1-9 by binding to the catalytic sites of ATP. The α-subunits of the inhibitory family of G protein ($G_i\alpha$) reduce ADCYs activity in an isoform-dependent manner. However, $G_s\alpha$ and $G_i\alpha$ do not have a competitive regulatory effect on ADCY5, and 6 (Sunahara, 2010). ADCY1-9 are mainly stimulated via $G_s\alpha$ by extracellular stimuli like hormones and neurotransmitters. These processes initiate G protein-coupled receptors (GPCRs) signaling cascades, which lead to elevated cAMP concentrations in a cell type dependent manner. Previous studies used forskolin (FSK) as a pharmacological activator of ADCY1-8 to raise cAMP levels (Sadana and Dessauer, 2009). Each isoform of ADCYs has a different affinity for $G_s\alpha$, and thus, ADCYs show individual concentration activity curves in the presence of $G_s\alpha$ (Harry et al., 1997). However, FSK, as an activator of ADCY1-8, increases the affinity to $G_s\alpha$. Furthermore, the absence of $G_s\alpha$ significantly reduces the affinity of FSK to ADCYs (Dessauer et al., 1997).

Cellular calcium (Ca^{2+}) levels can act as either positive or negative regulator of ADCYs activities. Influx of calcium via calcium channel is postulated as the primary source of intracellular Ca^{2+}. Calmodulin (CaM) acts as intracellular Ca^{2+}-sensor. Two studies demonstrated that all isoforms of tmACs (ADCY1-9) show suppressed activity in the presence of supramicromolar concentrations of Ca^{2+} (Ludwig and Seuwen, 2002; Sunahara, 2010). However, under physiological conditions, Ca^{2+}/CaM activates ADCY1, 3, and 8 and inhibits ADCY5 and 6 whereas, ADCY2, 4, and 7 are not affected (Ludwig and Seuwen, 2002; Sunahara, 2010).

ADCY1-9 are distributed in tissue-specific manner (Defer et al., 2000; Kleinboelting et al., 2014). ADCY1 is located in the dentate gyrus of the hippocampus and the cerebral cortex and contributes to memory formation. ADCY3 is present in the olfactory neuro-epithelium. ADCY5 is exhibited in cardiac myocytes and ADCY6 is exhibited in nonmyocyte cells in the chicken heart. Moreover, ADCY4, 5, 6, 7, and 9 are expressed in different regions of the kidneys (Defer et al., 2000).

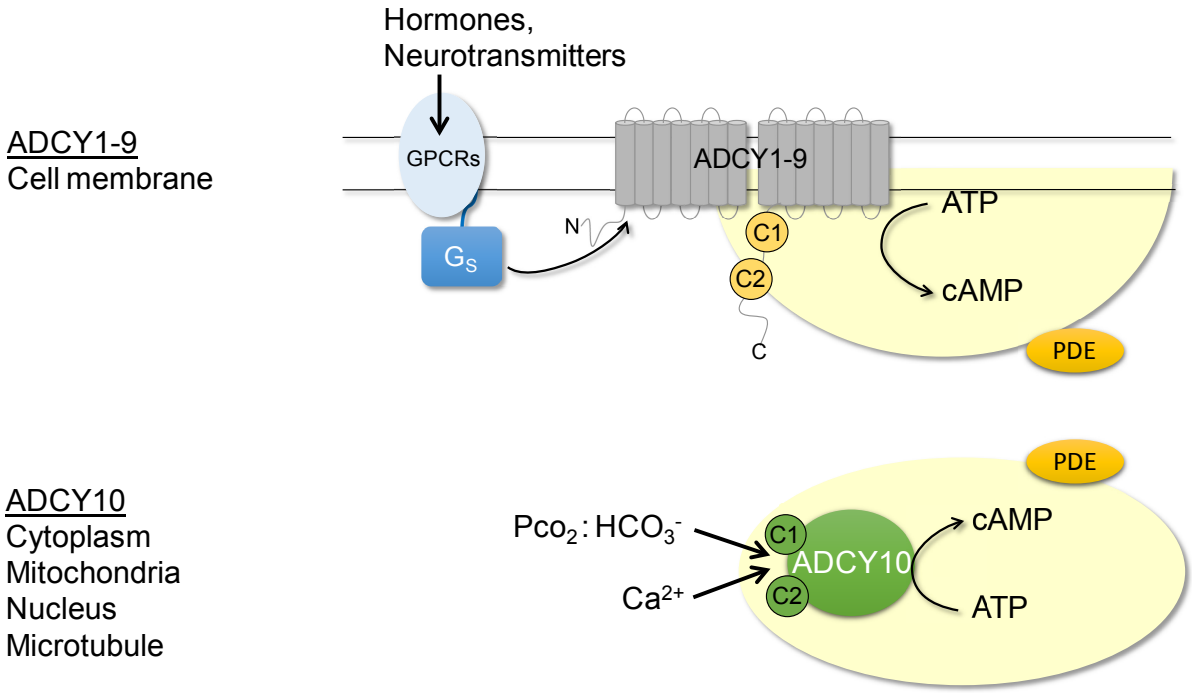

Figure 1. Cellular localization of adenylate cyclase isoforms (ADCYs). ADCYs synthesize cAMP from ATP. ADCY1-9 reside within the plasma membrane, and are stimulated by hormones or neurotransmitters via G protein-coupled receptors (GPCRs). ADCY10 localizes in the cytoplasm and sub-cellular domains like mitochondria, nucleus, and microtubule. ADCY10 is mainly activated by bicarbonate (HCO_3^-), calcium, and ATP. Intracellular cAMP is balanced by the degradation to AMP through phosphodiesterases (PDEs).

1.2.2 Adenylate cyclase type 10

Interestingly, another type of ADCYs known as ADCY10, also called soluble adenylate cyclase (sAC) does not possess the transmembrane domains. ADCY10 is insensitive to GPCRs and FSK. However, ADCY1-9 as well as ADCY10 contain two catalytic domains, C1 and C2 (Figure 1). The full length ADCY10 (~180 kDa) contains both catalytic domains and regulatory domains. These regulatory domains also contain auto-inhibitory domains (Kleinboelting et al., 2014). A truncated ADCY10 isoform (~50 kDA) occurs due to alternative splicing of ADCY10. The truncated isoform contains almost exclusively the catalytic domains C1 and C2. Generally, the truncated ADCY10 is ten times more active than the full length isoform due to the loss of the auto-inhibitory domains (Chaloupka et al., 2006; Kleinboelting et al., 2014; Tresguerres et al., 2014).

ADCY10 is localized throughout intracellular compartments like mitochondria, cytoplasm, nucleus, and centrioles (Tresguerres et al., 2011). Human ADCY10 is a conserved isoform that shows a high degree of similarity to the ADCY10 of cyanobacteria. In addition, ADCY10

can function in a pH-independent manner in the range of pH 7.0 - 8.5 (Chen et al., 2000).

In contrast to ADCY1-9, the full length as well as the truncated form of ADCY10 are sensitive to ATP, bicarbonate (HCO_3^-), Ca^{2+} (Chen et al., 2000; Pastor-Soler et al., 2003; Chaloupka et al., 2006; Kamenetsky et al., 2006; Kleinboelting et al., 2014) and/or other divalent cations like Co^{2+}, Mg^{2+}, and Mn^{2+}. ADCY10 serves as an intracellular ATP sensor and its activity varies depending on the intracellular ATP concentrations, typically in the range of 1-3 mM (Tresguerres et al., 2010). At high concentrations of ATP-Mg^{2+} (>6 mM), substrate inhibition occurs (Litvin et al., 2003). Ca^{2+} increases the substrate affinity of ADCY10 around ten folds compared to other divalent ions such as Mg^{2+} (Wiggins et al., 2018). Another study demonstrated that Ca^{2+} and HCO_3^- work synergistically to stimulate ADCY10 activity (Litvin et al., 2003). In addition, HCO_3^- induces an increase of Vmax (maximum velocity of the enzymatic catalyzed reaction) without altering Km (affinity of the enzyme to the substrate) for the substrate ATP-Mg^{2+} (Litvin et al., 2003). Therefore, Ca^{2+} supports substrate binding, and HCO_3^- increases the turnover. Furthermore, HCO_3^- reduces ATP inhibition (Litvin et al., 2003). Under laboratory conditions, Mn^{2+}-ADCY10 provides the highest activity; however, the physiologically endogenous Mn^{2+} concentrations are unable to activate ADCY10. Thus, physiologically Mg^{2+} is more relevant (Litvin et al., 2003; Wiggins et al., 2018).

Kleinboelting et al. (2013) analyzed the impact of the HCO_3^--binding site for activation of human ADCY10 in a protein crystallography study. They discovered that in the inactive state, the complex of Asp99 contains a β2-β3 overlap with the ion site region of Arg176. This phenomenon prevents the binding of FSK to Arg176 and leads to insensitivity of ADCY10 to FSK. The analysis of ADCY10 enzyme crystal structure showed that the HCO_3^--binding site is situated between Lys95 and Arg176. It was shown that the HCO_3^- binding site is the same site as the FSK binding site in tmACs (Kleinboelting et al., 2014). Moreover, they demonstrated that there was no change in the overall structure of ADCY10 after HCO_3^- binding. Instead, HCO_3^- induced “a loosening” of the protein conformation, enabling the catalytic motion. Besides, Arg176 acted as a lever connecting regulatory and active sites, whereas Lys95 remained unchanged upon HCO_3^- binding. However, Lys95 contributed to the regulation of HCO_3^- binding. The double mutant of Lys95Ala/Arg176Ala disrupted the side chain and as a result, no HCO_3^- activation was observed. In contrast, single mutant of Arg176Ala caused a desensitization of EC_{50} of ADCY10 from 12 mM to more than 30 mM HCO_3^- (Kleinboelting et al., 2014).

In vitro and *in vivo*, carbonic anhydrase (CA) converts the substrate carbon dioxide (CO_2) to HCO_3^-. The human body obtains CO_2 directly from cellular respiration and consequently, catalyzes it to HCO_3^-. HCO_3^- can be shuttled across plasma membranes via a variety of ion

transporting proteins (Tresguerres et al., 2010; Tresguerres et al., 2014; Roa and Tresguerres, 2017). Moreover, HCO_3^- acts as a buffer in the acid-base regulatory system of complex organisms. Taken together, HCO_3^- is present from cellular to organ level and is a key element of the homeostasis of the whole body system. Under resting conditions, average partial pressure of carbon dioxide (Pco_2) ranges between 40 mmHg in the aorta and 46 mmHg in the vena cava, equivalent to 24.0 and 24.6 mM HCO_3^- respectively. Increased cellular metabolism typically raises Pco_2. However, each organ has an individual venous Pco_2 level depending on its oxygen uptake and metabolic rate. The heart and the kidney have different Pco_2 at the level of their tissue capillaries at 50 and 40 mmHg respectively (Schmidt and Thews, 1987). These findings have raised questions concerning the roles of ADCY10 since it is directly activated by HCO_3^-.

CO_2 is constantly produced during mitochondrial respiration and consequently converted into HCO_3^- catalyzed by CA. Thus, ADCY10 is always stimulated under physiological conditions, raising the question whether cAMP produced by ADCY10 may have physiological functions. In line with this assumption, work from Sayner's group showed that the cellular location of intracellular cAMP production is critical for pulmonary endothelial barrier function, and can either lead to barrier tightening or disruption (Sayner et al., 2006; Sayner, 2011; Obiako et al., 2013), indicating the decisive role of cAMP for maintenance of vascular function. Furthermore, work from Das (2019) from the medical faculty Carl Gustav Carus, Institute of Physiology, TU-Dresden, could recently show that physiological HCO_3^- concentrations tighten the endothelial barrier function via activation of ADCY10 in a cultured model of human umbilical vein endothelial cells (HUVECs) (Das, 2019).

1.3 Intracellular cAMP distribution

Intracellular cAMP distribution is caused by at least four different processes.

1. Diffusion: cAMP produced by tmACs diffuses and activates its downstream effectors, PKA and Epac. The spreading of cAMP is dependent on the intracellular cAMP gradient. Agarwal et al. (2016) investigated the cAMP diffusion coefficient in HEK293 cells by using the fluorescent dye fluorescein. They found that the diffusion coefficient of cAMP in the cytoplasm is significantly lower compared to the free diffusion in an aqueous solution (Agarwal et al., 2016).

2. Endocytosis: There is evidence suggesting that GPCRs-ADCY1-9 complexes can be internalized via endocytosis under the influence of prolonged incubation with thyroid stimulating hormone (TSH). These endosomes were persistent and produced cAMP even after TSH administration was terminated (D Calebiro et al., 2010; Davide Calebiro et al., 2010).

3. ADCY10: ADCY10-generating cAMP is considered as a local cAMP source. It is found in intracellular domains including nucleus and microtubule (Zippin et al., 2003).

4. PDEs: PDEs play an essential role in cAMP distribution since they catalyzed cAMP to AMP. Furthermore, compartmentalized in close vincity of transmembrane and soluble ADCYs, PDEs form a diffusion barrier for cAMP. Thereby, balancing intracellular cAMP concentrations (Conti et al., 2014).

1.4 Effect of cAMP on cell proliferation

Previous studies demonstrated that cAMP produced from ADCY1-9 has either proliferative or anti-proliferative effects depending on cell types (Chen et al., 1998; Hanaoka and Guggino, 2000; Yamaguchi et al., 2000; Belibi et al., 2004; Loffler et al., 2008; Hewer et al., 2011; Wallace, 2011; Jang et al., 2012; Gold et al., 2013; Rodriguez et al., 2013; Lv et al., 2018). ADCY1-9 induced cell proliferation via the activation of downstream pathways of cAMP, such as Epac and PKA (Chen et al., 1998; Hanaoka and Guggino, 2000; Schmitt and Stork, 2001; Loffler et al., 2008; Jang et al., 2012; Rodriguez et al., 2013; Lv et al., 2018). In the context of the present work, it is interesting to note that activation of ADCY5 and 6, the major ADCYs express in endothelial cells, induce cell proliferation via PKA and Epac/Rap1 pathways in mesenchymal stem cells (Jang et al., 2012).

Gregory et al. (1992) used prostaglandins (PGEs) and FSK to stimulate ADCY1-9. They reported that PGEs induces an increase of cAMP production via GPCRs (Gregory et al., 1992). Many stimulators are capable of activating ADCY1-9 creating an extensive and complex network of ADCYs signaling cascades. Hence, ADCY1-9 are fundamental enzymes for complex organisms. Furthermore, PGEs stimulation of the human cancer cell line HT-29 resulted in a rise of intracellular cAMP concentrations. Ultimately, the increased cAMP induced cell proliferation of the cancer cells (Loffler et al., 2008). Furthermore, Hanaoke and Guggino (2000) showed that extracellular cAMP induced cell proliferation and cyst formation in autosomal dominant polycystic kidney disease (ADPKD) (Hanaoka and Guggino, 2000). However, several studies suggested that cAMP produced from ADCY1-9 has an anti-proliferative effect. One study stated that cAMP generated by ADCY1-9 inhibits cell proliferation and mitogenesis in the fibroblast cell line NIH 3T3 via Rap1 (Schmitt and Stork, 2001). Furthermore, an FSK-induced increase of cAMP levels caused a reduction of cell proliferation in a cell line of T-cell chronic lymphocytic leukemia (Rodriguez et al., 2013). A recent study by Lv et al. (2018) indicated that tumor spheres of the cell lines U87 and A172 reduced their sizes after incubation with combination of FSK and phosphodiesterase inhibitor (FSK-IBMX) (Lv et al., 2018).

The effects of cAMP on cell proliferation are summarized in Table 1.

Table 1. Controversial effect of cAMP on cell proliferation in different cell types.

Types of ADCYs	Cell types	Stimulator	cAMP downstream		Cell proliferation		Publication
			Epac	PKA	Activation	Inhibition	
	kidney microcyst	Sp-cAMP		+	+		Hanaoka and Guggino (2000)
1-8	HKC cells	Forskolin		+	+		Yamaguchi et al. (2000)
1-8	NIH 3T3 cells	Forskolin	+			+	Schmitt and Stork (2001)
1-9	HT-29 cells	Prostaglandin			+		Loffler et al. (2008)
	smooth muscle cells	8-cpct, 6-BNZ	+	+		+	Hewer et al. (2011)
10	LNCap, PC3	bicarbonate, 8-pcpt	+		+		Flacke et al. (2012)
1-9	hUCB-MSCs	Prostaglandin	+	+	+		Jang et al. (2012)
	isolated Schwann cells	6-MB cAMP		+	+		Bacallao and Monje (2013)
1-8	T-cell: Kit225	Forskolin		+		+	Rodriguez et al. (2013)
1-8	glioma stem cells (GSCs)	Forskolin				+	Lv et al. (2018)

In the past, the majority of studies on cAMP-mediated cell proliferation were focused on the transmembrane type (ADCY1-9). However, as it is illustrated in Section 1.3, the local distribution and the intracellular site of formation emerge to be critical determinant for specific cAMP effects. Thus, ADCY10 expressed in a variety of organelles including cell nucleus, might play a crucial role in cell cycle progression and cell proliferation.

Generally, cell proliferation is an increase of cell population by the parental cell division into two daughter cells. The daughter cells inherit the parental genetic materials and behave exactly like their parental cells. In addition, the division of progeny cells is symmetric and does not alter their properties, whereas uncontrolled cell proliferation is a hallmark characteristic of cancer. Throughout this work, if it is not mentioned otherwise, cell proliferation refers to mitosis (somatic cell division) only, and not to meiosis (reproductive cell division).

In healthy tissue, cell proliferation occurs only to support replenishment of cells that have died or been injured. For example, lymphocytes, hematopoietic cells, and epithelial cells from the duodenum have a turnover interval of 2-3 days. In contrast, cardiac myocytes and neurons have the longest turnover interval of around 14,800 and 16,425 days, approximately 40 and 45 years respectively (Richardson et al., 2014). However, among different cell types, the endothelium has a high turnover rate of more than 15% per year (Bergmann et al., 2015). Normally, most cell types in an adult body including endothelial cells, sustain quiescent at G_0 stage of cell cycle (Section 1.5). However, cells can reenter into the cell cycle again if it is needed (Cooper, 2000a).

Changes of cell number are an outcome of cell proliferation and cell loss due to differentiation or apoptotic cell death. In healthy tissues, cell growth and cell death are balanced by sophisticated physiological cell programs to maintain tissue homeostasis. In tumor cells, owing a pathophysiological transformed cell cycle control, it has been shown that ADCY10 might be a critical factor for tumor cell turnover (Flacke et al., 2013).

This thesis focuses on the specific influence of cAMP synthesized by ADCY10 in healthy cell proliferation.

1.5 Cell proliferation and cell cycle

Cell proliferation is an outcome of cell cycle progression. Generally, a eukaryotic cell has two stages of cell division, which are interphase and mitotic phase. Most cells remain quiescent at G_0 phase. When the appropriate stimuli are present, cells can enter the first gap phase (G_1). Cell cycle progression is primarily modulated by phosphatases and kinases. To proliferate, a parental cell is required to go through cell cycle transition. Eukaryotic cells have evolved the so-called cell cycle checkpoints. These checkpoints mainly maintain genomic integrity by detecting DNA damage, incomplete DNA synthesis, and subsequently activate cell cycle arrest. Under physiological conditions, cells are able to pass through checkpoints. The cell cycle continues and the cell replicates into two daughter cells (Schafer, 1998; Berridge, 2014).

Cell division can be divided into interphase and mitotic phase. G_1, S, and G_2 phases belong to interphase whereas, mitotic phase only contains M phase.

1.5.1 Interphase

The phases of interphase are illustrated in Figure 2.

G_1 phase (the first gap) is the beginning phase of interphase. During this period, cells are preparing for DNA (deoxyribonucleic acid) synthesis by synthesizing RNA (ribonucleic acid) and proteins. Cyclin D, E and cyclin-dependent kinases (CDKs) 2, 4, and 6 are dominant in this phase.

S phase (synthesis phase) is the phase after G_1. Cells in S phase synthesize DNA. Under physiological conditions, the human genome of a somatic cell has a diploid set of 23 pairs of chromosomes. During S phase, each chromosome is replicated. In the late stage of S phase, each chromosome contains two identical sister chromatids. Thus, the DNA content doubles during S phase. Cyclin A and CDK2 play a role in cell cycle transition from S to G_2 phase.

G_2 phase (the second gap) occurs after the DNA synthesis is finished. Cells are preparing themselves for mitotic phase and cytokinesis. Cells are also forming mitotic spindles and kinetochore to separate the two daughter cells. In this phase, DNA proofreading occurs to ensure that the DNA was properly replicated before entering mitosis. Cyclin A and CDK1 play a role in cell cycle progression from G_2 to M phase.

1.5.2 Mitotic phase (M phase)

The mitotic phase includes mitosis, separation of the nucleus, and cytokinesis, separation into two daughter cells. Mitosis consists of prophase, prometaphase, metaphase, anaphase, and telophase. The purpose of having mitosis is, to separate the two sister chromatids of each chromosome into two new daughter cells. The biomechanical forces required for chromatid separation are accomplished by the reorganization of microtubules of the bipolar mitotic spindles. The mitotic spindles will segregate the two sister chromatids to opposite poles of the cell by equal force. Microtubules connect the spindle pole via proteins called kinetochores with the centromere of each chromosome. This is needed for force transduction. After that, cytokinesis occurs; actin and myosin form a contractile ring creating cell cleavage. As a result, the parental cell is separated into two new daughter cells (Cooper, 2000b).

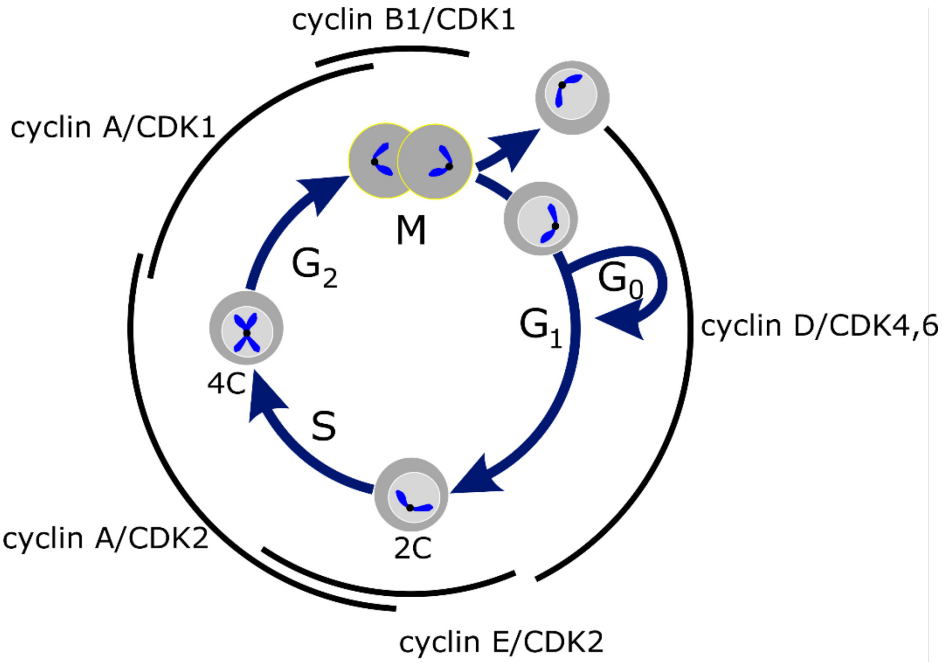

Figure 2. Cell cycle stages of a somatic cell. Cell cycle stages consist of two major phases: interphase (G_1, S, G_2) and mitotic phase (M). Each phase is characterized by specific cyclins and CDKs. Generally, interphase is the longest period of cell cycle time due to DNA synthesis. In contrast, mitosis takes the least time to divide a parental cell into two daughter cells. DNA content is described as follows: 2C: single diploid chromosome set, 4C: double diploid chromosome set.

1.5.3 Cyclin-dependent kinases (CDKs)

Cell cycle regulatory proteins are mediated during the progression of the cell cycle. Synthesis and destruction of regulatory proteins are determined by strict chronological regulations. The main regulatory components of the cell cycle are cyclin-CDK complexes. In order to become active, CDKs are required to be dephosphorylated to form a complex with their specific cyclins. This complex initiates transition to the next phase. Correct cell cycle progression depends on ubiquitin-mediated proteolysis of cyclins. Therefore, cell cycle transitions from one phase to another are irreversible due to the regulated degradation of specific cyclins in each phase (Heim et al., 2017). For example, for the transition from G_2 to M phase, dephosphorylated CDK1 associated with cyclin B1 is required. These cyclin B1/CDK1 complexes accumulate further as cell progresses to the late M phase, where it is ubiquitinated and subsequently degraded. Cells that are not ready to progress in the cell cycle due to insufficient growth, malnutrition, or DNA damage, will arrest in G_2 (Rowley et al., 1992; Strasser-Wozak et al., 1998; DiPaola, 2002).

In fact, the regulation of CDKs is complex as can be seen at the example of the cyclin B1/CDK1 auto amplification loop. The regulation of cyclin B1/CDK1 depends on the upstream pathways of the kinase WEE1 and the phosphatase Cdc25. Both depend on the activity of PP2A (Section 1.5.4) Throughout the cyclin B1/CDK1 dependent auto-amplification loop, cyclin B1/CDK1 directly activates Cdc25 through positive feedback and inhibits WEE1 via negative feedback (Hara et al., 2012; Jeong and Yang, 2013). Taken together, the regulation of cyclin B1/CDK1 mainly works cooperatively with other proteins in this auto-amplification loop.

1.5.4 Protein phosphatases (PPs)

Protein phosphatase 1 (PP1) and phosphatase 2A (PP2A) are members of Ser/Thr PPs, and are involved in cell cycle progression (Heim et al., 2017; Manic et al., 2017). A review from Manic (2017), pointed out that PP2A promotes the alignment of sister chromatids in mitosis by stabilizing kinetochore fibers (Manic et al., 2017). Under physiological conditions, PP2A controls cell cycle transition in interphase and mitotic phase (Wlodarchak and Xing, 2016). Recent studies have focused on PP2A as therapeutic target for cancer and inflammation (O'Connor et al., 2018; Clark and Ohlmeyer, 2019; Remmerie and Janssens, 2019).

Cell cycle progression is the result of a balanced intermittent phosphorylation of CDKs and PPs, determining their active states. For example, the inhibition of PP2A by okadaic acid (OA) induces down-regulation of CDK1 and subsequently, accumulation of cells in G_2/M phases (Gong et al., 2015). This finding is consistent with a study from Cervone et al. (2018), where PP2A was shown to regulate CDK1 via the spindle assembly checkpoint (Cervone et al., 2018).

1.5.5 Cell cycle checkpoints

Checkpoints are involved in the prevention of phase transition when cells are not ready to progress through the cell cycle. There are several checkpoints monitoring how the cell progresses in each phase. This mechanism diminishes possible replication mistakes, such as chromosome segregation or incomplete DNA synthesis. Therefore, checkpoints play an essential role in the prevention of cancer.

There are four known control checkpoints in the cell cycle. First, the unreplicated-DNA checkpoint, between G_2 and M phase, inhibits cells with unfinished DNA replication to enter mitosis. Second, the spindle-assembly checkpoint, during M phase, prohibits cells with improper mitotic spindle assembly to proceed to anaphase. Third, the chromosome-segregation checkpoint, during the transition from ana- to telophase, ensures the correct location of segregated daughter chromosomes and promotes mitotic exit. Fourth, the DNA-damage checkpoint, which takes place multiple times during the cell cycle, blocks defective cells to traverse the G_1, S, or G_2 phase through tumor suppressor protein p53 regulation (Lodish, 2012).

1.6 cAMP in diseases and pathophysiology

The second messenger cAMP is synthesized in response to upstream primary messengers such as hormones, neurotransmitters or prostaglandins (PGEs) (Bar and Hechter, 1969; Steer, 1975). Basal concentrations of cAMP regulate homeostasis of cells and organs. However, it has been shown that impairment of the local cAMP concentrations correlates with the progression of pathological processes and various diseases like heart failure, cataract, diabetes, cancer (Gold et al., 2013), inflammation, polycystic kidney disease, as well as cell aging and death (Ehses et al., 2003; Belibi et al., 2004; Wallace, 2011; Ladilov and Appukuttan, 2014; Torres and Harris, 2014). In the past decades, many studies have been focusing on the impact of cAMP on cell proliferation. However, these reports interpreted the effects of transmembrane adenylate cyclase (ADCY1-9) by using direct stimulators such as epinephrine, PGEs, and FSK (Yamaguchi et al., 2000; Chen et al., 2007; Madamanchi, 2007; Loffler et al., 2008; Gold et al., 2013; Bar-Shavit et al., 2016; Liu et al., 2016).

In vitro studies showed that the direct pharmacological activation of ADCY1-8 by FSK induces tumor-genesis, invasion, and metastasis (Bar-Shavit et al., 2016; Liu et al., 2016). These findings indicated that cAMP generated by tmACs might be a key player of physiological and pathophysiological cell proliferation. At least 18 hormones play a role in stimulation of ADCY1-9 activity like TSH, serotonin, and vasopressin (Steer, 1975). Several studies reported increased ADCY1-9 activity due to β-adrenergic receptor (β-ARs) stimulation (Yamaguchi et

al., 2000; Loffler et al., 2008; Gold et al., 2013; Liu et al., 2016). This effect was linked to a long-QT syndrome, which is a potentially deadly disease associated with cardiac ventricular tachycardia (Chen et al., 2007). Another study suggested that continuous over-activation of the β-ARs desensitized GPCRs. Additionally, phosphoinositide-3-kinase (PI3K), a downstream signaling element of cAMP, was identified to be affected by decreased β-ARs function and associated with reduced cardiac contractility. Taken together, the impaired β-AR signaling pathway can cause chronic heart failure (Madamanchi, 2007).

In summary, many stimulators are capable of activating ADCY1-9 creating a vast and redundant complex network of ADCY signaling cascades. Certainly, cAMP produced by ADCY1-9 is involved in various diseases. However, the exact role of ADCY10 in physiological processes like cell growth, cell cycle control, cell division as well as in pathophysiological states remains to be elucidated.

2. Aims

The present study was performed to analyze the role of ADCY10 in cell proliferation and cell cycle control. It is hypothesized that ADCY10 regulates cell proliferation and cell cycle control due to its characteristic compartmentation within cells and specific mode of activation by HCO_3^-. Since the endothelium, forming the inner lining of the whole cardiovascular system, is exposed to alternating bicarbonate concentrations due to functional adaptation responses of the body, this study is performed in a model of cultured human umbilical vein endothelial cells (HUVECs) expressing ADCY10.

Thus, the following objectives were raised to assess this hypothesis:

1. Does ADCY10 induce cell proliferation in human endothelial cells via HCO_3^-?
2. If objective 1 is applicable, how does ADCY10 regulate cell cycle control?
3. Which of the known downstream pathways of ADCY10, in particular Epac and PKA, play a dominant role in the regulation of the cell cycle?
4. Does ADCY10 influence PP2A activity to control cell cycle progression?
5. Does ADCY10 share common signaling pathways with ADCY1-9 during cell proliferation?

It is expected that the present study will provide novel insight into a not yet identified function of the soluble adenylate cyclase and will expand the knowledge about the impact of ADCY10 on cell cycle control, cell proliferation, and finally tissue homeostasis.

3. Experimental design and methods

Supplemental data for material……...…..page 86

3.1 Isolation and culturing of HUVECs

3.1.1 Isolation of HUVECs

Solutions and materials:

Phosphate-buffered saline (PBS)	X ml
Collagenase II dissolved in PBS	0.25 mg/ml
Gelatin	0.5%
Ethanol	70%
Rinsing solution:	
Medium M199	X ml
Fetal calf serum (FCS)	10%
Penicillin/streptomycin (Pen/Strep)	1%
Culture medium A:	
Medium M199	X ml
FCS	10%
Pen/Strep	1%
Endothelial cell growth supplement from bovine pituitary (WF)	12 µg/ml

The umbilical cords were collected from the obstetric and gynecology department, University Hospital Dresden. The permission was given by the Ethikkommission of the Medical Faculty Carl Gustav Carus of TU Dresden (permission EK 203112005). The protocol was adapted from Jaffe el al. (1973) (Jaffe et al., 1973). The ends of the umbilical cord were immerged shortly in 70% ethanol for disinfection. Afterwards, the umbilical cord was cut again at both ends. Then, it was cannulated and perfused with PBS to remove blood residue. The lumen of the vein was then filled with collagenase II solution for 11 min at 37 °C. After the incubation, the umbilical cord was massaged to promote the detachment of HUVECs. Consecutively, the collagenase II solution containing endothelial cells was removed and collected in a 50 ml Falcon tube. Further, the vein was perfused with 30 ml of rinsing solution, which was collected in the same 50 ml Falcon tube to inactivate the collagenase. The effluent was centrifuged for 5 min at 250 x *g* at room temperature (RT). The supernatant was discarded and the cell pellet was resuspended with culture medium A.

T25 flask was coated with 5 ml 0.5% gelatin for 30 min at 37 °C. The excessive gelatin was aspirated right before adding the cell suspension. After overnight incubation at 37 °C and 5%

CO_2, cells were extensively washed with PBS to remove the unattached non-endothelial cells and cell debris. Adherent cells were incubated in 5 ml of culture medium A at 37 °C and 5% CO_2. The medium was changed every 48 h.

3.1.2 Culturing of HUVECs

Solutions and materials:

1X HBSS	X ml
Trypsin-ethylenediaminetetraacetic acid (EDTA)	0.05%
Culture medium B:	
Medium M199	X ml
Sodium bicarbonate ($NaHCO_3 \rightarrow Na^+ + HCO_3^-$)	{0, 24, 40} mM
FCS	{2, 10} %
Pen/Strep	1%
Sodium pyruvate	1%
200 nM L-glutamine	1%
SupplementPack Endothelial cell GM (Promocell):	
Human epidermal growth factor (hEGF)	0.1 ng/ml
Endothelial cell growth supplement (ECGS/H)	4 µl/ml
Hydrocortisone (HC)	1 µg/ml
Human basic fibroblast growth factor (bhFGF)	1 ng/m
HEPES*	(50 mM)

* HEPES was only used as a pH buffer, when Pco_2 concentrations were altered due to experimental conditions ($Pco_2 \neq 5\%$).

48 h prior to the experiment, the medium was changed to culture medium B (2% FCS, 24 mM HCO_3^-). The cells were allowed to grow and become a confluent monolayer. At the beginning of the experiment, the cells were washed with HBSS and subsequently incubated with 900 µl of trypsin/EDTA solution until the cells started to detach as observed under microscopic control. Consecutively, 100 µl FCS was added to inactivate trypsin/EDTA. The trypsin solution containing HUVECs was collected and centrifuged for 5 min, 400 x *g*. Thereafter, the cell pellet was resuspended in 1 ml culture medium B. 10 µl of the cell suspension was taken and counted with a hemocytometer. Then, cells were seeded according to the experimental designs. Experiments were performed with HUVECs from passage 1.

3.1.2.1 Cell cycle synchronization in G_0/G_1 phases

Starvation culture medium C:	
Medium M199	X ml
Sodium bicarbonate ($NaHCO_3$)	24 mM
FCS	0.2%
Pen/Strep	1%
100 mM Sodium pyruvate	1%
200 nM L-glutamine	1%
SupplementPack Endothelial cell GM (Promocell):	
Human epidermal growth factor (hEGF)	0.1 ng/ml
Endothelial cell growth supplement (ECGS/H)	4 µl/ml
Hydrocortisone (HC)	1 µg/ml
Human basic fibroblast growth factor (bhFGF)	1 ng/m

For cell proliferation assays, 50,000 HUVECs were seeded in 3.5 cm^2 culture dishes with culture medium B (2% FCS, 24 mM HCO_3^-). After 24 h, the cells were washed once with HBSS to dilute FCS residue. Then, the cells were put into starvation culture medium C (0.2% FCS) for 15, 18, and 24 h at 37 °C and 5% CO_2. The protocol was adapted from Jackman and O'Connor (Jackman and O'Connor, 2001).

Cell synchronization was initially verified at 15 h, 18 h, and 24 h by FACS analysis. In brief, cells were stained for DNA content to differentiate cell cycle phases - G_0/G_1, S, G_2/M (Section 3.3.2).

The result showed that after 18 h of starvation, cell synchronization was achieved in G_0/G_1. At this time point, around 80% of the total cell population is in G_0/G_1 phases. This method was chosen because it is free of external drugs and allows the cells to intrinsically coordinate cell synchronization.

3.2 Experimental designs

This section illustrates the individual experimental protocols to address the objectives of this study.

3.2.1. Experimental design for objective 1, 2, and 5

Objective 1: Does ADCY10 induce cell proliferation in HUVECs via HCO_3^-?

Objective 2: If objective 1 is applicable, how does ADCY10 regulate cell cycle control?

Objective 5: Does ADCY10 share common signaling pathways with ADCY1-9 during cell proliferation?

Experimental Design: HCO_3^- levels directly stimulate ADCY10 activity. To observe whether ADCY10 induces cell proliferation via HCO_3^-, the experimental groups were arranged as 0, 24 (control group), and 40 mM HCO_3^-. These HCO_3^- concentrations are equivalent to conditions of humidified air with 0%, 5%, and 8% CO_2. After starvation, cells were incubated in culture medium B (10% FCS) at 0, 24, and, 40 mM HCO_3^- for up to 72 h. The pharmacological inhibitor of ADCY10, 10 µM KH7, was used to reassure the effect of ADCY10 on cell proliferation (culture medium B with 10% FCS, 24 mM HCO_3^-). Further stimuli or inhibitors of downstream pathways were used to assess objective 2 and 5. The cells were collected for analysis at different time points, every 12 or 24 h. Cell number and cell cycle stages were assessed by FACS analysis. Proteins were collected for Western blot analysis. The localizations of proteins (ADCY10, α-Tubulin, PP2A) were assessed by immunofluorescence (Section 3.3.3).

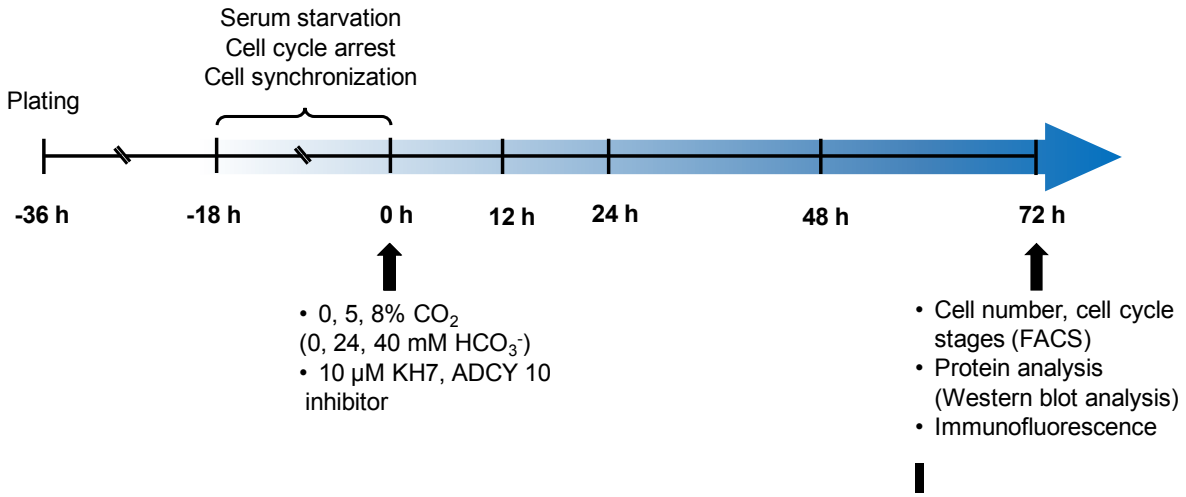

Figure 3. Diagram of the experimental design for objective 1, 2, and 5. HUVECs were seeded 36 h before the experiment started. Cells were incubated in starvation medium C (0.2% FCS) 18 h prior to the experiment to induce cell synchronization in G_0/G_1 phases. At 0 h, HUVECs were incubated in culture medium B (10% FCS) with HCO_3^- concentrations according to their conditions or 10 µM KH7 (ADCY10 inhibitor). Cell populations were collected at 12, 24, 48, and 72 h. Cell number and cell cycle stages were analyzed by FACS analysis. Protein levels were measured by Western blot analysis.

3.2.2. Experimental design for objective 3

Objective 3: Which of the known downstream pathways of ADCY10, in particular Epac and PKA, play a dominant role in the regulation of the cell cycle?

Experimental Design: ADCY10 is producing cAMP under *in vitro* conditions. Epac and PKA are downstream signaling pathways of ADCY10. Specific direct inhibition and activation of Epac and PKA demonstrate their roles in cell proliferation. For inhibition experiments, ADCY10 activated by 24 mM HCO_3^- were compared against inhibition of Epac using ESI-09 and PKA using H-89. Additionally, ADCY10 was inhibited by KH7. Therefore, the experimental groups were: control (24 mM HCO_3^-), 10 µM KH7, 25 µM ESI-09, and 10 µM H-89. For activation experiments of Epac and PKA, the influence of ADCY10 was inhibited using KH7 to differentiate between downstream pathways. Epac and PKA were individually activated by cAMP agonists, 8-pcpt-2'-o-me-cAMP for Epac and 6-BNZ-cAMP for PKA. Therefore, the experimental groups were: control (24 mM HCO_3^-), 10 µM KH7, 10 µM KH7 plus 0.1 mM 8-pcpt-2'-o-me-cAMP, and 10 µM KH7 plus 0.1 mM 6-BNZ-cAMP. After starvation, cells were incubated in culture medium B (10% FCS, 24 mM HCO_3^-) for up to 48 h. The cells were collected for analysis at different time points, either at 12, 24, or 48 h. Cell number and cell cycle stages were assessed by FACS analysis. Proteins were collected for Western blot analysis.

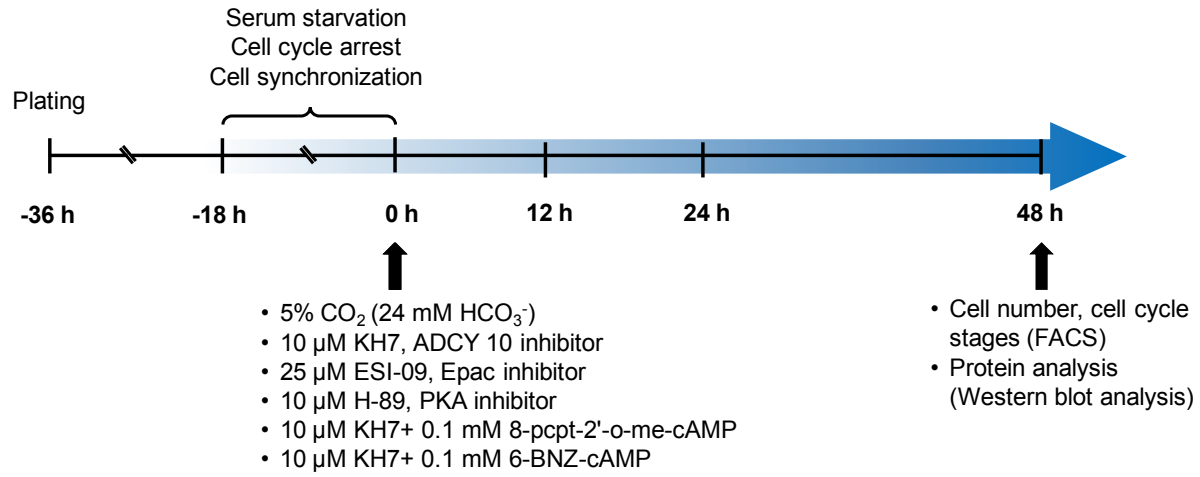

Figure 4. Diagram of the experimental design for objective 3. HUVECs were seeded 36 h before the experiment started. Cells were incubated in starvation medium C (0.2% FCS) 18 h prior to the experiment to induce cell synchronization in G_0/G_1 phases. At 0 h, HUVECs were incubated in culture medium B (10% FCS, 24 mM HCO_3^-) with inhibitors and activators according to protocol. Cell populations were collected at 12, 24, and 48 h. Cell number and cell cycle stages were analyzed by FACS analysis. Protein levels were measured by Western blot analysis.

3.2.3. Experimental design for objective 4

Objective 4: Does ADCY10 influence PP2A activity to control cell cycle progression?

Experimental Design: The balance of kinases and phosphatases is essential for cell cycle progression. In general, PP2A dephosphorylates CDK1 to enter mitotic phase. Specific inhibitors of ADCY10 (KH7) and PP2A (OA) were applied to investigate the effect of ADCY10 on PP2A. The experimental groups were: control (24 mM HCO_3^-), 10 µM KH7, 5 nM OA. To further investigate whether ADCY10 regulates PP2A activity via PKA or Epac, cAMP agonists for Epac (8-pcpt-2'-o-me-cAMP) and PKA (6-BNZ-cAMP) were used in a combination with ADCY10 inhibitor (µM KH7). Therefore, the experimental groups were: control (24 mM HCO_3^-), 10 µM KH7, 10 µM KH7 plus 0.1 mM 8-pcpt-2'-o-me-cAMP, and 10 µM KH7 plus 0.1 mM 6-BNZ-cAMP. After starvation, cells were incubated in culture medium B (10% FCS, 24 mM HCO_3^-) for up to 48 h. The cells were collected for analysis at different time points, either at 12, 24, or 48 h. Cell number and cell cycle stages were assessed by FACS analysis. Proteins were collected for Western blot analysis. Cell lysates were also assessed for PP2A activity. The localizations of proteins were assessed by immunofluorescence (Section 3.3.3).

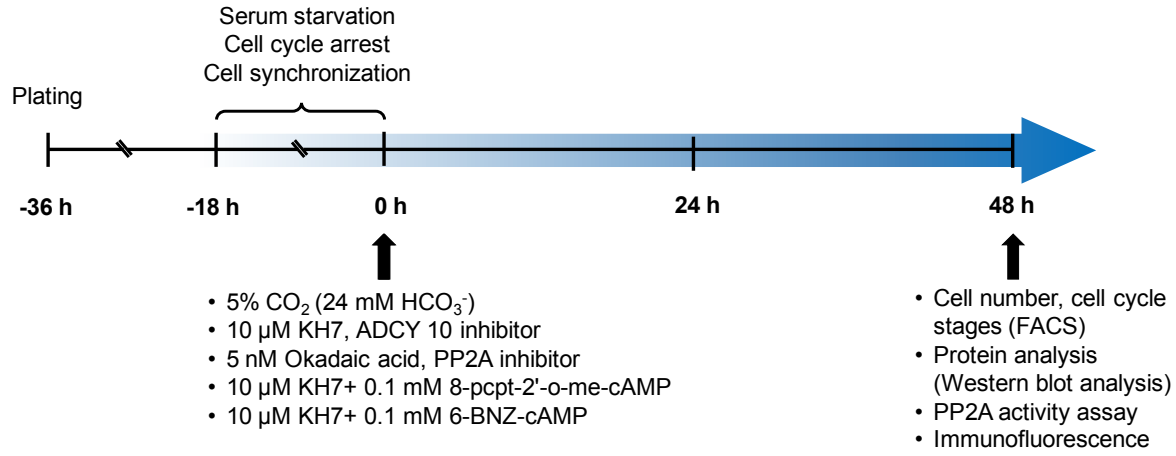

Figure 5. Diagram of the experimental design for objective 4. HUVECs were seeded 36 h before the start of the experiment. Cells were incubated in starvation medium C (0.2% FCS) 18 h prior to the experiment to induce cell synchronization in G_0/G_1 phases. At 0 h, HUVECs were incubated in culture medium B (10% FCS, 24 mM HCO_3^-) with inhibitors and activators according to protocol. Cell populations were collected at 12, 24, and 48 h. Cell number and cell cycle stages were analyzed by FACS analysis. Protein levels were measured by Western blot analysis.

3.3 Methods

3.3.1 Cell proliferation assay

Solutions and materials:

1X Hanks' balanced salt solution (HBSS)	X ml
Trypsin-ethylenediaminetetraacetic acid (Trypsin-EDTA)	0.05%
Culture medium B (Section 3.1.2)	X ml
Starvation culture medium C (Section 3.1.2.1)	X ml

HUVECs were isolated from individual umbilical cords and cultured until confluence. Then, HUVECs were trypsinized by using 0.05% Trypsin EDTA and seeded at a concentration of 50,000 cells per 3.5 cm^2 dish using culture medium B (2% FCS, 24 mM HCO_3^-). After 24 h, cell synchronization in G_0/G_1 was induced by incubation with starvation culture medium C for 18 h. The method was adapted from Jackman and O'Connor (Jackman and O'Connor, 2001). Afterwards, culture medium B (10% FCS) with either 0, or 24, or 40 mM HCO_3^- was added according to the experimental groups. This allowed the cells to potentially continue cell cycle progression.

Specific inhibitors for ADCY10, Epac, and PKA were used. This included 10 µM KH7, 25 µM ESI-09, and 10 µM H-89 respectively. The cells were collected every 12 or 24 h by ethanol fixing and then proceeded to flow cytometry (Section 3.3.2).

3.3.2 Fluorescence-activated cell sorting (FACS) analysis

3.3.2.1 Analyzed cell cycle status by double staining of Hoechst 33342/Pyronin Y

Solutions and materials:

HUVECs	
1X PBS	X ml
Ethanol	70%
FACS buffer:	
1X PBS	X ml
FCS	2%
Ethylenediaminetetraacetic acid (EDTA)	1 mM
Hoechst 33342/Pyronin Y staining solution:	
Hoechst 33342, DNA stain	2 µg/ml
Pyronin Y, RNA stain	4 µg/ml

Effects of HCO_3^- activated ADCY10 on cell proliferation and cell cycle stages were determined by FACS analysis of Hoechst 33342/Pyronin Y double staining. Proliferating cells in G_1 contain elevated amount of intracellular RNA compared to quiescent cells (G_0), hence, FACS analysis was used to differentiate the cell cycle phases. Cell number and cell cycle stages were assessed as described by Kim and Sederstrom (Kim and Sederstrom, 2015). After the cells were collected (3.3.1), they were resuspended in 0.5 ml PBS to wash out remaining FCS. Consecutively, 4.5 ml pre-chilled 70% ethanol (−20 °C) were added dropwise while vortexing. The cells were required to be incubated at −20 °C overnight. Before performing FACS analysis, the cells were centrifuged for 3 min at 300 × *g* at RT to eliminate residual ethanol. Then, the ethanol supernatant was removed and discarded. Afterwards, the cells were washed twice with 5 ml FACS buffer and then centrifuged for 5 min at 200 × *g* at RT. The supernatant was discarded. Subsequently, the cell pellet was resuspended with 150 µl freshly prepared Hoechst 33342/Pyronin Y staining solution. Consequently, the 150 µl resuspended stained cells were pipetted into a flat bottom 96 well plate and analyzed by a flow cytometer MACSQuant Analyzer 10 (Miltenyi Biotec GmbH, Bergisch Gladbach, Germany). Data obtained from flow cytometry were analyzed by FlowJo™ (FlowJo LLC, Ashland, Oregon, USA) Software (Figure 6).

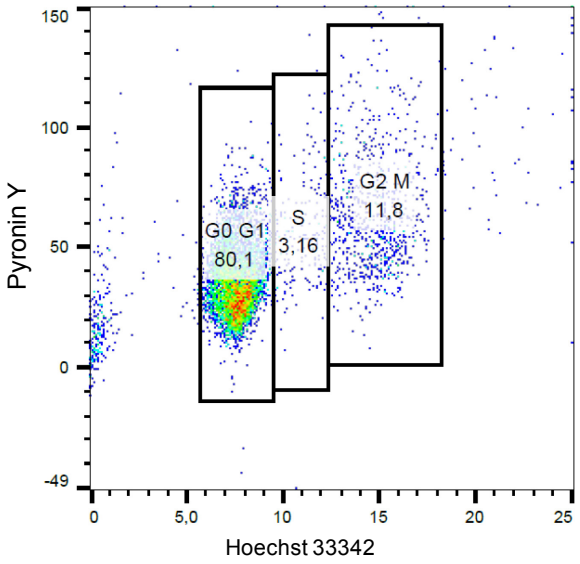

Figure 6. FACS analysis enables the differentiation between cell cycle phases. The data were obtained by using FACS analysis double staining with Hoechst 33342/Pyronin Y. HUVECs were incubated with starvation medium C (0.2% FCS) at 5% CO_2 for 18 h. FACS analysis allows to differentiate cell cycles stages such as G_0/G_1, S, G_2/M. The graph demonstrates that more than 80% of the cells are in G_0/G_1 after cell synchronization.

3.3.3 Immunofluorescence

Solutions and materials:

Falcon™ chambered cell culture slides	
HUVECs	
Paraformaldehyde	4%
Triton X 100	0.25%
1X PBS	X ml
PBS Tween (PBST):	
1X PBS	X ml
Tween 20	0.1%
Blocking-buffer and antibody-dilution buffer:	
Bovine serum albumin (BSA)	4%
Mounting solution	
Axio Observer.Z1 microscope	

Falcon™ chambered cell culture slides were used in this experiment. HUVECs were seeded at 5,000 cells per chamber and were allowed to grow for 48 h after exposure to 24 mM HCO_3^-. Immunofluorescence was used to assess the localization of ADCY10 throughout the cell cycle as well as colocalization with tubulin or PP2A. DAPI was used to stain DNA inside the nucleus.

Primary antibodies

Antibody	**Dilution**	**Dilution buffer**
Anti-ADCY10	1:150	4% BSA
Anti-α Tubulin	1:150	4% BSA
Anti-PP2A	1:100	4% BSA
DAPI	1:20	4% BSA

Secondary antibodies

Antibody	**Dilution**	**Dilution buffer**
Anti-Mouse, TRITC-conjugate	1:250	4% BSA
Anti-Rabbit, FITC-conjugate	1:250	4% BSA

Protocol: Culture medium B (10% FCS, 24 mM HCO_3^-) was removed. Subsequently, pre-warmed 4% paraformaldehyde was directly added to the HUVECs monolayer at 37 °C for 15 min. Then, the fixed cells were washed 3 times for 5 min each with 1X PBS. Afterwards, 0.25% Triton X 100 was added for 15 min at RT for plasma membrane permeabilization. Consecutively, cells were washed 3 times for 10 min each with 1X PBS at RT. Afterwards, cells were incubated with 4% bovine serum albumin (BSA) at 4 °C overnight to block non-specific binding. The fixed cells were then probed with primary antibody at 4 °C overnight under constant shaking, followed by 3 times washing 10 min each with 1X PBST at RT. DAPI was added together with the secondary antibodies and cells were incubated for 1 hour at RT. The samples were then washed 5 times 10 min each with 1X PBST and mounted with mounting solution. Immunoreactivity was visualized with an Axio Observer.Z1 (Carl Zeiss Jena GmbH; Jena, Germany) microscope.

3.3.4 Protein analysis

GSK-3β, CREB, MEK1/2, and ERK1/2 are known ADCY1-9 downstream targets with effects on cell proliferation. To assess whether ADCY10 shares downstream targets with ADCY1-9 (Objective 5), protein content and phosphorylation of these proteins was by Western blot analysis.

3.3.4.1 Preparation of Samples

Lysis buffer:

1X Radioimmunoprecipitation assay (RIPA) buffer	X ml
Phosphatase/protease inhibitors tablets (1 tablet/10 ml)	
Dithiothreitol (DTT)	10 mM
Benzonase®	50 IU/ml
Magnesium chloride ($MgCl_2$)	2 mM

Protocol: Cells were lysed using RIPA buffer with additional phosphatase and protease inhibitors with constant shaking for 5 min at RT. Consecutively, 50 IU/ml Benzonase® and 2 mM $MgCl_2$ were added into the lysate to reduce viscosity and prevent cell clumping. The sample was scraped and the lysate was collected in a 1.5 ml Eppendorf tube. Then, the cell lysates were used for protein assay to evaluate total protein concentration.

3.3.4.2 Protein Assay

Solutions and materials:

Pierce® bicinchoninic acid (BCA) Protein Assay Kit:	X ml
Working solution (BCA reagent A: BCA reagent B)	(50:1)
2 mg/ml Albumin standard	
2X Laemmli buffer	X ml
4X Laemmli buffer	X ml
96 well plate	
ClarioSTAR microplate reader	

Protein content of the lysate was quantified using Pierce® bicinchoninic acid (BCA) protein assay kit. In brief, a set of diluted albumin standards and protein samples were prepared in 0.6 ml Eppendorf tubes as described in Table 2**.**

Table 2. Preparation of diluted albumin (BSA) standards.

Standard No.	2 mg/ml BSA (µl)	ddH_2O (µl)
1	0	25
2	2.5	22.5
3	5	20
4	10	15
5	15	10
6	20	5
	Lysate (µl)	ddH_2O (µl)
Protein sample	10	15

Deionized distilled water (ddH_2O)

Subsequently, the working solution was freshly prepared with a ratio of 50:1 of reagent A: reagent B. Then, 200 µl of working solution was added into albumin standards and protein samples. The reagents were vortexed. All samples and standard tubes were then incubated at 37 °C for 30 min. Afterwards, each tube was vortexed. 200 µl of each tube were taken and pipetted into a 96 well plate. The colorimetric values were detected using a microplate reader at wavelengths of 540-590 nm (Clariostar, BMG Labtech, Ortenberg, Germany). According to the measured protein concentrations, either 4X or 2X Laemmli buffer was added to the primary lysate to standardize a protein amount of 25 µg for Western blotting. Protein samples were denatured for 3 min at 95 °C and used immediately or stored at –20 °C. Analysis continued with gel electrophoresis (Section 3.3.4.3).

3.3.4.3 Sodium dodecyl sulfate - polyacrylamide gel electrophoresis (SDS-PAGE)

Solutions:

Separating gel buffer:
1.5 M Tris/HCl; pH 8.8
Stacking gel buffer:
0.5 M Tris/HCl; pH 6.8
10X Gel running buffer:

Tris	250 mM
Glycine	2.0 M
SDS	10%

Table 3. Composition of SDS-gel.

Components	Separating gels	Stacking gel
	12%	5%
30% Mixed acrylamide	6 ml	0.83 ml
Deionized distilled water	4.9 ml	2.8 ml
Separating gel buffer	3.8 ml	--------
Stacking gel buffer	--------	1.26 ml
10% SDS	0.15 ml	0.05 ml
Tetramethylethylenediamine (TEMED)	0.012 ml	0.010 ml
10% Ammonium persulfate (APS)	0.15 ml	0.05 ml

Protocol: After cleaning the glass plates with water and ethanol, the gel apparatus (Bio-Rad) was assembled. The separating solution was prepared as described in Table 3. Consecutively, the separation solution was poured into the gel apparatus (around 8 cm). Then, it was layered with ddH_2O. The gel was let to polymerize for 45 min at RT. The layer of water was removed and the stacking gel solution was poured on top of the polymerized separating gel. A comb was inserted to form wells for the protein samples. The stacking gel was let to polymerize for 30 min at RT. After removing the comb, 1X running gel buffer was added to the chamber and the wells were washed using a syringe. Protein samples were loaded into the wells. The gel was run at a constant voltage of 60 volts for the first 30 min. Then, the voltage was changed to 120 volts until bromophenol blue had passed through the gel.

3.3.4.4 Western blotting

Proteins separated by SDS-PAGE were transferred onto a nitrocellulose membrane by semi-dry blotting. Afterwards, proteins of interest were immunodetected using specific antibodies.

Solutions and materials:

Nitrocellulose membrane
Thin filter paper
Blotting chamber
Transfer buffer:

Tris-HCl pH 7.6	25 mM
Glycine	192 mM
Methanol	20%

Protocol: Six sheets of filter paper and nitrocellulose membrane were cut to the size of the gel dimensions. Then, they were submerged in transfer buffer for at least 15 min to ensure proper binding. The blotter was prepared in the following way: First, the platinum anode was wetted with transfer buffer. Consequently, the first thin filter paper was placed at the center of the

platinum plate. Air bubbles were excluded out by rolling the roller on top of the filter paper in one direction. The same procedure was repeated with another two sheets of soaked filter paper. The nitrocellulose membrane was placed on top of the filter sheets. Thereafter, the transfer buffer was poured on top of the nitrocellulose transfer membrane. Air bubbles were avoided. The SDS-gel was placed on top of the nitrocellulose membrane. Excess transfer solution and air bubbles were removed by using a roller. Consecutively, the other three wetted filter papers were laid on top of the gel one after the other as described above. The stainless steel cathode lid was used to assemble the apparatus and screws were tightened to ensure protein transfer. Transfer was achieved by applying 1.5 mA/cm^2 current for 1.5 h at RT.

3.3.4.5 Staining of transferred proteins

Solutions:

Ponceau-S solution:	
Ponceau-S	0.10%
Acetic acid	5%
ddH_2O	
10X Tris-buffered saline + 0.1% Tween (TBST):	
Tris/HCl (pH 7.4)	100 mM
Sodium chloride (NaCl)	1.6 M
Tween	0.1%

To estimate the efficiency of the protein transfer (Section 3.3.4.4), the membrane was stained with Ponceau-S solution, a reversible stain that produces pink bands on a light background. Prior to the staining, the nitrocellulose membrane was washed with ddH_2O for 5 min, incubated in Ponceau-S solution for 5 s at room temperature. Subsequently, the membrane was destained by washing in ddH_2O until protein bands became apparent. This allowed the verification of complete and correct protein transfer. The membrane was washed with TBST under constant shaking until the Ponceau-S stain was completely removed. In order to identify individual protein bands, the membrane was proceeded to immunoblotting using specific antibodies (Section 3.3.4.6).

3.3.4.6 Immunodetection of proteins

To identify an individual protein band, the protein of interest was detected using a specific primary antibody. Then, the primary antibody was labeled using a secondary antibody.

Solutions and materials:

10X Tris-buffered saline (TBS):	
Tris/HCl (pH 7.4)	100 mM
Sodium chloride (NaCl)	1.6 M
10X TBST:	
Tris/HCl (pH 7.4)	100 mM
Sodium chloride (NaCl)	1.6 M
Tween	0.10%
Bovine serum albumin (BSA) in 1XPBST	4%
Shaker	
Fusion® FX7 chemiluminescence system	
Enhanced chemiluminescence (ECL) reagent	

Primary antibodies

Antibody	**Dilution**	**Dilution buffer**
Anti-MEK1/2~p	1:1000	4% BSA
Anti-ERK1/2~p	1:1000	4% BSA
Anti-CREB~p	1:2000	4% BSA
Anti-GSK-3β	1:1000	4% BSA
Anti-PP2A	1:1000	4% BSA
Anti-cyclin B1	1:1000	4% BSA
Anti-WEE1	1:1000	4% BSA
Anti-vinculin	1:1000	4% BSA
Anti-GAPDH	1:10000	4% BSA

Secondary antibodies, horseradish peroxidase (HRP)-labeled:

Antibody	**Dilution**	**Dilution buffer**
Anti-Mouse IgG	1:5000	4% BSA
Anti-Rabbit IgG	1:5000	4% BSA

Protocol: After a brief washing in ddH_2O and TBST, the membrane was blocked in 4% BSA at 4ºC overnight. After blocking, the membrane was incubated with a primary antibody at 4ºC overnight. This was followed by three washings with TBST each time for 10 min at RT. Then,

the membrane was incubated with a HRP conjugated secondary antibody for 1 hour at RT. Afterwards, the membrane was washed three times with TBST each time for 10 min at RT. ECL was added as a substrate of HRP to develop the protein bands on the membrane. Fusion® FX7 (Peqlab Biotechnologie GbmH, Erlangen, Germany) system was used for detection of fluorescent signals. Loading of equal amounts of protein was controlled by detection of glyceraldehyde-3-phosphate dehydrogenase (GAPDH) or vinculin. The intensity of protein bands were analyzed using Bioprofil Bio1D (version 15.06a) (Vilber Lourmat Sté, Collégien, France). This resulted in a semi-quantitative estimate of protein amount.

3.3.4.7 Stripping and reprobing the membrane

Solutions:

Restore™ Plus Western Blot Stripping Buffer	X ml
1X TBST	X ml

To reprobe a membrane with antibody against another protein of a similar size, bound antibodies were removed by incubating the membrane with pre-warmed (37 °C) stripping buffer. The stripping buffer was poured onto the membrane. Then, the membrane was incubated for 10 min at RT under constant shaking. Subsequently, the membrane was washed with TBST buffer, blocked and reprobed (Section 3.3.4.6) with appropriate antibodies.

3.3.5 PP2A activity assay

PP2A phosphatase activity measurements were done by following a protocol provided by RediPlate™ 96 EnzChek® Serine/Threonine Phosphatase Assay Kit (R-33700) from Thermo Fisher Scientific (Waltham, Massachusetts, USA).

Solutions and materials:

RediPlate 96 EnzChek serine/threonine phosphatase assay microplate	
1X reaction buffer for RediPlate serine/threonine phosphatase:	
Tris-HCl (pH 7.0)	X ml
Calcium chloride ($CaCl_2$)	0.2 mM
BSA	250 µg/mL
Tween 20	0.10%
40 mM $NiCl_2$	1 mM
ClarioSTAR microplate reader	

Protocol: According to Warfel and D'Agnillo, protein samples were lysed in RIPA buffer containing protease inhibitors. Protein contents in lysates were determined using protein assay protocol (3.3.4.2). For PP2A activity assay, samples with an amount of 4 µg protein were

prepared from lysates (Warfel and D'Agnillo, 2009). The kit components were warmed for 20 min at RT. The RediPlate 96 EnzChek microplates came pre-coated with a fluorescence standard according to Table 4. Further, all wells of a plate were pre-coated with the phosphatase substrate 6, 8-difluoro-4-methylumbelliferyl phosphate (DiFMUP). PP2A dephosphoralyses DiFMUP into DiFMU, which could be detected by the plate reader.

Table 4. Reference standards for the RediPlate 96 Serine/Threonine phosphatase assay kit.

Well	Amount of DiFMU
A	5000 pmol
B	3000 pmol
C	1500 pmol
D	500 pmol
E	100 pmol
F	50 pmol
G	10 pmol
H	0 pmol

Consecutively, 100 µl 1X reaction buffer were pipetted into the standard wells whereas 50 µl were pipetted into sample and negative control wells. The coated phosphatase substrate was solubilized by repetitive pipetting with 1X reaction buffer during the addition. Subsequently, 50 µl of sample solutions containing 4 µg of protein were added into sample wells. While extra 50 µl 1X reaction buffer was added into negative control wells. A multichannel pipette was used to mix the solutions inside the wells. Then, the microplate was incubated for 30 min in a darkplace at RT. The CalrioSTAR microplate reader was used to measure fluorescence at 358 nm excitation and 452 nm emission. Phosphatase activity was calculated based on the values of the standard wells and negative controls.

3.3.6 Data analysis

Data were summarized as mean ± SEM of 3-5 experiments using independent cell preparations. Significance among groups was determined using one-way analysis of variance ANOVA followed with Student-Newman-Kuel test (GraphPad Inplot, ISI software, or PRISM). Changes in parameters within the same group were assessed by multiple ANOVA analysis or paired T-test. Probability values (p-values) of less than 0.05 were considered significant ($p < 0.05$).

4. Results

4.1 Colocalization and translocation of ADCY10 and α-Tubulin during the cell cycle of HUVECs.

To analyze the localization of ADCY10 and the mitotic spindle apparatus during cell cycle, HUVECs were cultured in normal culture medium in presence of the physiological concentration of 24 mM HCO_3^-, balanced by 5 % (vol/vol) CO_2 in humidified atmosphere for 48 h. Afterwards, ADCY10 and α-Tubulin, as mitotic spindle marker, were detected by indirect immunofluorescence microscopy as described in Section 3.3.3. DNA was stained by DAPI.

During interphase, ADCY10 was found to be localized within the nucleus in a speckle -like pattern and distributed diffusely in the cytoplasmic compartment (Figure 7). In contrast to ADCY10, α-Tubulin was scattered throughout the cytoplasm and showed only a low signal in the nucleus. During the mitotic phase (prophase, metaphase, anaphase, telophase, and cytokinesis), cell size became smaller, most probable due to chromosome condensation. In the prophase, ADCY10 was found to be colocalized with α-Tubulin at the centrosomes. Additionally, ADCY10 was dispersed throughout the whole cell. During metaphase and anaphase, ADCY10 and α-Tubulin were found to be colocalized along the mitotic spindles. Interestingly, ADCY10 and α-Tubulin showed high fluorescence signals at the contractile ring, the side of cell separation during cytokinesis. In summary, as shown by immunofluorescence microscopy, ADCY10 is translocated to the developing spindle apparatus during mitotic phase, suggesting an essential role of ADCY10 in cell division.

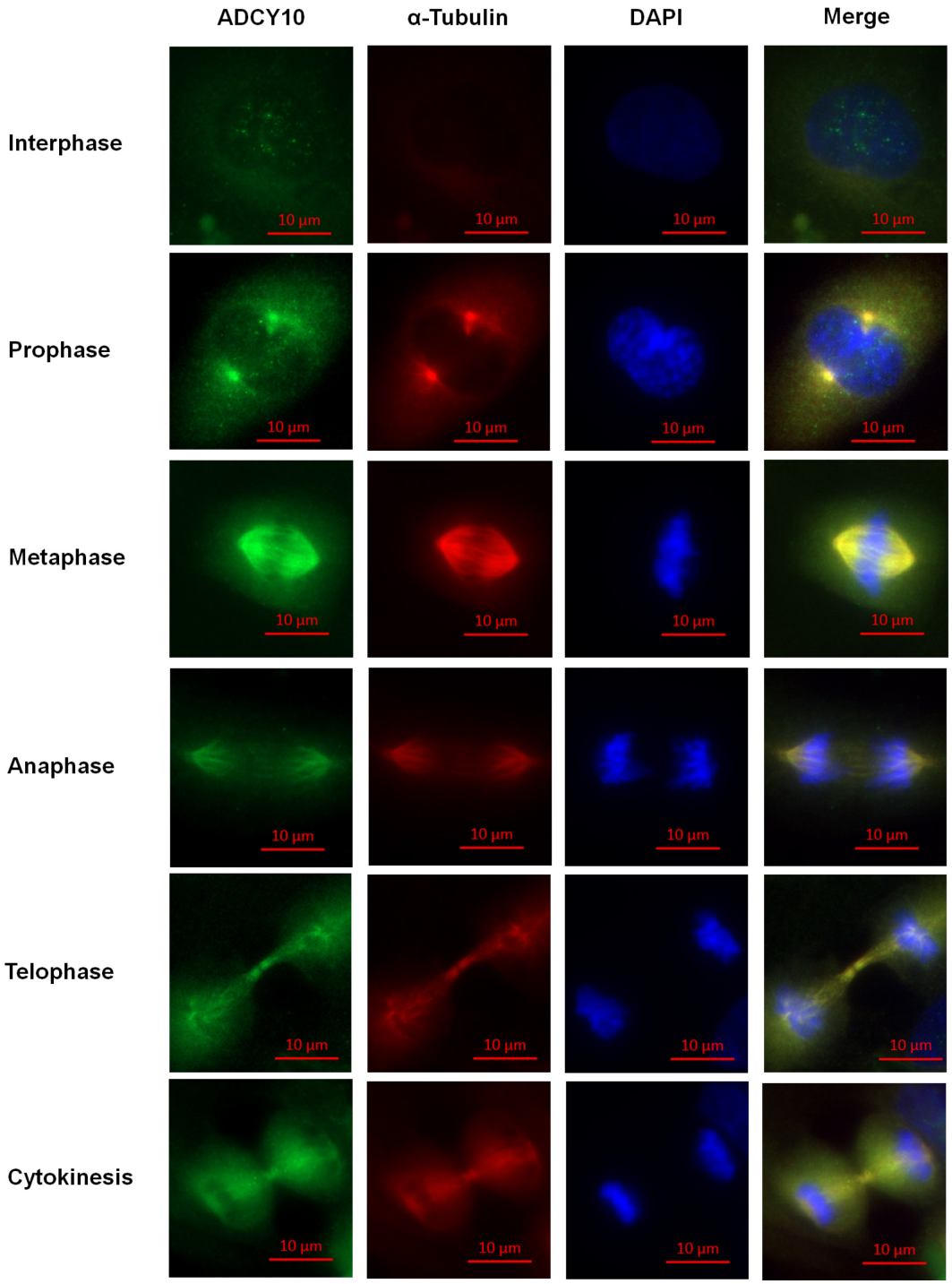

Figure 7. Translocation of ADCY10 during cell division. HUVECs were incubated in culture medium buffered by 25 mM HEPES at pH 7.4 containing 24 mM HCO_3^- balanced by 5 % (vol/vol) CO_2 in humidified atmosphere. Afterwards, cells were fixed with 4% paraformaldehyde. ADCY10 was detected by a combination of anti-ADCY10-antibody corresponding FITC-conjugated anti-rabbit-antibody (green). α-Tubulin was detected by a combination of anti-α-Tubulin-antibody corresponding TRITC-conjugated anti-mouse-antibody (red). DNA was stained using DAPI (blue). The merge of these channels show that ADCY10 and α-Tubulin are colocalized during mitosis, but not during interphase.

4.2 ADCY10 induces cell proliferation by modulating cell cycle progression of HUVECs

To test whether HCO_3^- promotes cell proliferation via the activation of ADCY10, HUVECs were incubated with different concentrations of HCO_3^- and cell number was measured at different time points. Cells were synchronized in G_0/G_1 by serum withdrawal (Section 3.1.2.1). Subsequently, the cells were exposed to 0, 24, and 40 mM HCO_3^-, where 24 mM HCO_3^- is equivalent to 5% CO_2 representing the physiological control. The pharmacological inhibitor KH7 was used to block ADCY10 activity.

4.2.1 HCO_3^- promotes cell proliferation of HUVECs

Cells were collected every 12 h for 72 h. Thereafter, cell number and cell cycle stages were determined by flow cytometry analysis (Figure 8 and 9). Within each group, the cell number was normalized to the cell number at 12 h. Here cell number is presented as a percentage. The results showed that 24 mM HCO_3^- induced an exponentially shaped increase of cell number. However, at 0 mM HCO_3^- the increase in cell number is greatly reduced. At 72 h, the group exposed to 0 mM HCO_3^- showed approximately a three-folds decrease in cell number compared to control. Interestingly, there was no further increase of cell number when cells were exposed to 40 mM HCO_3^- compared to control (Figure 8A). Therefore, it can be concluded that HUVECs have approximately 24 h doubling time under physiological conditions (Figure 8A). However, deficiency of HCO_3^- in HUVECs caused a prolongation of doubling time to approximately 48 h.

The same sets of cells also processed to analyze whether HCO_3^- regulates cell cycle control. In line with that, cell cycle stages were assessed using flow cytometry (Section 3.3.2). As shown in Figure 9, cell cycle progression from G_1 to S and G_2 to M phase is delayed at 0 mM compared to 24 mM HCO_3^-. The most prominent differences of cell cycle phases between groups were observed at 24 h after cell synchronization. Data from measurements at later time points, suggested that cells accumulated in S and G_2/M phases. On the contrary, 40 mM HCO_3^- neither caused a delay of cell cycle progression nor accumulation of cells in G_2/M phases compared to 24 mM HCO_3^- (Figure 9). Thus, these findings indicate that HCO_3^-, at physiological concentration level, stimulates cell proliferation by triggering cell cycle progression in human endothelial cells.

4.2.2 Pharmacological inhibition of ADCY10 reduces cell proliferation of HUVECs

To prove whether HCO_3^- promotes cell proliferation via the activation of ADCY10, KH7, an established pharmacological inhibitor for ADCY10, was applied. Optimum concentration for ADCY10 inhibition was determined in a series of pilot experiments. Therefore, 10 µM KH7 was used to inhibit ADCY10 in all further experiments. As depicted in Figure 8B, 10 µM KH7 repressed the increase in cell number in the presence of 24 mM HCO_3^-. Furthermore, the data suggested that the proliferation of HUVECs was decreased due to a delay of cell cycle progression (Figure 10). Delayed cell cycle progression became apparent by an accumulation of cells in G_2/M phases compared to control (Figure 10C). Regarding cell proliferation and cell cycle phases, 0 mM HCO_3^- and 10 µM KH7 showed similar results. Furthermore, these results suggested that 10 µM KH7 had a stronger effect on blocking cell proliferation at 48 and 72 h than 0 mM HCO_3^-, this was observed both when the data were compared directly, as well as when the different inhibitors (0 mM HCO_3^- and 10 µM KH7) were compared to their individual control groups (Figure 8C).

In conclusion, these results suggest that HCO_3^- stimulates cell proliferation and triggers cell cycle progression in human endothelial cells via modulating the activity of ADCY10.

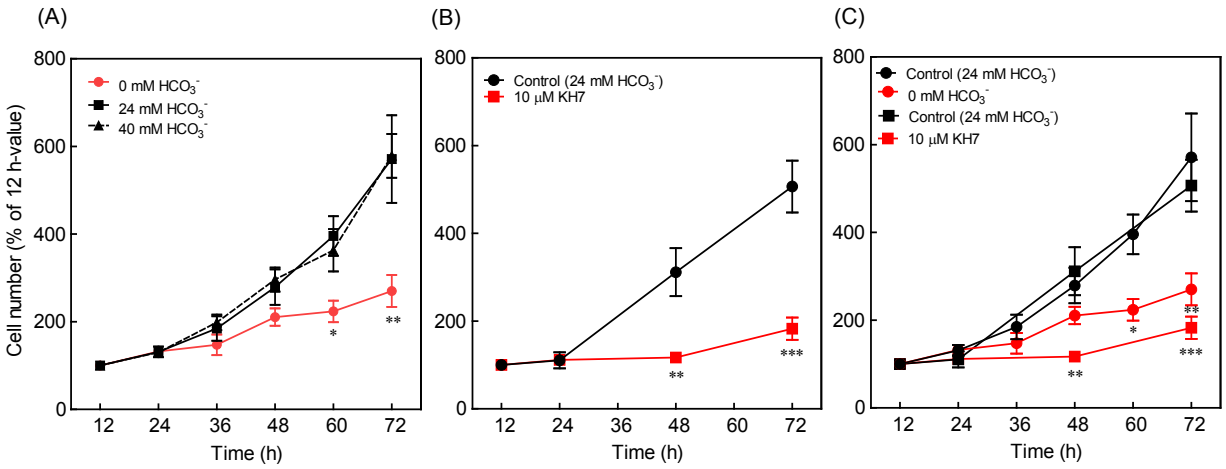

Figure 8. Inhibition of ADCY10 activity suppresses cell proliferation. The data were obtained by using FACS analysis of double stained cells with Hoechst 33342 and Pyronin Y. HUVECs were incubated in culture medium buffered by 50 mM HEPES at pH 7.4 **(A)** containing 0 mM, 24 mM or 40 mM HCO_3^- balanced by 0, 5 or 8% (vol/vol) CO_2 in humidified atmosphere. Cells were collected every 12 h for 72 h. **(B)** containing 24 mM HCO_3^- and 10 µM KH7, a specific ADCY10 inhibitor, for 72 h. **(C)** comparison of cell number from (A) and (B). Cells were collected at 12, 24, 48, and 72 h. Data are mean ± SEM from 5-7 independent preparations of cells from different umbilical cords. * p-value < 0.05, ** p-value < 0.01, *** p-value < 0.001 using one-way ANOVA.

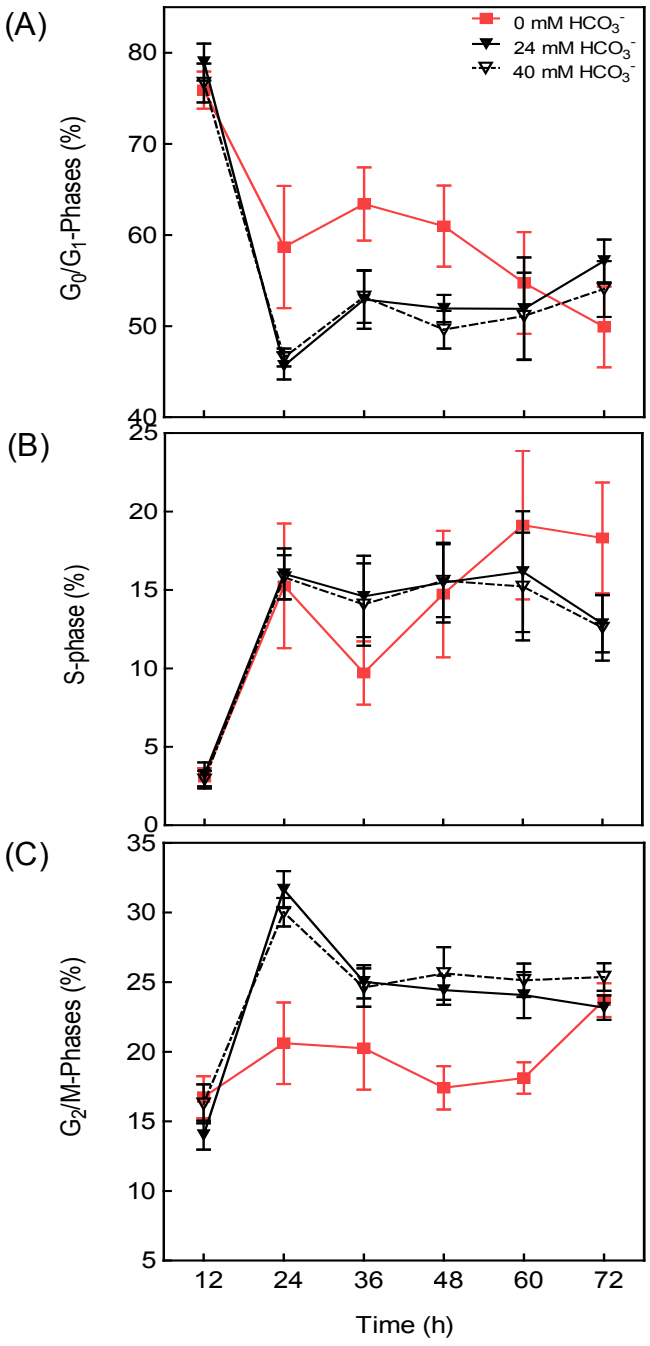

Figure 9. Inhibition of ADCY10 activity using 0 mM HCO_3^- delays cell cycle progression. The data were obtained by using FACS analysis after double staining of HUVECs with Hoechst 33342 and Pyronin Y. Cells were incubated in culture medium buffered by 50 mM HEPES at pH 7.4 containing 0 mM, 24 mM or 40 mM HCO_3^- balanced by 0, 5 or 8% (vol/vol) CO_2 in humidified atmosphere. The percentage of cells in **(A)** G_0/G_1 phases, **(B)** S phase and **(C)** G_2/M phases are depicted. Data are mean ± SEM from 5-7 independent preparations of cells from different umbilical cords. The presented data are derived from the same measurements as in Figure 8A using further analytical methods to estimate cell populations in different cell cycle stages.

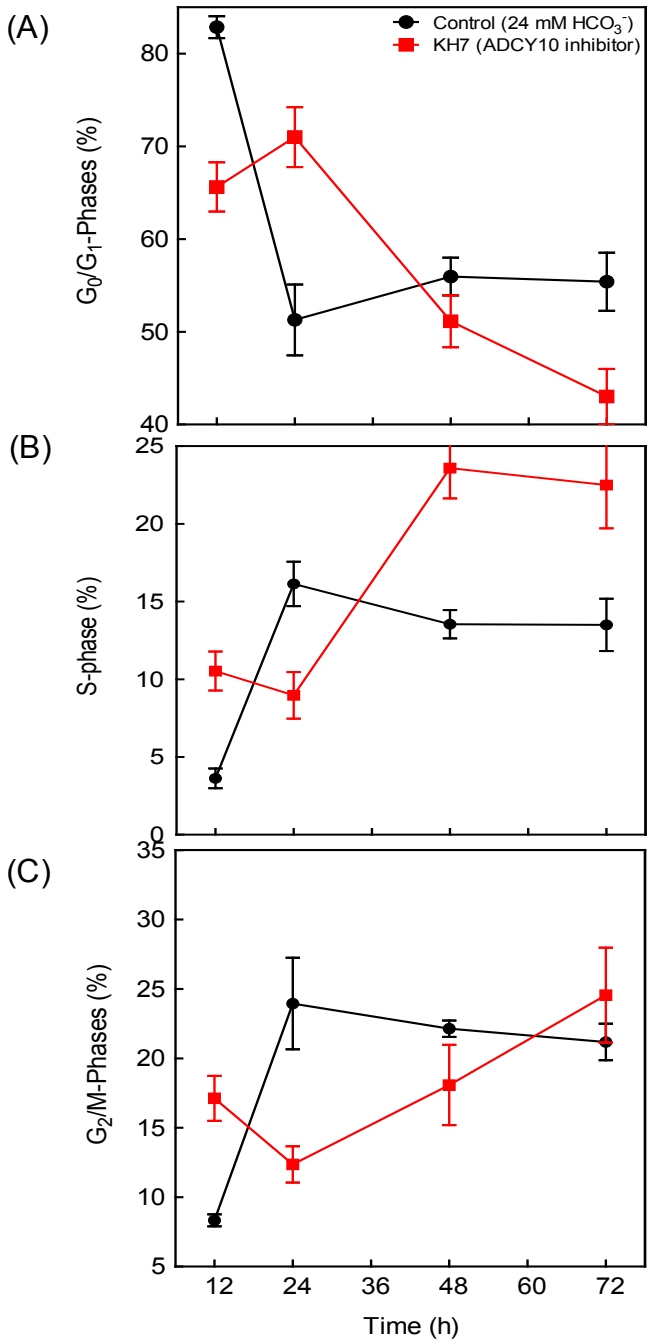

Figure 10. Inhibition of ADCY10 activity using KH7 delays cell cycle control of HUVECs. The data were obtained by using FACS analysis after double staining of HUVECs with Hoechst 33342 and Pyronin Y. Cells were incubated in culture medium buffered by 25 mM HEPES at pH 7.4 containing 24 mM HCO_3^- balanced by 5 % (vol/vol) CO_2 in humidified atmosphere. In a set of experiments the medium contained 10 µM KH7, an inhibitor of ADCY10. The percentage of cells in **(A)** G_0/G_1 phases, **(B)** S phase and **(C)** G_2/M phases are depicted. Data are mean ± SEM from 5-7 independent preparations of cells from different umbilical cords. The present data are derived from the same measurements as in Figure 8B using further analytical methods to estimate cell populations in different cell cycle stages.

4.2.3 ADCY10 controls cyclin B1 content.

As mentioned previously, the data obtained by flow cytometry suggested that inhibition of ADCY10 delays cell cycle progression, causes cell accumulation in G_2/M phases (Figure 10C), leading consecutively to a suppression of cell proliferation. However, flow cytometry fails to differentiate between cells arrest in G_2 or M phase, because the DNA content of cells in both phases are equal. To investigate whether the majority of cell accumulation in G_2/M phases (Figure 9C and 10C) was arrested in either G_2 or M phase, Western blot analysis was used to determine the cyclin B1 protein levels, as a mitotic phase marker. The experiments were performed by using the same cell proliferation assay as in Section 4.2. Okadaic acid (OA), a specific inhibitor of the protein phosphatase 2A (PP2A) was used at optimum concentration to completely block PP2A in endothelial cells (Knapp et al., 1999) as a positive control, since it can induce cell retention in G_2 stage (Gong et al., 2015). Samples from each group were collected at 48 h, since OA treated cells did not survive until 72 h. As shown in Figure 11, the presence of 10 µM KH7 or 5 nM OA as well as absence of HCO_3^- in the medium reduces the cyclin B content by 50 % compared to control in HUVECs. This indicates that the majority of arrested cells in G_2/M phases after ADCY10 inhibition were in G_2 phase supporting the concept that inhibition of ADCY10 obviously blocks the transition of endothelial cells from G_2 to M phase. This raises the question by which mechanism ADCY10 can accomplish a G_2 to M phase transition.

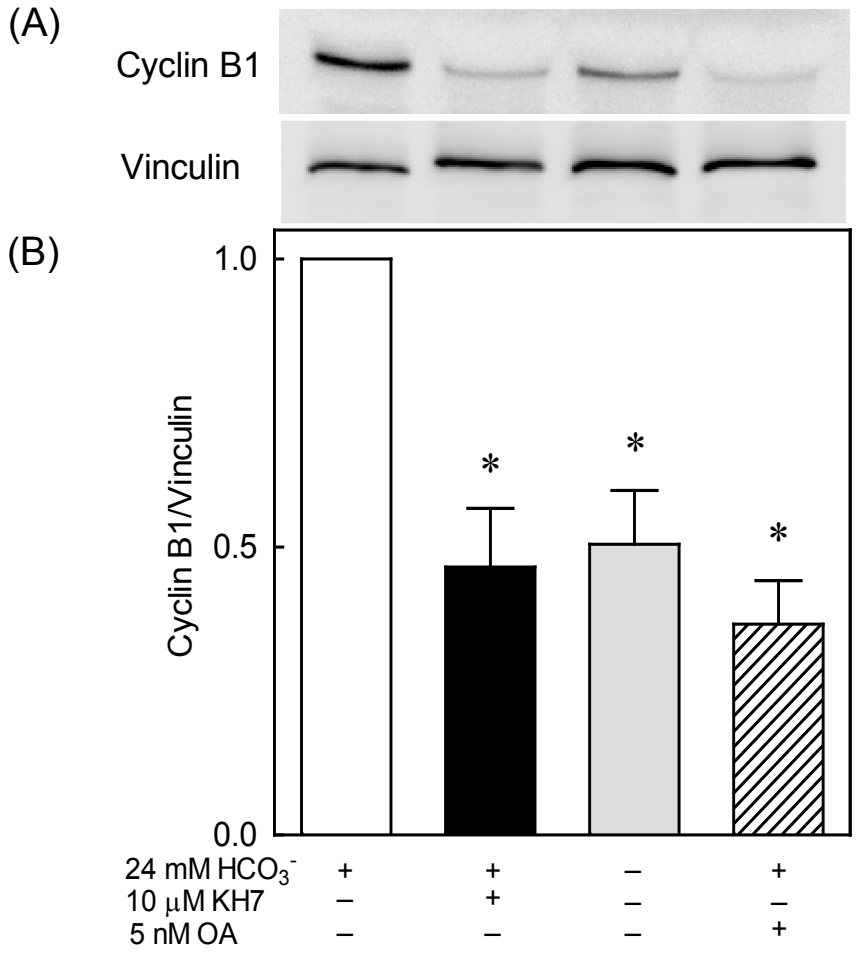

Figure 11. ADCY10 is necessary for cyclin B1 accumulation in HUVECs. Cells were incubated in culture medium buffered by 50 mM HEPES at pH 7.4 containing 24 mM HCO_3^- balanced by 5 % (vol/vol) CO_2 in humidified atmosphere for 48 h. In a set of experiments, the medium contained 10 µM KH7, an inhibitor of ADCY10 or 5 nM OA, an inhibitor of PP2A. In another set the medium did not contained HCO_3^-. **(A)** Representative Western blot of cyclin B1 and vinculin used as loading control. **(B)** Densitometries of cyclin B1 relative to vinculin. Data are mean ratio ± SEM from 4 independent preparations of cells from different umbilical cords. * p-value < 0.05 compared to control.

4.3 Epac and PKA control cell proliferation and cell cycle regulation

The objective of this study was to determine which effector proteins of ADCY10 play a dominant role for regulating cell proliferation and cell cycle control. There are four effector proteins identified as cAMP effector proteins, which are Epac, PKA, CNGs as well as HCNs, and PDEs (Yang et al., 2006; Cheng et al., 2008; Sassone-Corsi, 2012). However, this thesis only focused on the effect of ADCY10 via Epac and PKA on cell proliferation and cell cycle control.

4.3.1 Epac modulates cell proliferation

To identify whether ADCY10 may control cell proliferation via Epac, a specific Epac inhibitor (ESI-09) was applied. The experimental procedure followed the same protocols for cell synchronization and consecutively cell proliferation assay as described in Sections 3.1.2.1 and 3.3.1. In this set of experiments the assays were terminated after 48 hours because cells did not survive any longer in presence of ESI-09.

As shown in Figure 12, ESI-09 decreased the cell number at 24 and 48 h compared to control. The control group showed approximately doubling time of 24 h whereas, inhibition of Epac resulted in a doubling time of approximately 128 h. In contrast to control, the cell fractions in G_0/G_1-phases did not drop (Figure 13A), while the cell fractions in G_2/M phases did not increase (Figure 13 C) and both remained almost constant at their control levels throughout the whole period of observation, respectively. This is consistent with the increase in doubling time and can be interpreted that ESI-09 caused cell cycle arrest mainly in G_0/G_1. Consequently, fewer amounts of cells transited to S and G_2/M phases.

In conclusion, inhibition of Epac was associated with suppressed cell proliferation. However, an arrest of cell cycle after Epac inhibition was observed in G_0/G_1 phases rather than S or G_2/M phases as it was present after ADCY10 inhibition. Thus, Epac inhibition causes a different cell cycle arrest compared to ADCY10 inhibition. Hence, Epac might not qualify as a major downstream target of ADCY10 for cell proliferation and cell cycle regulation.

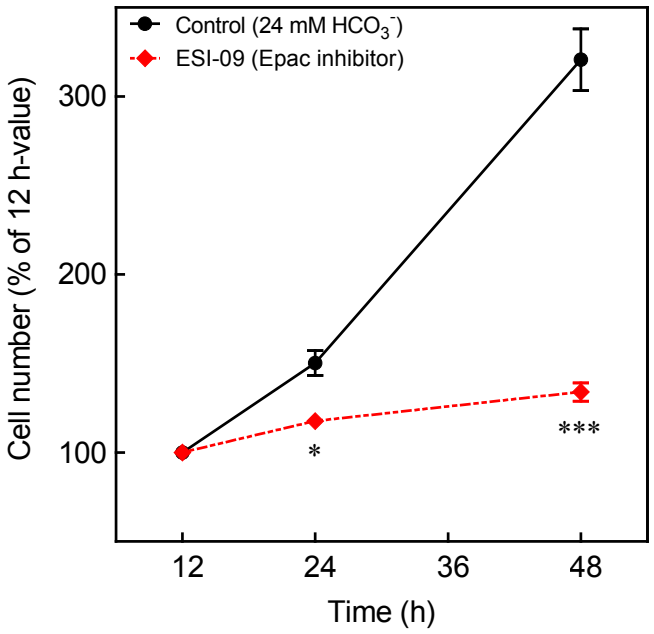

Figure 12. Inhibition of Epac represses cell proliferation. The data were obtained using FACS analysis of double stained cells with Hoechst 33342 and Pyronin Y. HUVECs were incubated in culture medium buffered by 25 mM HEPES at pH 7.4 containing 24 mM HCO_3^- balanced by 5 % (vol/vol) CO_2 in humidified atmosphere. In a set of experiments, the medium contained 25 µM ESI-09, an Epac inhibitor. Cells were collected at 12, 24, and 48 h. The cell number was normalized to the 12 h time point of each group. Data are mean ± SEM from 3 independent preparations of cells from different umbilical cords. * p-value < 0.05, *** p-value < 0.001 using one-way ANOVA.

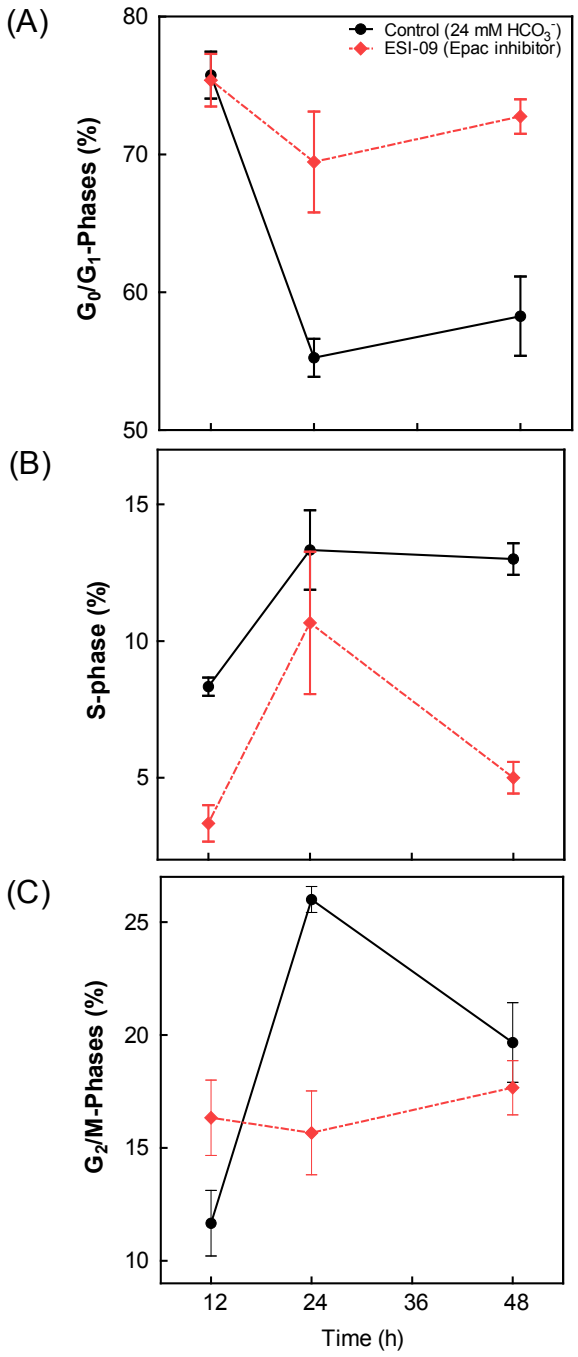

Figure 13. Inhibition of Epac restricts cells in G_0/G_1. The data were obtained by using FACS analysis of double stained cells with Hoechst 33342 and Pyronin Y. Cells were incubated in culture medium buffered by 25 mM HEPES at pH 7.4 containing 24 mM HCO_3^- balanced by 5 % (vol/vol) CO_2 in humidified atmosphere. In a set of experiments, the medium contained 25 µM ESI-09, an Epac inhibitor. Cells were collected at 12, 24, and 48 h. The percentage of cells in **(A)** G_0/G_1 phases, **(B)** S phase and **(C)** G_2/M phases are depicted. Data are mean ± SEM from 3 independent preparations of cells from different umbilical cords. The present data are derived from the same measurements as in Figure 12 using further analytical methods to estimate cell populations in different cell cycle stages.

4.3.2 PKA controls cell proliferation

Since Epac has to be excluded as downstream target triggering G_2/M-phases arrest, the hypothesis was tested whether PKA is the effector of cAMP derived from ADCY10 in this process. If this were the case, inhibition of PKA in HCO_3^--supplemented endothelial cells should reduce cell proliferation due to cell cycle arrest in G_2/M phases. To elucidate this question, experiments were conducted by using an adapted version of cell proliferation protocol as described in Section 3.3.1. In these experiments, two pharmacological PKA inhibitors of different chemical structures, the PKA inhibitor peptide PKI and the chemical inhibitor H-89, were applied. Since both inhibitors may have distinct different modes of action (Murray, 2008), both were tested in two independent sets of experiments to confirm a consistent effect of PKA on cell proliferation.

In both sets of experiments, HUVECs were incubated under control conditions in presence of 24 mM HCO_3^- balanced by 5 % (vol/vol) CO_2 at pH 7.4. Treated cells in both sets also obtained the ADCY10 inhibitor KH7 (10 µM), the Epac inhibitor ESI-09 (25 µM), the PKA inhibitor peptide PKI (10 µM) or the chemical PKA inhibitor H-89 (10 µM). After 48 h cells were collected for FACS analysis. The data were used to determine total cell number and accumulation of cells in G_2/M phases. As shown in Figure 14A, PKI caused an increase of cell number by 40 % compared to 24 mM HCO_3^-, whereas H-89 suppressed cell number by around 35% compared to HCO_3^--control (Figure 15A). Furthermore, both pharmacological and chemical different PKA inhibitors did not cause accumulation in G_2/M-phases in HUVECs (Figure 14B, 15B). In contrast, the KH7-treated group showed consistent accumulation of cells in G_2/M phases (Figures 14B, 15B) and ESI-09 caused similar effect as previously recorded (Figure 12).

In summary, although PKA unequivocally plays an important role in cell proliferation, its inhibition did not lead to cell accumulation in G_2/M-phase, indicating that ADCY10 and PKA may not share a common pathway in cell proliferation and cycle control. On the other hand, it was shown that deficiency of PKA plays a role in either activation or inhibition of cell proliferation. This effect might be associated with broadened roles of PKA in different pathways. Later on throughout this thesis, H-89 was used as the only PKA inhibitor.

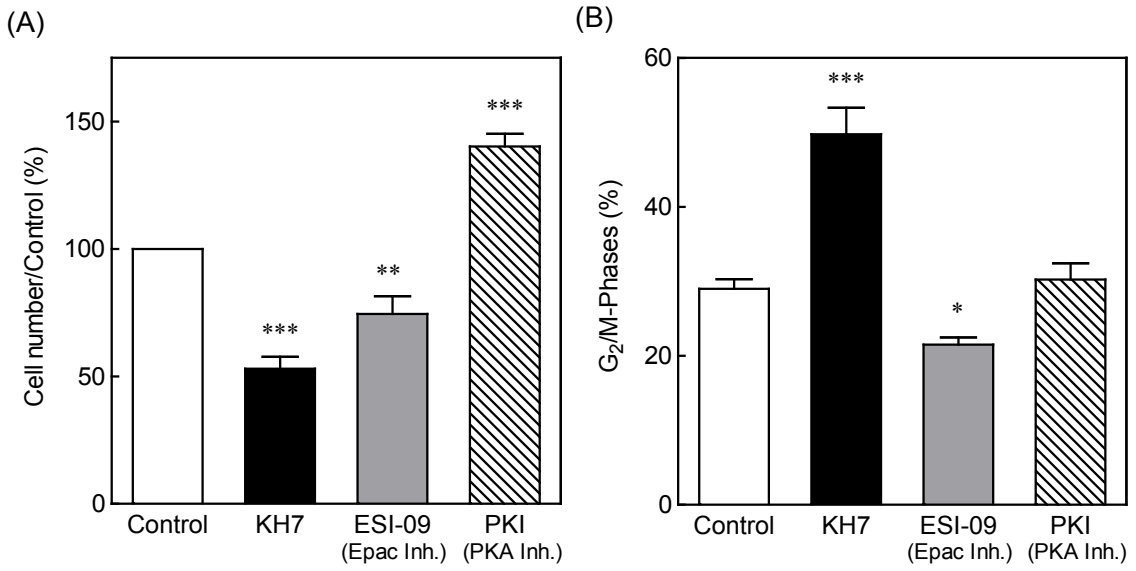

Figure 14. Inhibition of PKA using PKI induced cell proliferation. The data were obtained by using FACS analysis of double stained HUVECs with Hoechst 33342 and Pyronin Y. Cells were incubated in culture medium buffered by 25 mM HEPES at pH 7.4 containing 24 mM HCO_3^- balanced by 5 % (vol/vol) CO_2 in humidified atmosphere. In a set of experiments, the medium also contained the ADCY10 inhibitor KH7 (10 µM), the Epac inhibitor ESI-09 (25 µM) or the PKA inhibitor peptide PKI (10 µM). Cells were collected at 48 h. **(A)** Percentage of cell number normalized to control. **(B)** Percentage of cells in G_2/M-phases. Data are mean ± SEM from 4 independent preparations of cells from different umbilical cords. * p-value < 0.05, ** p-value < 0.01, *** p-value < 0.001 compared to control, using one-way ANOVA.

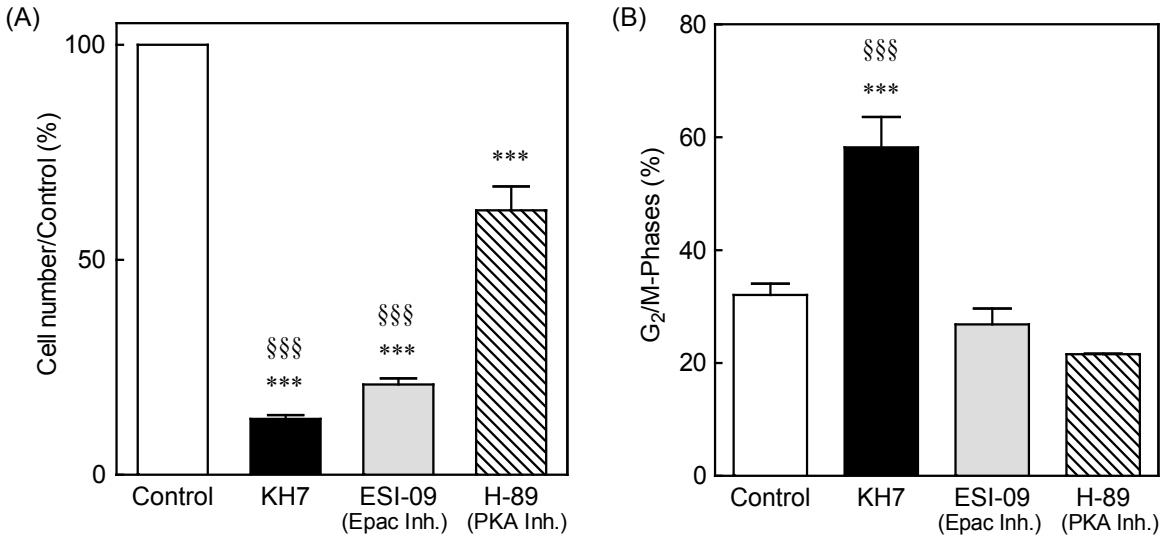

Figure 15. Inhibition of PKA using H-89 represses cell proliferation. The data were obtained by using FACS analysis of double stained HUVEC with Hoechst 33342 and Pyronin Y. Cells were incubated in culture medium buffered by 25 mM HEPES at pH 7.4 containing 24 mM HCO_3^- balanced by 5 % (vol/vol) CO_2 in humidified atmosphere. In a set of experiments, the medium also contained the ADCY10 inhibitor KH7 (10 µM), the Epac inhibitor ESI-09 (25 µM) or the chemical PKA inhibitor peptide H-89 (10 µM). Cells were collected at 48 h. **(A)** Percentage of cell number normalized to control. **(B)** Percentage of cells in G_2/M-phases. Data are mean ± SEM from 4 independent preparations of cells from different umbilical cords. *** p-value < 0.001 compared to control. §§§ p-value < 0.001 compared to H-89-treated group, using one-way ANOVA.

4.3.3 Interaction of Epac and PKA modulates cell proliferation and cell cycle control

As shown so far, inhibition of Epac or PKA may affect cell proliferation. Regarding Epac, inhibition of this signaling element downstream of cAMP induced cells retention in G_0/G_1 phases and increased doubling time. However, inhibition of PKA let to contradictory effects. It could be suspected that both proteins are essential for the orchestration of cell proliferation and cell cycle control. However, the results of the present study apparently did not share similarities with the obtained results when ADCY10 was inhibited. Therefore, it was hypothesized that ADCY10 may modulate both Epac and PKA simultaneously to regulate cell cycle progression. For these reasons, an activator-driven experimental approach was chosen to validate the impact of Epac and PKA on cell cycle progression under ADCY10 inhibition. In other words, it was assumed that under the inhibition of ADCY10 either Epac or PKA could unblock the arrested cells from G_2 and induces cell proliferation. Therefore, specific cAMP analogs were used for Epac and PKA activation.

In these sets of experiments, HUVECs were incubated under the same control conditions as in Section 4.3.2. Treated cells also obtained the ADCY10 inhibitor KH7 (10 µM), KH7 plus the Epac activator 8-pcpt-2'-o-me-cAMP (0.1 mM, 8-pcpt-cAMP), or KH7 plus the PKA activator 6-BNZ-cAMP (0.1 mM cAMP analog for PKA). The cells were synchronized prior to the experiment as described in Section 3.1.2.1. The cells were collected after 48 h and analyzed for cell number and cell cycle phases by FACS analysis. The cell number was normalized to the control.

4.3.3.1 Effect of Epac and PKA on cell proliferation under ADCY10 inhibition

As shown in Figure 16, KH7 alone consistently suppressed cell proliferation compared to control group. This is in accordance with data shown before (Figure 8). Copresence of the PKA agonist 6-BNZ-cAMP plus KH7 partly increased cell proliferation compared to KH7 alone, whereas the copresence of Epac agonist 8-pcpt-cAMP plus KH7 had no effect on cell number compared to KH7 alone (Figure 16).

4.3.3.2 Effect of Epac and PKA on cell cycle control under ADCY10 inhibition

The detailed analysis of the cell cycle phases confirmed that KH7 decreased cell population in G_0/G_1 phases and increased cell population in G_2/M phases compared to control (Figure 17). The PKA agonist 6-BNZ-cAMP increased cell population in G_0/G_1 phases while it reduced cell accumulation in G_2/M-phases compared to KH7 alone (Figure 17). Regarding the S phase, there was no significant difference among groups compared to KH7 alone (Figure 17B).

Conversely, compared to the cells treated with KH7 alone, the combination of the Epac agonist 8-pcpt-cAMP with KH7 caused no difference in the cell population in any of the cell cycle phases (Figure 17).

The present data show that the PKA agonist 6-BNZ-cAMP, but not the Epac one, is able to overcome the G_2/M-phase arrest in presence of KH7. This effect is in accordance with the observed increase of cell population in G_0/G_1 phases. On the other hand, these data support the concept that ADCY10 may trigger cell cycle progression via stimulation of G_2 to M-phase transition in PKA-dependent manner.

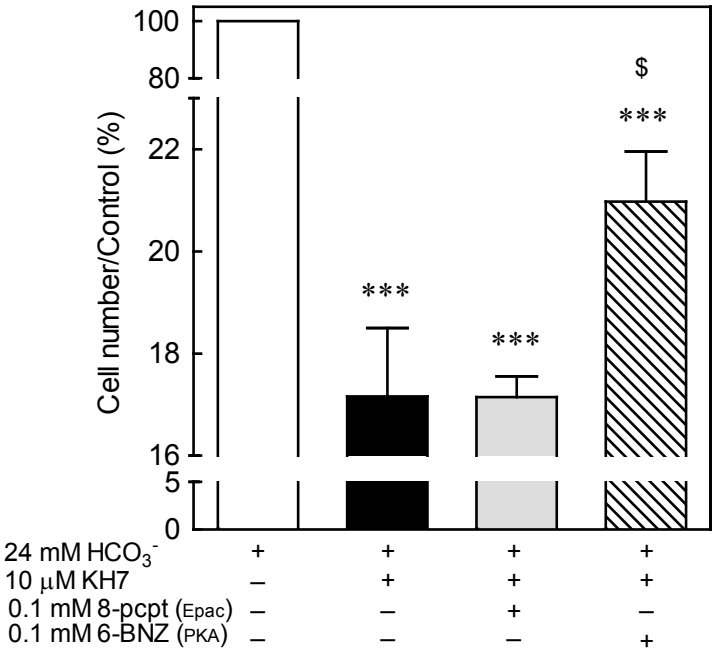

Figure 16. PKA agonist partially increases cell proliferation under ADCY10 inhibition. The data were obtained by using FACS analysis of double stained cells with Hoechst 33342 and Pyronin Y. Cells were incubated in culture medium buffered by 25 mM HEPES at pH 7.4 containing 24 mM HCO_3^- balanced by 5 % (vol/vol) CO_2 in humidified atmosphere. In a set of experiments, the medium also contained the ADCY10 inhibitor KH7 (10μM), KH7 + Epac agonist 8-pcpt-2'-o-me-cAMP (0.1 mM 8-pcpt) or KH7 + PKA agonist 6-BNZ-cAMP (0.1 mM 6-BNZ). Cells were collected at 48 h. Data are mean ± SEM from 4 independent preparations of cells from different umbilical cords. *** p-value < 0.001 compared to control, using one-way ANOVA, $ p-value < 0.05 compared to KH7-treated group, using paired T-test.

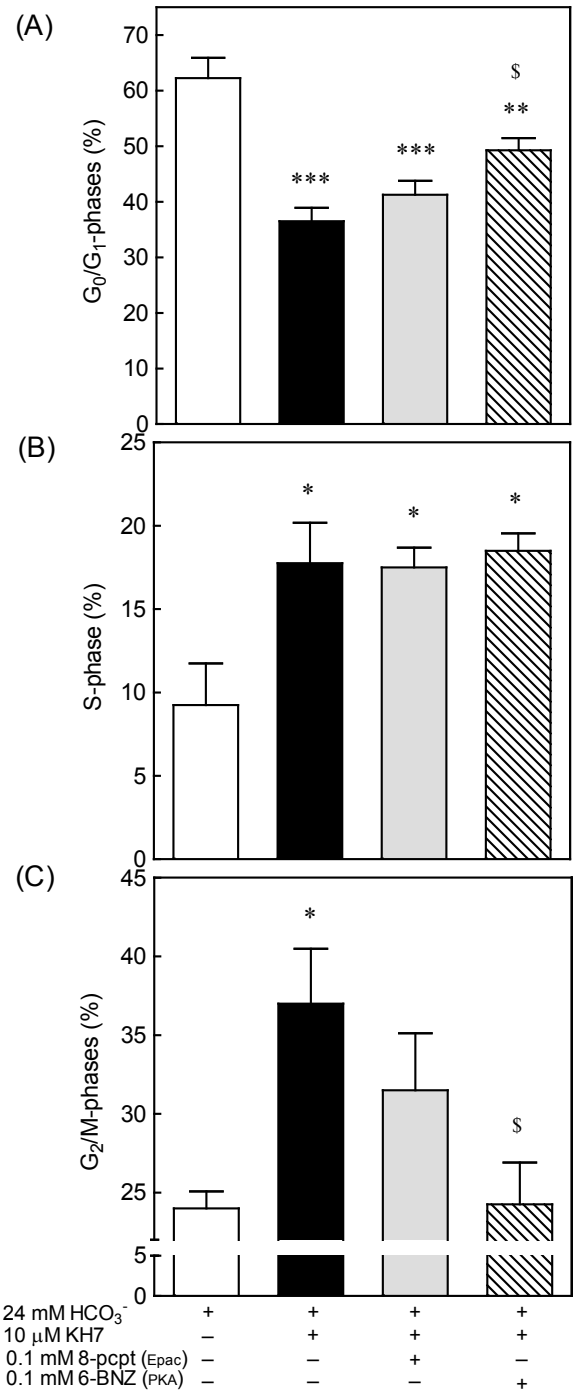

Figure 17. PKA prohibits cell cycle arrest in G_2 under ADCY10 inhibition. The data were obtained by using FACS analysis of double stained cells with Hoechst 33342 and Pyronin Y. Cells were incubated in culture medium buffered by 25 mM HEPES at pH 7.4 containing 24 mM HCO_3^- balanced by 5 % (vol/vol) CO_2 in humidified atmosphere. In a set of experiments, the medium also contained the ADCY10 inhibitor KH7 (10μM), KH7 + Epac agonist 8-pcpt-2'-o-me-cAMP (0.1 mM 8-pcpt) or KH7 + PKA agonist 6-BNZ-cAMP (0.1 mM 6-BNZ). Cells were collected at 48 h. Data are mean ± SEM from 4 independent preparations of cells from different umbilical cords. * p-value < 0.05 , ** p-value < 0.01, *** p-value < 0.001 compared to control, using one-way ANOVA, $ p-value < 0.05 compared to KH7-treated group, using paired T-test.

4.4 ADCY10 modulates regulatory kinases and phosphatases

Since the PKA agonist did not fully reverse the effects of KH7, it was hypothesized that ADCY10 may regulate kinases and phosphatases, which can directly affect the cell cycle transition, rather than via Epac and PKA alone.

As mentioned in the introduction regarding the roles of kinases and phosphastase in cell cycle progression (Section 1.5.3 and 1.5.4), it was tested whether the cyclin B1/CDK1 auto-amplification loop is involved in the underlying mechanisms of cell cycle arrest in G_2 phase after ADCY10 inhibition. Even though, this mechanism is assumed to act via Epac and PKA independent, inhibitors were used to assess this hypothesis.

4.4.1 ADCY10 affects WEE1 expression

To determine whether inhibition of ADCY10 affects WEE1 expression via Epac or PKA, inhibitors for ADCY10, Epac, and PKA were applied. In a set of experiments, the cells were incubated under control conditions in presence of 24 mM HCO_3^- balanced by 5 % (vol/vol) CO_2 at pH 7.4. Treated cells obtained the ADCY 10 inhibitor KH7 (10 µM), the Epac inhibitor ESI-09 (25 µM), and the PKA inhibitor H-89 (10 µM). The cells were lysed and collected at 48 h. Subsequently, Western blot analysis was performed in order to detect WEE1 levels using the anti-WEE1 antibody (Section 3.3.4.4). As shown in Figure 18, there is no significant difference in WEE1 expression among the groups using one-way ANOVA, indicating that WEE1 expression is independent of Epac and PKA. However, ADCY10 inhibition reduces WEE1 expression compared to control using paired T-test, indicating that WEE1 is regulated at least in part via ADCY10.

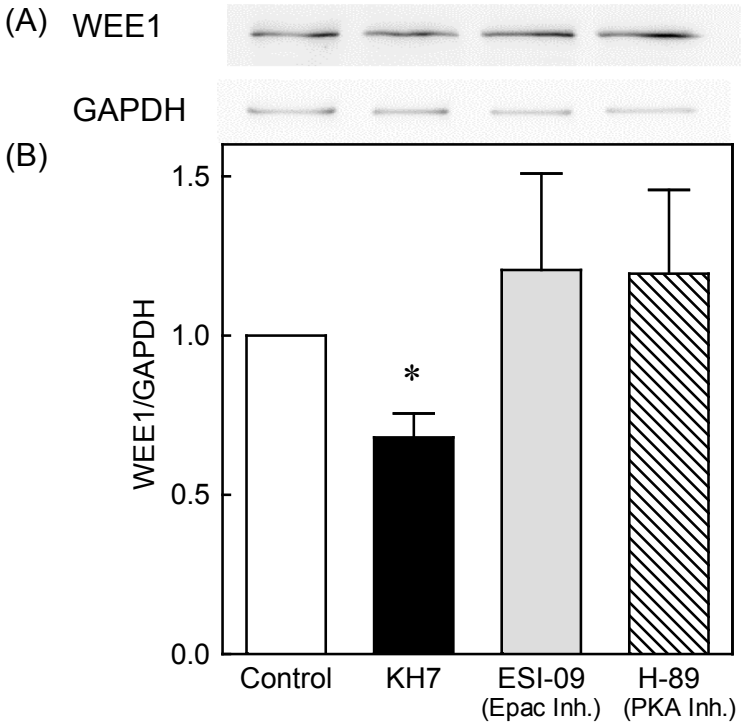

Figure 18. ADCY10 induces an increase of WEE1 protein level independent of Epac and PKA. Cells were incubated in culture medium buffered by 25 mM HEPES at pH 7.4 containing 24 mM HCO_3^- balanced by 5 % (vol/vol) CO_2 in humidified atmosphere. In a set of experiments, the medium also contained the ADCY10 inhibitor KH7, the Epac inhibitor ESI-09 (25 µM) or the PKA inhibitor H-89 (10 µM). **(A)** Representative Western blot of WEE1 and GAPDH used as loading control. **(B)** Densitometric evaluation of WEE1 relative to GAPDH and normalized to control. Data are mean ± SEM from 4 independent preparations of cells from different umbilical cords. * p-value < 0.05 compared to control, using paired T-test.

4.4.2 ADCY10 mediates PP2A in cell proliferation and cell cycle control

In addition to WEE1, PP2A is another component of the cyclin B1/CDK1 auto-amplification loop. Therefore, it was tested whether ADCY10 may control cell proliferation and cell cycle regulation via PP2A.

4.4.2.1 PP2A regulates cell proliferation and cell cycle control

To analyze whether PP2A affects cell proliferation and cell cycle phases, a specific inhibitor for PP2A, OA, was used. In a set of experiments, the cells were incubated under control conditions in presence of 24 mM HCO_3^- balanced by 5 % (vol/vol) CO_2 at pH 7.4. Treated cells obtained 5 mM OA. After 48 h, the cells were collected and analyzed by FACS for cell number and cell cycle stages. As shown in Figure 19A, inhibition of PP2A suppressed cell proliferation by approximately 50% compared to control. In addition, inhibition of PP2A induced cell accumulation in G_2/M phases (Figure 19B). These data are in accordance with the blot analysis shown in Figure 11, revealing that PP2A inhibition decreased cyclin B1 content, a marker for cells in mitosis. Thus, these data indicate that deficiency of PP2A induces cell cycle arrest in G_2 phase.

In conclusion, inhibition of PP2A showed a suppression of cell proliferation and cell cycle arrest in G_2. These results were in accordance with those after ADCY10 inhibition. Therefore, this data provides evidence that ADCY10 controls cell proliferation and cell cycle regulation via PP2A.

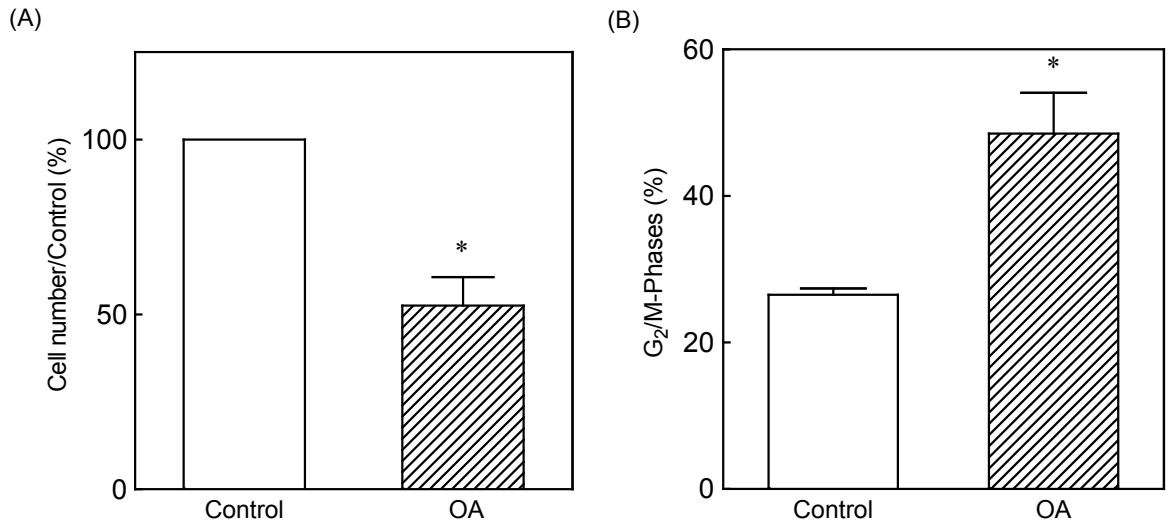

Figure 19. PP2A suppresses cell proliferation and induces cell accumulation in G_2/M phases. The data were obtained by using FACS analysis of double stained cells with Hoechst 33342 and Pyronin Y. Cells were incubated in culture medium buffered by 25 mM HEPES at pH 7.4 containing 24 mM HCO_3^- balanced by 5 % (vol/vol) CO_2 in humidified atmosphere. In a set of experiments, the medium also contained the PP2A inhibitor Okadaic acid (OA, 5 nM). Cells were collected at 48 h. Data are mean ± SEM from 4 independent preparations of cells from different umbilical cords. * p-value < 0.05, using paired T-test

4.4.2.2 ADCY10 and PP2A increase expression during mitotic phase

In the next step, it was studied whether PP2A relates to ADCY10 during cell division using immunofluorescence microscopy. Cells were seeded into an 8-well culture slide from Falcon™ and were cultured in a medium buffered by 25 mM HEPES at pH 7.4 containing 24 mM HCO_3^- balanced by 5 % (vol/vol) CO_2 in humidified atmosphere for 48 hours. Afterwards, cells were fixed and stained with antibodies raised against ADCY10 and PP2A. As shown in the upper three panels of Figure 20, ADCY10 (green) is mainly localized within the nucleus in a speckle pattern during interphase. Considerably less ADCY10 staining was found in the cytoplasm. Likewise, there was no signal for PP2A. The lower panel of Figure 20 shows two dividing cells during mitotic phase. ADCY10 positive staining was found to be dispersed throughout the entire cell body and less localized compared to interphase. Similar to ADCY10, PP2A shows a dispersed pattern throughout the entire cell. Additionally, PP2A positive staining was found at the contractile ring at the side of cell separation. In addition, ADCY10 also stained the contractile ring during late cytokinesis (Figure 7). This data indicates that ADCY10 and PP2A change expression levels as well as localization throughout the cell cycle.

In conclusion, ADCY10 and PP2A increase their expression during mitosis. It can be suggested that ADCY10 and PP2A might cooperate during mitotic phase.

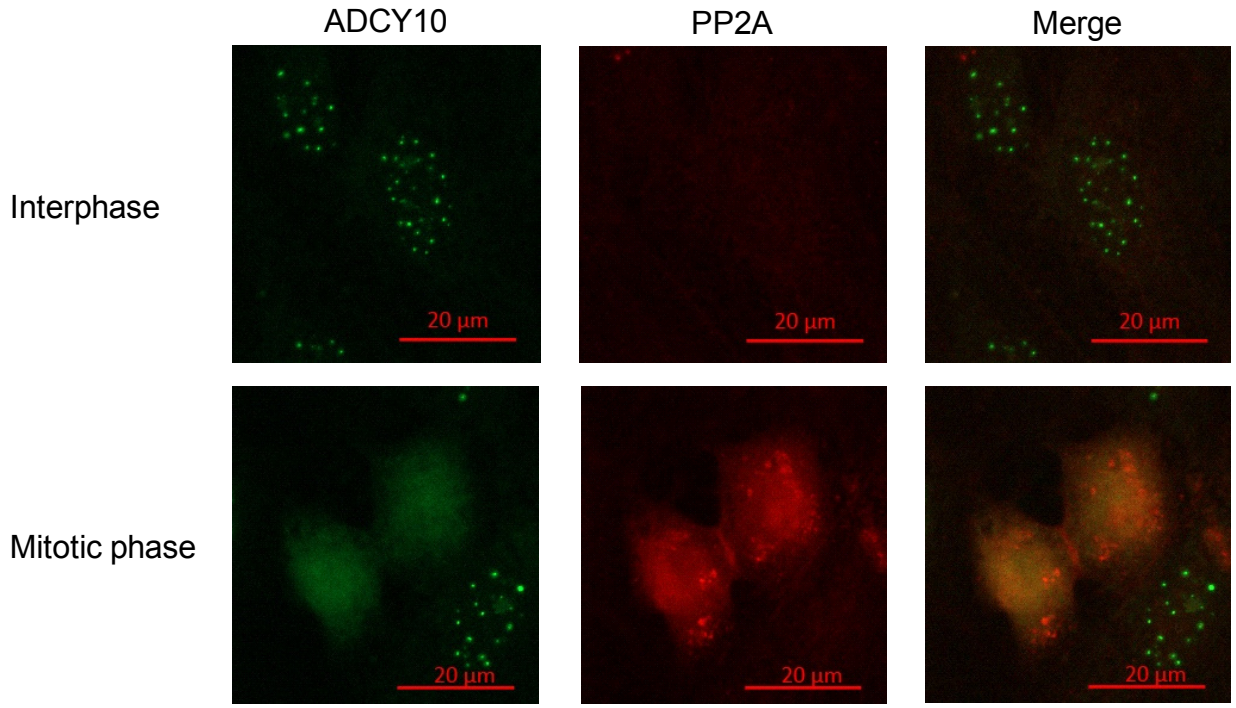

Figure 20. ADCY10 and PP2A change expression localization during the cell cycle. HUVECs were incubated in culture medium buffered by 25 mM HEPES at pH 7.4 containing 24 mM HCO_3^- balanced by 5 % (vol/vol) CO_2 in humidified atmosphere. Afterwards, cells were fixed with 4% paraformaldehyde. ADCY10 was detected by a combination of anti-ADCY10-antibody corresponding FITC-conjugated anti-rabbit-antibody (green). PP2A was detected by a combination of anti-PP2A-antibody corresponding TRITC-conjugated anti-mouse-antibody (red). Data show localization of ADCY10 and PP2A in two adjacent cells during interphase (upper panel) and two daughter cells during mitotic phase (lower panel). The merge of both channels show that ADCY10 and PP2A are colocalized during mitosis, but not during interphase.

4.4.2.3 ADCY10 sustains PP2A activity

As shown so far, inhibition of PP2A suppresses cell proliferation and causes cell accumulation in G_2 (Section 4.4.2.1). A similar effect was observed under ADCY10 inhibition suggesting that PP2A and ADCY10 are involved in cell cycle progression. Hence, immunostaining showed colocalization of ADCY10 and PP2A during cell division (Figure 20). To clarify whether PP2A is a downstream signaling molecule of ADCY10, PP2A activity was analyzed under ADCY10 inhibition. In a set of experiments, OA (PP2A inhibitor) was used as positive control of PP2A inhibition. HUVECs were incubated in culture medium buffered by 25 mM HEPES at pH 7.4 containing 24 mM HCO_3^- balanced by 5 % (vol/vol) CO_2 in humidified atmosphere. Phosphatase activity was measured at 24, 48, and 72 h (Section 3.3.5). The phosphatase assay applied in these analyses detects the activity of both PP1 and PP2. Since OA is a specific PP2A inhibitor at low concentrations, the observed inhibition of phosphatase activity throughout this section, can be attributed to PP2A activity only.

As shown in Figure 21, inhibition of ADCY10 suppressed PP2A activity at 48 h and 72 h by approximately 50% compared to the control group. This result was consistent with the inhibition of PP2A using OA. Unfortunately, OA induced cell death beyond 48 h of incubation, so that the cells could not be collected and experiments had to be terminated. In summary, inhibition of ADCY10 led to an inhibition of PP2A activity to the same degree as direct PP2A inhibition suggesting that PP2A is a downstream signaling molecule of ADCY10 and might be a key factor of the ADCY10 mediated cell cycle progression through G_2 phase.

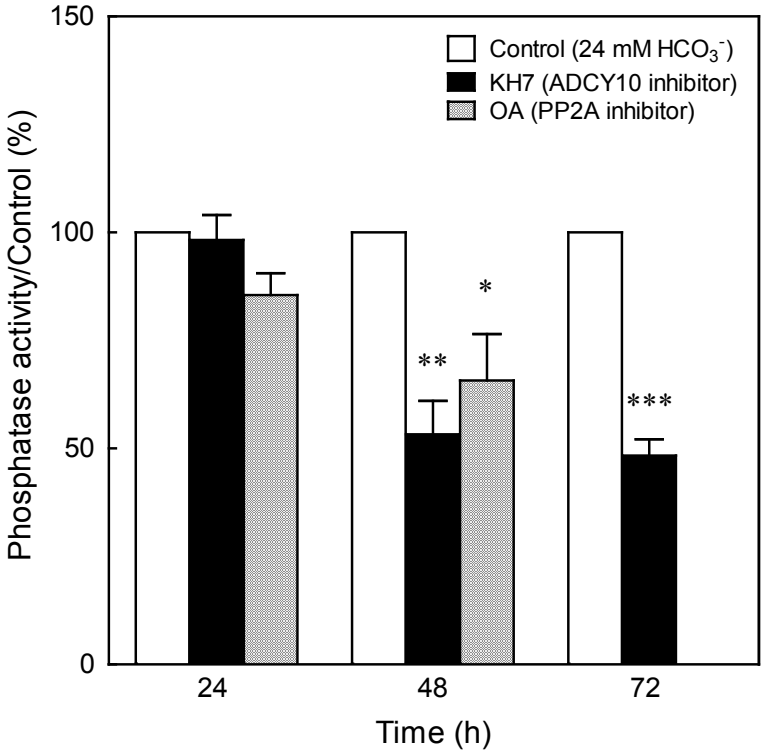

Figure 21. Inhibition of ADCY10 suppresses PP2A activity at 48 and 72 h. HUVECs were incubated in culture medium buffered by 25 mM HEPES at pH 7.4 containing 24 mM HCO_3^- balanced by 5 % (vol/vol) CO_2 in humidified atmosphere. In a set of experiments, the incubation medium also contained the ADCY10 inhibitor KH7 (10 µM) or the PP2A inhibitor OA (5 nM) as positive control. Cells were collected at 24, 48, and 72 h. Whole cell lysates were collected using RIPA buffer with protease inhibitor. Data are mean ± SEM from 4-6 independent preparations of cells from different umbilical cords. * p-value < 0.05, ** p-value < 0.01, *** p-value < 0.001 compared to control at the same time point, using one-way ANOVA.

4.4.2.4 Inhibition of ADCY10 has no effect on PP2A content

To confirm whether inhibition of ADCY10 affected PP2A content, Western blot analysis was performed. Cells were incubated in culture medium buffered by 25 mM HEPES at pH 7.4 containing 0 or 24 mM HCO_3^- balanced by 0 or 5 % (vol/vol) CO_2 in humidified atmosphere, respectively**.** In a set of experiments, the medium also contained the ADCY10 inhibitor KH7 (10 µM) or the PP2A inhibitor OA (5 nM) for 48 h. The cell lysates were collected and analyzed by Western blotting (Section 3.3.4). As shown in Figure 22A, neither inhibition of ADCY10 by the pharmacological blocker KH7 nor by HCO_3^- deprivation affects the expression of PP2A compared to control. Surprisingly, suppression of PP2A by OA resulted in increased PP2A expression by around 60% compared to the control group (Figure 22B).

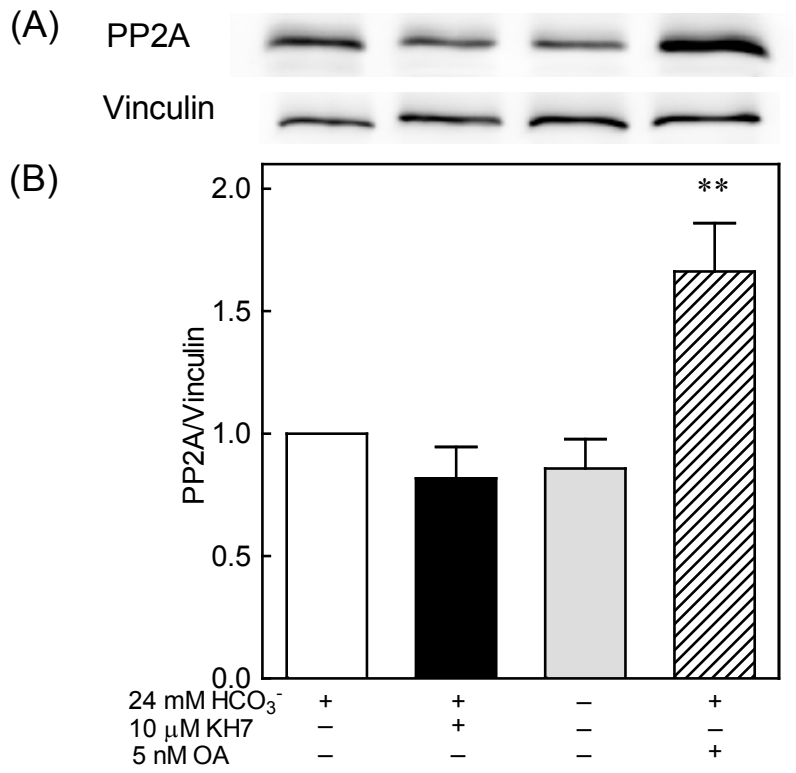

Figure 22. Inhibition of ADCY10 has no effect on PP2A content. HUVECs were incubated in culture medium buffered by 25 mM HEPES at pH 7.4 containing 0 or 24 mM HCO_3^- balanced by 0 or 5 % (vol/vol) CO_2 in humidified atmosphere, respectively. In a set of experiments, the medium also contained the ADCY10 inhibitor KH7 (10 μM) or the PP2A inhibitor OA (5 nM) for 48 h. **(A)** Representative Western blot of PP2A and vinculin used as loading control. **(B)** Densitometric evaluation of PP2A related to vinculin. Data are mean ratio ± SEM of 4 independent preparations of cells from different umbilical cords. ** p-value < 0.01 compared to control, using one-way ANOVA.

4.4.2.5 ADCY10 regulates PP2A activity independently from Epac and PKA

As shown in Section 4.3.3.2, a PKA agonist was able to unblock the arrested cells from G_2 under ADCY10 inhibition. In addition, inhibition of ADCY10 for 48 h caused a reduction of PP2A activity (Section 4.4.2.3), which likely led to cell accumulation in G_2 (Sections 4.2.2 and 4.4.2.1). To examine whether ADCY10 modulates PP2A activity through Epac or PKA, PP2A activity was measured under ADCY10 inhibition in combination with either Epac agonist (8-pcpt-cAMP) or PKA agonist (6-BNZ-cAMP). HUVECs were incubated in culture medium buffered by 25 mM HEPES at pH 7.4 containing 24 mM HCO_3^- balanced by 5 % (vol/vol) CO_2 in humidified atmosphere, respectively. In a set of experiments, the medium also contained the ADCY10 inhibitor KH7 (10 µM), KH7 plus 8-pcpt-cAMP (0.1 mM) or KH7 plus 6-BNZ (0.1 mM) for 48 h. Subsequently, phosphatase activity was measured as described in Section 3.3.5.

As shown in Figure 23, inhibition of ADCY10 by KH7 suppressed PP2A activity, which is consistent with the results in Section 4.4.2.3. However, presence of the Epac and PKA agonists had no effect on PP2A activity compared to KH7 alone. Therefore, it can be concluded that PP2A activity is directly regulated by ADCY10 rather than by its downstream targets Epac or PKA.

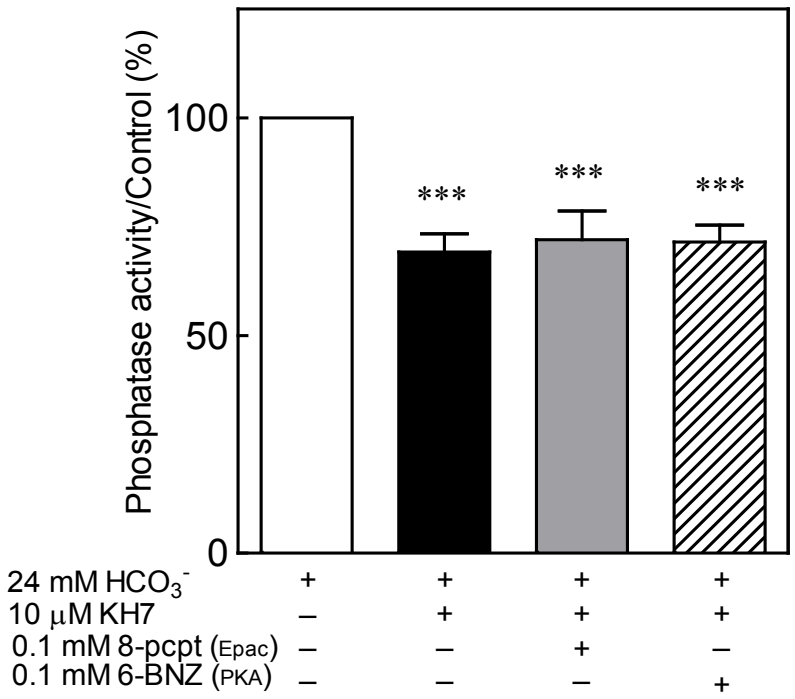

Figure 23. ADCY10 regulates PP2A activity independently of Epac and PKA. HUVECs were incubated in culture medium buffered by 25 mM HEPES at pH 7.4 containing 24 mM HCO_3^- balanced by 5 % (vol/vol) CO_2 in humidified atmosphere, respectively. In a set of experiments, the medium also contained the ADCY10 inhibitor KH7 (10 μM), KH7 plus the Epac agonist 8-pcpt-cAMP (0.1 mM) or KH7 plus the PKA agonist 6-BNZ-cAMP (0.1 mM) for 48 h. Cells were collected at 48 h. Whole cell lysates were collected using RIPA buffer with protease inhibitor. Data are mean ± SEM of 8 independent preparations of cells from different umbilical cords. *** p-value < 0.001 compared to control, with one-way ANOVA.

4.5 ADCY10 induces classical pathways of cell proliferation

Cell proliferation is modulated by different pathways involving ADCY1-9. The present thesis focuses on ERK1/2 (MAPK pathway), Glycogen synthase kinase-3β (GSK-3β), and cAMP response element-binding protein (CREB) as possible downstream targets of ADCY10 mediated signaling mechanism (Della Fazia et al., 1997; Yamaguchi et al., 2000; Zhang and Liu, 2002; Delghandi et al., 2005; Yang et al., 2006; Chambard et al., 2007; Jang et al., 2012; Sun et al., 2015). MAPK pathway induces cell proliferation in mammalian cells via three different signaling cascades by phosphorylation of their downstream targets at Ser/Thr (Zhang and Liu, 2002; MacCorkle and Tan, 2005). ERK, JNK, and p38 pathways belong to MAPK pathway. JNK and p38 can be stimulated together with growth factors, cytokines, and stress. However, ERK pathway is stress-independent and can be stimulated by growth factors and

cytokines. Therefore, the present thesis focuses on ERK as it is considered a physiological non-inflammatory pathway of cell proliferation.

Cells were incubated in culture medium buffered by 25 mM HEPES at pH 7.4 containing 24 mM HCO_3^- balanced by 5 % (vol/vol) CO_2 in humidified atmosphere, respectively. In a set of experiments, the medium also contained the ADCY10 inhibitor KH7 (10 μM), the Epac inhibitor ESI-09 (25 μM), or the PKA inhibitor H-89 (10 μM) for 48 h**.** Afterwards, protein lysates were collected and analyzed using Western blotting (Section 3.3.4.4). Densitometries of each protein were normalized by GAPDH. Furthermore, densitometric values of each HUVEC source were normalized by their own control. Therefore, control group is shown without SEM (Figures 24, 25, and 26).

4.5.1 ADCY10 induces cell proliferation via MAPK pathway

The aim of this section was to examine whether ADCY10 induces cell proliferation via ERK pathway. Therefore, the phosphorylation of MEK1/2 and ERK1/2 were measured. The inhibitors for ADCY10, Epac, and PKA were used to assess the individual effects of ADCY10, Epac, and PKA on MAPK pathway. As shown in Figure 24, inhibition of ADCY10 reduced the phosphorylation of MEK1/2 compared to control. Furthermore, Epac inhibition showed a similar effect compared to ADCY10 inhibition. In contrast, inhibition of PKA had no effect on phosphorylation of MEK1/2 compared to control. However, inhibition of PKA by H-89 resulted in a reduction of HUVEC number as shown by FACS analysis in Figure 15.

In accordance with the data on MEK1/2 phosphorylation, inhibition of ADCY10 or Epac significantly reduced phosphorylation of ERK1/2 compared to control (Figure 25). In contrast, PKA inhibition did not alter the amount of phosphorylated ERK1/2. Thus, ADCY10 and Epac but not PKA influenced the state of phosphorylated ERK1/2 and MEK1/2. Furthermore, this data provides evidence that PKA controls cell proliferation independently of ERK pathway.

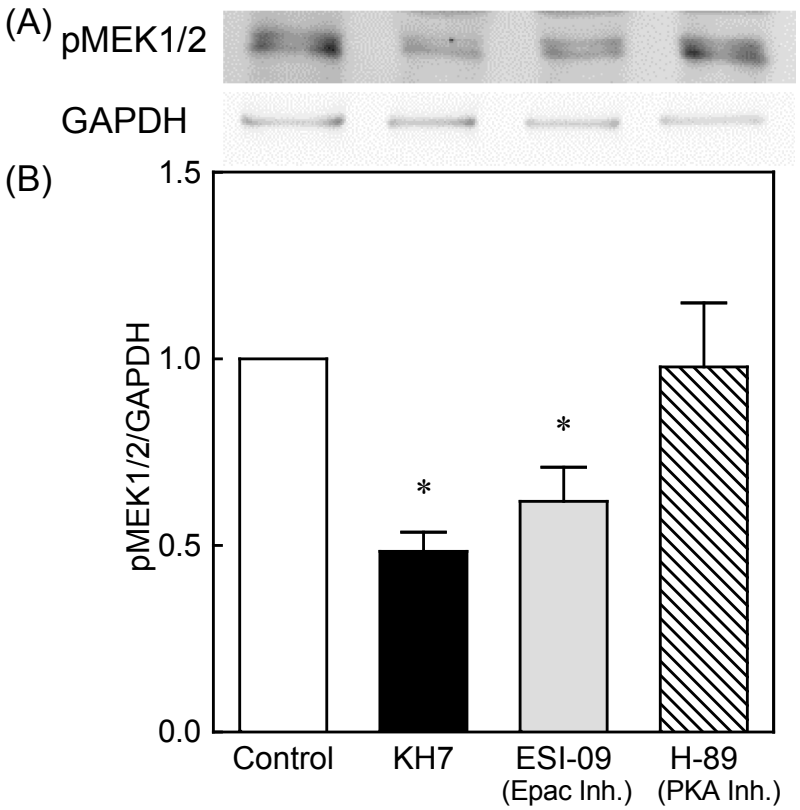

Figure 24. Inhibition of either ADCY10 or Epac represses phosphorylation of MEK1/2. Cells were incubated in culture medium buffered by 25 mM HEPES at pH 7.4 containing 24 mM HCO_3^- balanced by 5 % (vol/vol) CO_2 in humidified atmosphere, respectively. In a set of experiments, the medium also contained the ADCY10 inhibitor KH7 (10 µM), the Epac inhibitor ESI-09 (25 µM), or the PKA inhibitor H-89 (10 µM) for 48 h. **(A)** Representative Western blot of pMEK1/2 and GAPDH used as loading control. **(B)** Densitometries of pMEK1/2 relative to GAPDH. Data are mean ± SEM from 4 independent preparations of cells from different umbilical cords. * p-value < 0.05 compared to control, using one-way ANOVA.

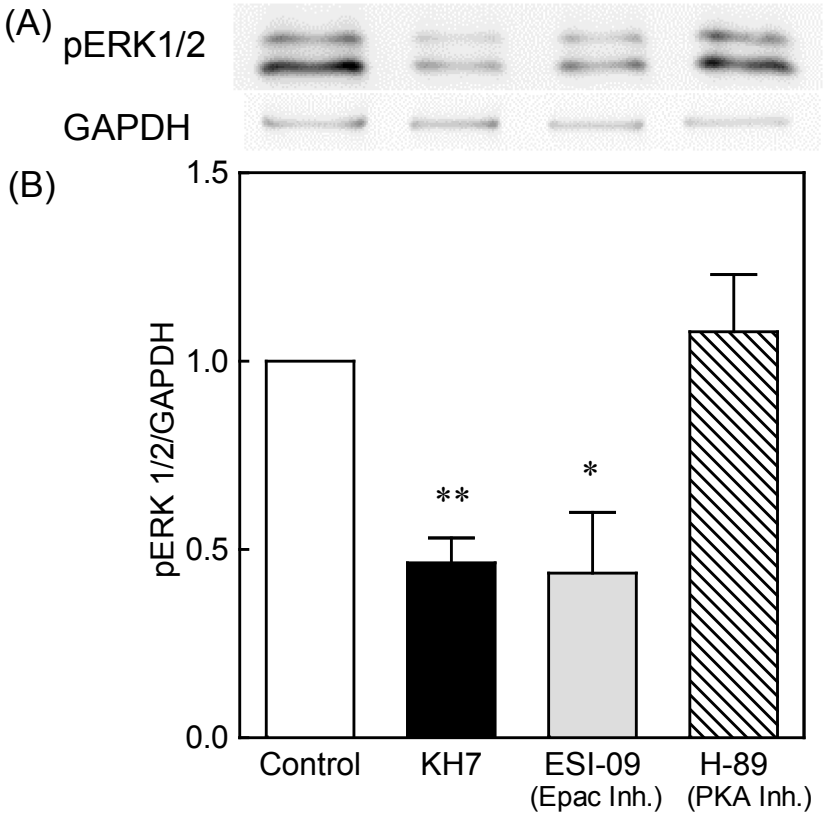

Figure 25. Inhibition of either ADCY10 or Epac represses the phosphorylation of ERK1/2. Cells were incubated in culture medium buffered by 25 mM HEPES at pH 7.4 containing 24 mM HCO_3^- balanced by 5 % (vol/vol) CO_2 in humidified atmosphere, respectively. In a set of experiments the medium also contained the ADCY10 inhibitor KH7 (10 μM), the Epac inhibitor ESI-09 (25 μM), or the PKA inhibitor H-89 (10 μM) for 48 h. **(A)** Representative Western blot of pERK1/2 and GAPDH used as loading control. **(B)** Densitometries of pERK1/2 relative to GAPDH. Data are mean ± SEM from 4 independent preparations of cells from different umbilical cords. * p-value < 0.05 compared to control, using one-way ANOVA.

4.5.2 ADCY10 has no effect on phosphorylation of GSK-3β or CREB signaling pathways.

Apart from MAPK, other downstream candidates of ADCY1-9, like GSK-3β or CREB, are reported to be upregulated by cAMP and thereby inducing cell proliferation (Ichiki, 2006; Sun et al., 2008).

To evaluate whether ADCY10 shares these signaling pathways with ADCY1-9 in cell proliferation, phosphorylation of GSK-3β and CREB was determined. As shown in Figure 26, inhibition of ADCY10, Epac, or PKA had no effect on phosphorylation of GSK-3β and CREB, indicating that ADCY10 did not induce cell proliferation via GSK-3β or CREB pathways. Significance was tested using one-way ANOVA.

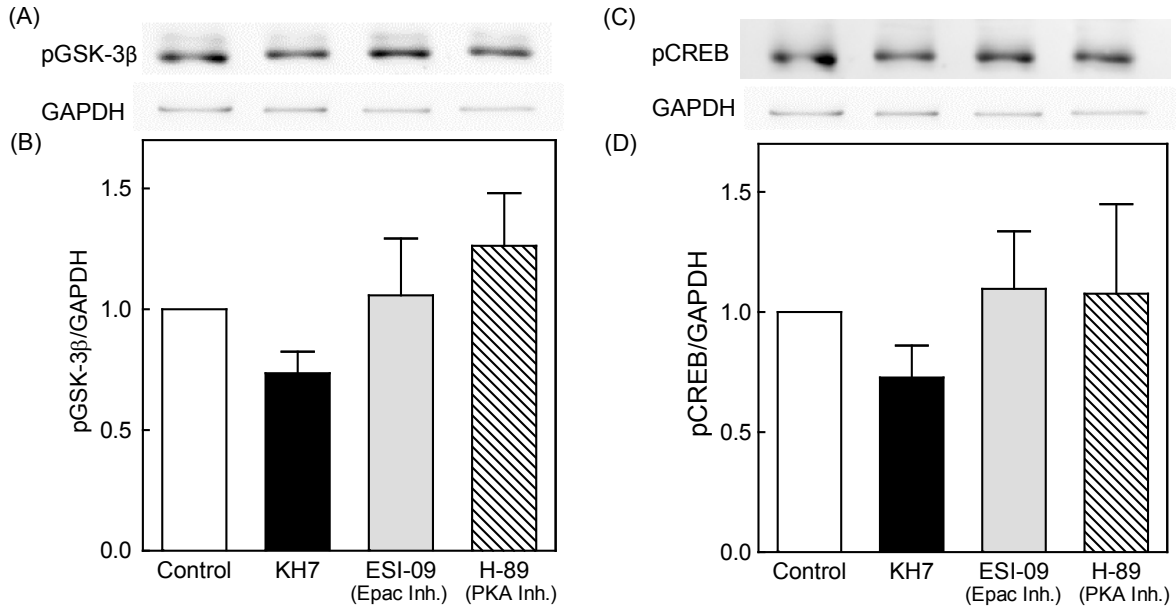

Figure 26. ADCY10 has no effect on phosphorylation of GSK-3β and CREB. Cells were incubated in culture medium buffered by 25 mM HEPES at pH 7.4 containing 24 mM HCO_3^- balanced by 5 % (vol/vol) CO_2 in humidified atmosphere, respectively. In a set of experiments, the medium also contained the ADCY10 inhibitor KH7 (10 μM), the Epac inhibitor ESI-09 (25 μM), or the PKA inhibitor H-89 (10 μM) for 48 h. Immunoblot membranes show phosphorylation bands of **(A)** GSK-3β and **(C)** pCREB signaling molecules with loading control GAPDH. Under the immunoblot membranes, densitometry comparing between **(B)** GSK-3β and **(D)** pCREB normalized to loading control GAPDH. Data are mean ± SEM from 4 independent preparations of cells from different umbilical cords.

4.6 ADCY10 and ADCY1-9 promote cell proliferation

To compare the effects of ADCY10 and ADCY1-9 in cell proliferation and cell cycle regulation, the cell proliferation assay was used (Section 3.3.1). FSK was applied as an activator of transmembrane ADCYs. The Ca^{2+} insensitive ADCY5 and 6 are considered as the dominant isoforms of transmembrane ADCYs in HUVECs (Manolopoulos et al., 1995). Therefore, the absence of FSK was considered to correlate to the non-active state of transmembrane ADCYs. Furthermore, ADCY10 was either activated by HCO_3^- and Ca^{2+} or inhibited by KH7.

Cells were incubated in culture medium buffered by 25 mM HEPES at pH 7.4 containing 24 mM HCO_3^- balanced by 5 % (vol/vol) CO_2 in humidified atmosphere, respectively. The experiment consisted of nine groups: 24 mM HCO_3^- (control), 10 µM KH7, combination of 10 µM KH7 with various concentration of FSK at 0.1, 1, 5, 10 µM, as well as combination of 24 mM HCO_3^- with various concentration of FSK at 1, 5, 10 µM (without KH7). After HUVEC synchronization, cells were exposed to the above mentioned conditions for 72 h. FACS analysis was performed as described in Section 3.3.2.

As shown in Figure 27, inhibition of ADCY10 by KH7 significantly suppressed cell number by approximately 4 times compared to control. Simultaneous activation of ADCY10 via HCO_3^- and transmembrane ADCYs via FSK resulted in a tendency of increased cell number compared to control. However, more intensive cell proliferation was prohibited by limited growth area under these conditions. In contrast, 0.1, 1, 5, and 10 µM FSK could reverse the effect of ADCY10 inhibition by KH7. Cell number in these groups showed no significant difference compared to control.

In addition to cell proliferation, cell cycle stages were also assessed (Figure 28). As shown already in Figure 10, inhibition of ADCY10 by KH7 induced G_2 cell accumulation. However, FSK abolished the effect of KH7. There was no cell accumulation in G_2/M phases after treated with 1, 5, and 10 µM of FSK (Figure 28).These data indicate that both ADCY10 and ADCY1-9 induce cell proliferation. Furthermore, the combined activation of ADCY10 and ADCY1-9 promoted higher cell proliferation compared to ADCY10 alone. Collaboration of ADCY10 and ADCY1-9 may lead to over proliferation.

In conclusion, ADCY 1-9 and ADCY10 are essential for cell proliferation in HUVECS. If either transmembrane ADCYs or the soluble ADCY are deficient, stimulation of the respective other type can balance cell proliferation redundantly.

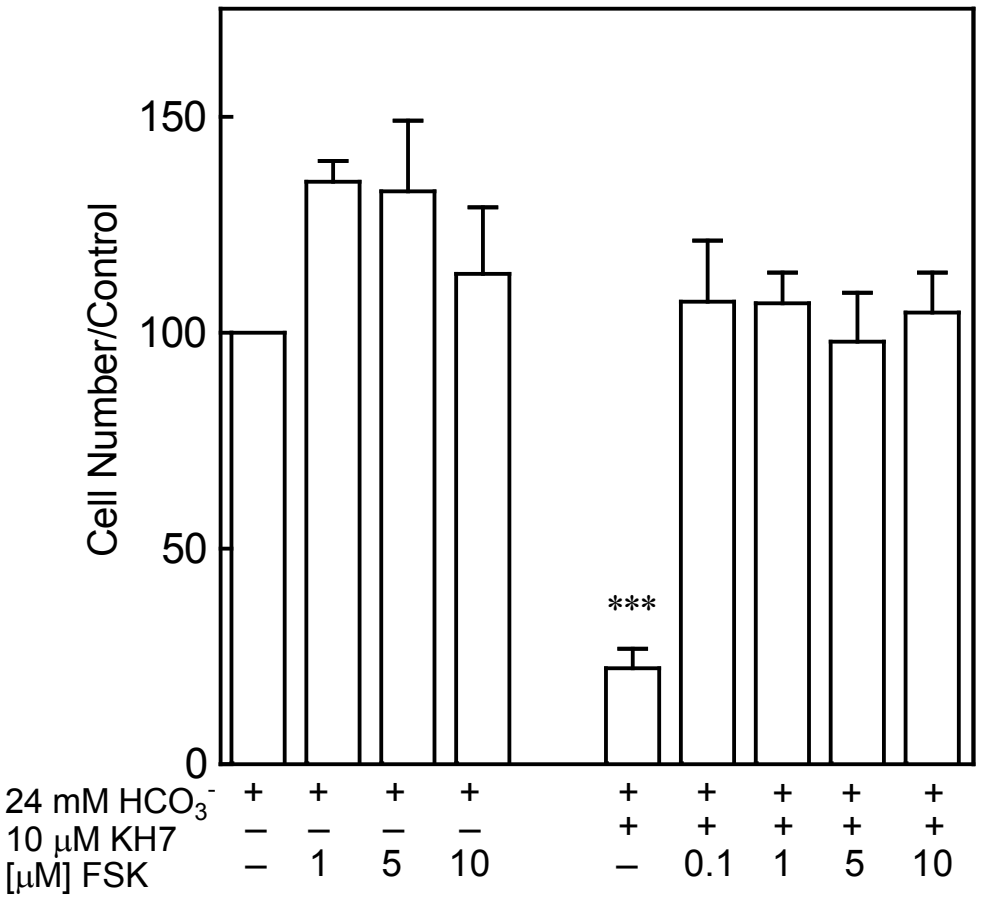

Figure 27. ADCY1-9 as well as ADCY10 promote cell proliferation. The data were obtained by using FACS analysis of double stained cells with Hoechst 33342 and Pyronin Y. HUVECs were exposed to 24 mM HCO_3^- (control), 10 μM KH7, and 0.1, 1, 5, 10 μM FSK according to experimental design at pH 7.4, 5% CO_2. Cells were collected at 72 h. Data are mean ± SEM from 3 independent preparations of cells from different umbilical cords. *** p-value < 0.001 compared to control, using one-way ANOVA.

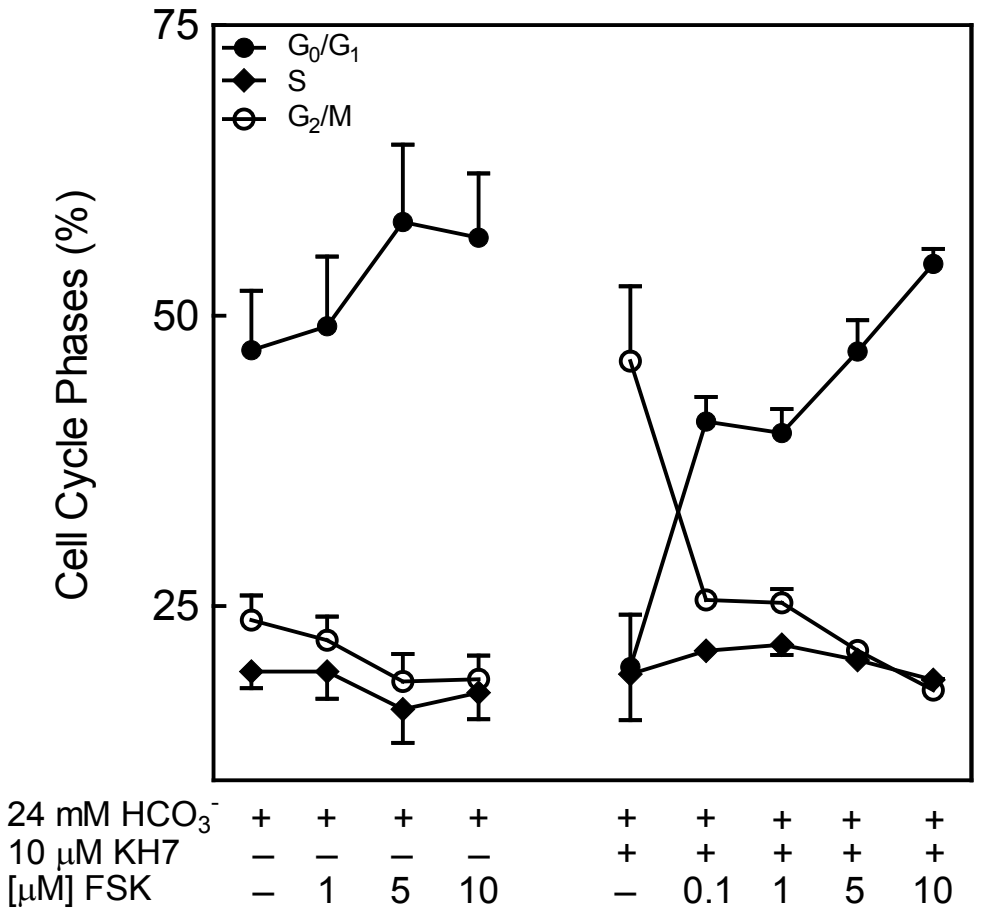

Figure 28. ADCY1-9 as well as ADCY10 promote cell cycle progression from interphase to mitotic phase. The data were obtained by using FACS analysis of double stained cells with Hoechst 33342 and Pyronin Y. HUVECs were exposed to 24 mM HCO_3^- (control), 10 μM KH7, and 0.1, 1, 5, 10 μM FSK according to experimental design at pH 7.4, 5% CO_2. Cells were collected at 72 h. Data are mean ± SEM from 3 independent preparations of cells from different umbilical cords.

5. Discussion

The main objective of the present study aimed to extend the current understanding of the role of ADCY10 and its downstream pathways on cell proliferation. The activation of ADCY10 via HCO_3^- induces cell proliferation. Lack of ADCY10 activity results in delayed cell cycle progression and accumulation of cells in G_2 phase as it was shown by decreased cyclin B1 level. Epac and PKA were identified as possible downstream targets of ADCY10 in cell proliferation. Epac promotes G_1/S transition and cell proliferation via phosphorylation of MEK1/2 and ERK1/2 (MAPK pathway) whereas PKA plays a role to promote cell cycle transition from interphase to mitotic phase. Furthermore, this work revealed that PP2A is a main downstream pathway of ADCY10 independent of Epac and PKA to regulate cell proliferation and cell cycle transition.

5.1 ADCY10 regulates HUVECs proliferation by controlling cell cycle progression

The current study used various HCO_3^- concentrations (Figure 8). The physiological concentration of HCO_3^- was sufficient to maintain cell proliferation, while supraphysiological concentrations of HCO_3^- (40 mM) did not induce further cell proliferation. This result can be explained in two different ways. First, PDEs catalyzed excessive amount of cAMP (Fischmeister, 2006) and second, cAMP produced at 24 mM HCO_3^- is already adequate for optimal cell growth of HUVECs.

In addition, the physiological concentration of 24 mM HCO_3^- in this *in vitro* study was used to mimic HCO_3^- concentration of plasma *in vivo*. The plasma HCO_3^- is a major buffer system of blood and maintains the pH value in the range of 7.35 - 7.45. However, the intracellular HCO_3^- concentration is much lower, approximately 10 mM (Guyton and Hall, 2012). This is consistent with findings that the EC_{50} value for isolated ADCY10 is 12 mM HCO_3^- (Kleinboelting et al., 2014). In addition, the saturating kinetics of the sigmoidal concentration response curve as described by Kleinboelting et al. (2014) support the finding of this study that supraphysiological concentrations beyond 24 mM HCO_3^- have little to no impact on ADCY10 activity. Furthermore, intracellular cAMP compartments are critical for cAMP function (Pozdniakova and Ladilov, 2018). Thus, the influence of HCO_3^- concentrations might be over- as well as underestimated in general *in vitro* studies due to its use as a common pH regulator.

Immunostaining demonstrated that ADCY10 localizes within nucleus and cytoplasm during

interphase. However, during mitotic phase, ADCY10 translocates from nucleus to cytoplasm and is localized intensively on the mitotic spindles as indicated by α-Tubulin staining (Figure 7). This result was consistent with the work from Zippin et al. (2003) that demonstrated the compartmentalization of ADCY10 throughout the nucleus and the cell body (Zippin et al., 2003). Additionally, ADCY10 modulates motility in sperms, where it is localized in the midpiece of the sperm tail together with tubulin (Hess et al., 2005). Despite the obvious difference in biological models (sperm motility vs. cell division), ADCY10 colocalizes in both systems with tubulin. Furthermore, it was previously described that ADCY10 dependent cAMP signaling is strictly compartmentalized (Raju et al., 2019). Hence, it might be a key regulator of the mitotic spindle and therefore interfere directly with underlying biomechanical apparatus of mitosis despite its role as a general regulator of cell cycle progression.

Various studies have demonstrated that cAMP production of ADCY10 depends on HCO_3^- (Chen et al., 2000; Tresguerres et al., 2010). This study showed that HCO_3^- induces cell proliferation under physiological conditions (24 mM HCO_3^-) via ADCY10. In contrast, inhibition of ADCY10 caused a delay of cell cycle progression consequently led to cell cycle arrest in G_2, as confirmed by decreased cyclin B1 level. Regarding ADCY10 inhibition, a specific inhibitor of ADCY10 KH7 had a stronger effect on cell proliferation and cell cycle regulation compared to 0 mM HCO_3^- (Figure 8C). One possible explanation for the stronger effect of KH7 compared to 0 mM HCO_3^- is, there is still the presence of other ADCY10 stimulators in the absence of bicarbonate. ADCY10 can be stimulated by HCO_3^-, Ca^{2+}, and ATP (Wiggins et al., 2018). Therefore, KH7 completely blocks ADCY10 activity. In contrast, other stimulators such as Ca^{2+} and ATP are still able to stimulate ADCY10 in the absence of HCO_3^-.

Flacke et al. (2013) found that ADCY10 is highly expressed in prostate cancer cell lines. Furthermore, their results indicated that the overexpression of ADCY10 was associated with increased cell growth and inhibition of ADCY10 blocked cell proliferation of these cancer cells effectively. The results of this thesis were consistent with the findings that Flacke et al. (2013) observed, that is an arrest of cells in G_2 phase after ADCY10 inhibition (Flacke et al., 2013). Taken together, ADCY10 is not only an essential regulator of cell cycle under physiological conditions, but further qualifies as a potential therapeutic target in prostate cancer.

5.2 ADCY10 controls cell cycle progression via Epac and PKA

The regulation of the cell cycle is a sophisticated system with various control mechanisms and checkpoints (Heim et al., 2017).

The arrest of cell cycle in G_2 due to deficiency of ADCY10 as found as a major findings in the current thesis which generates the obvious question regarding to which underlying mechanisms contribute to the complex downstream network of ADCY10 that supports cell division. Throughout this thesis, Epac, PKA, and PP2A were investigated as possible downstream candidates of ADCY10 in the context of cell division and cell cycle progression. Different experiments including direct inhibition as well as direct stimulation were performed, leading to an elaborate understanding of the orchestration of different pathways.

The cells were synchronized in G_0/G_1 phases due to nutrition insufficiency using serum withdrawal. Kaplon et al. (2015) described that serum triggers G_0/G_1 transition as indicated by increased cyclin D level, which is an indicator for G_1 phase (Kaplon et al., 2015). In addition, in order to reenter normal cell cycle, serum is required to provide sufficient energy and nutrition for biomass synthesis (Kalucka et al., 2015). An important link between physiological appearance of mitochondria and their metabolic rate was found to be determined for correct cell cycle transition (Finkel and Hwang, 2009). Increasing ATP levels from Krebs cycle increase cyclin E levels which are required for G_1/S transition. As described in Section 4.3.1, Epac inhibition was associated with cell arrest in G_0/G_1 phase (Figure 13). In this context, Epac was found to colocalize with mitochondria (Qiao et al., 2002). Beyond the role of Epac in insulin secretion, Epac was found to be essential in general cellular energy homeostasis (Valsecchi et al., 2013; Almahariq et al., 2014). Regarding the influence of Epac on cell cycle progression, this thesis provides evidence that Epac influences cell cycle transition of G_1/S phases rather than G_2/M phases as observed after ADCY10 inhibition (Section 4.3.1).

In Section 4.3.2, the two PKA inhibitors PKI and H-89 led to contradicting results with regard to cell proliferation. A previous study describes that PKA inhibitors have widespread nonspecific effects (Murray, 2008). Thus, results from the experiments of direct inhibition of PKA have to be regarded with caution as it does not provide sufficient evidence. The experimental strategy was therefore switched towards Epac and PKA activators.

Activation experiments were performed after ADCY10 inhibition via KH7. These led to the expected cell arrest in G_2 (Section 4.3.3.2). Under this condition, the addition of PKA agonists released cells from G_2 phase. This finding is consistent with two results of Vandame et al. (2014). First, PKA inhibition led to incorrect DNA alignment and DNA segregation during metaphase and second, PKA localized at the centrosomes (Vandame et al., 2014). Taken together, this indicates that PKA is essential for cell division as a downstream mechanism of

ADCY10.

In contrast to PKA, the addition of Epac agonists did not influence the cell number nor the cell cycle phases during ADCY10 inhibition. Flacke et al. (2013) found evidence that Epac rather than PKA or PP2A played an essential role in a prostate cancer cell line (Flacke et al., 2013). Even though both studies were conducted *in vitro*, cancerous cells might use Epac as a dominant pathway to induce cell proliferation. Taken together, Epac plays a role in the transition of G_1/S phase as indicated above under physiological conditions. Furthermore, it has no effect on cells arrested in G_2 as it was induced by ADCY10 inhibition.
Considering both influences of PKA and Epac as illustrated by Figures 16 and 17 in a quantitative approach, it becomes obvious that ADCY10 might operate cell proliferation via Epac and PKA synergistically or through pathways other than Epac and PKA in the given biological system.

5.3 PP2A is a main downstream molecule of ADCY10 to regulate cell proliferation and cell cycle progression

The cyclin B1/CDK1 complex triggers mitotic entry. Figure 29 illustrates the auto-amplification loop of cyclin B1/CDK1. The activation of this complex occurs to be all-or-none fashion at the transition to M phase. Therefore, to initiate the auto amplification activation, a sufficient amount of cyclin B1/CDK1 is required to convert this switch-like mechanism (Heim et al., 2017). This loop consists of the positive feedback of Cdc25 activation and the double negative loop of WEE1 inhibition (Figure 29). These phosphatase Cdc25 and kinase WEE1 create a unique extreme steady state which is either “on” or “off” (Forester et al., 2007; Perry and Kornbluth, 2007; Heim et al., 2017). In addition, PP2A was found to be a key regulator of G_2/M cell cycle transition by balancing cyclin B1/CDK1 via WEE1 and Cdc25 (Hara et al., 2012; Jeong and Yang, 2013).

This current study demonstrated that inhibition of ADCY10 suppresses WEE1 level (Section 4.4.1), cyclin B1 content (Section 4.2.3), and PP2A activity (Section 4.4.2.3). Therefore, deprivations of these three main components lead to a malfunction of the cyclin B1/CDK1 auto-amplification loop. In summary, inhibition of ADCY10 prohibits the initiation of the cyclin B1/CDK1 auto-amplification loop, which results in cell cycle arrest in G_2.

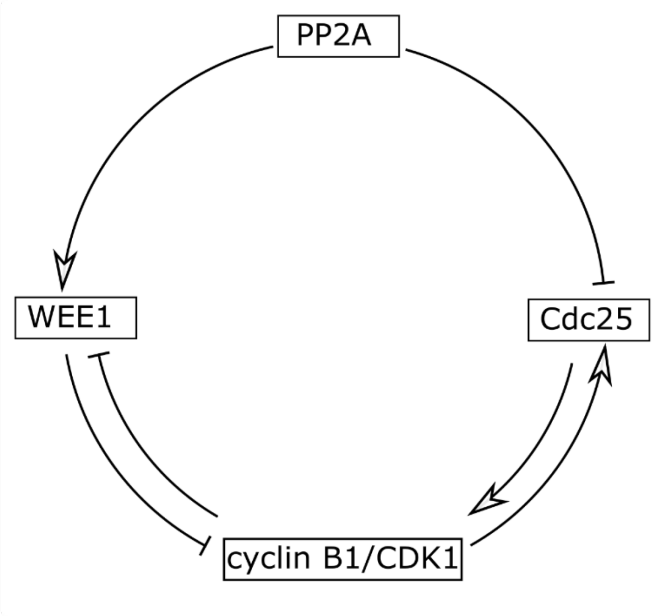

Figure 29. Cyclin B1/CDK1 auto-amplification loop. PP2A, WEE1, Cdc25, and cyclin B1/CDK1 regulate cell cycle transition from G_2/M phase within an auto-amplification loop. This loop consists of the positive feedback of Cdc25 activation and the negative loop of WEE1 inhibition. Arrows indicate activation and dashes represent inhibition.

Various studies identify PP2A as an essential molecule that plays a role in cell cycle regulation (Lechward et al., 2001; Wlodarchak and Xing, 2016; Heim et al., 2017). PP2A is one of the most predominant serine-threonine phosphatases in most cells. Previous studies demonstrated that PP2A has a positive role in mitotic entry in *Saccharomyces cerevisiae* (Lin and Arndt, 1995; Jiang, 2006). This is consistent with data from Gong et al. (2015), where inhibition of PP2A by OA led to cell accumulation in G_2 via suppression of CDK1 in a pancreatic cancer cell line PANC-1 (Gong et al., 2015). Regarding the role of ADCY10, there is evidence indicating that cAMP regulates PP2A either directly or indirectly via PKA (Feschenko et al., 2002; Ahn et al., 2007; Dodge-Kafka et al., 2010; Leslie and Nairn, 2019). This thesis provides evidence that PP2A activity is regulated independently of either Epac or PKA (Figure 23). This is further supported by the colocalization of ADCY10 and PP2A during mitosis and cytokinesis (Figure 19). Additionally, previous studies showed that PP2A colocalized with tubulin during mitosis (Sontag et al., 1995; Horn et al., 2007). Thus, there seem to be strong local connection between ADCY10, tubulin, as well as the central regulator of mitotic entry, PP2A.

Furthermore, ADCY10 and PP2A inhibition showed similar patterns of reduced cell proliferation and increased cell accumulation in G_2 as well as decreased cyclin B1 content

(Figures 11 and 20).

The PP2A activity assay showed a decreased PP2A activity after 48 and 72 h of ADCY10 inhibition (Section 4.4.2.3). Interestingly, this effect was correlated with the cell accumulation in G_2 phase under ADCY10 inhibition (Section 4.2.2). However, 24 h after synchronization, cells were not accumulated in G_2 and did not show decreased PP2A activity compared to control (Figure 21). Surprisingly, there was an increase of PP2A content after PP2A inhibition using OA. Even though, PP2A inhibition using OA suppressed PP2A activity. These results suggested a negative feedback regulation of PP2A.

Taken together, lack of cAMP from ADCY10 causes decreased cyclin B1 and WEE1 content as well as decreased PP2A activity. These observations reflect the general “off” state of the cyclin B1/CDK1 auto-amplification loop.

Currently, the data demonstrated that ADCY10 controls cell proliferation and cell cycle in HUVECs via the central regulator PP2A independently of Epac and PKA.

5.4 ADCY10 induces cell proliferation via MAPK pathway

MAPK pathway is known to stimulate cell proliferation and mitogenesis (Zhang and Liu, 2002; Chambard et al., 2007; Mebratu and Tesfaigzi, 2009; Sun et al., 2015). Blocking ADCY10 and Epac resulted in a suppression of MAPK pathway whereas, inhibition of PKA had no effect on phosphorylation of MEK1/2 and ERK1/2 compared to control (Section 4.5.1). These results were harmonious with the result from cell proliferation assay (Section 4.2 and 4.3).

Jang et al. 2012 claimed that cAMP produced from ADCY1-9 stimulated cell proliferation via GSK-3β (Jang et al., 2012) or CREB (Della Fazia et al., 1997). However, the current study demonstrated no correlation between phosphorylation state of GSK-3β or CREB and ADCY10 activity (Section 4.5.2). In conclusion, ADCY10 induces cell proliferation via Epac/MAPK pathway. Furthermore, ADCY10 did not share the common signal pathways to induce cell proliferation with ADCY1-9.

The current understanding of this thesis regarding the role of ADCY10 on G_2/M transition is summarized in Figure 30.

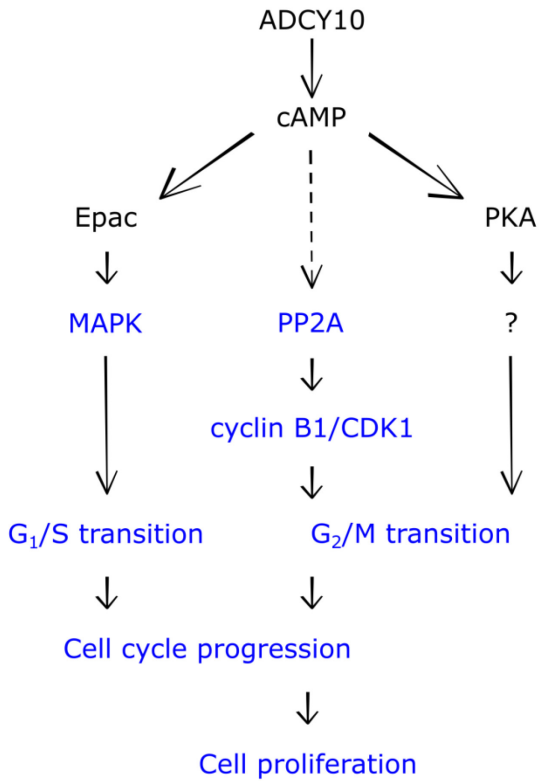

Figure 30. Summary of the current study: ADCY10 induces cell proliferation via Epac, PKA, and PP2A pathways. ADCY10 produces cAMP. cAMP activates Epac, PKA, and PP2A. Epac induces G_1/S transition via ERK1/2 whereas PKA promotes cell cycle transition of G_2/M phase via an unidentified pathway. Moreover, PP2A is identified as a downstream pathway of ADCY10, which regulates cyclin B1/CDK1 content and subsequently promotes cell cycle transition of G_2/M phase. There is no link between Epac and PKA on PP2A. In conclusion, ADCY10 regulates cell cycle progression and cell proliferation via Epac, PKA, and PP2A. The dashed line indicates an either direct or indirect pathway. The blue texts represent work found in this study.

5.5 Activated-transmembrane type of ADCYs is the alternative source of cAMP when ADCY10 is deprived in cell proliferation.

The current study showed that after FSK-activated tmACs can abolish the effect of KH7-suppressed ADCY10 in cell proliferation. Activation of tmACs by FSK and ADCY10 by HCO_3^- generate the comparable amount of cell number. However, a tendency of increased cell number was observed when tmACs and ADCY10 together stimulation. Due to the limited growth area of the culture dish used in this experiment, therefore, this study could not provide the evidence that tmACs have a stronger proliferative effect compared to ADCY10 since tmACs can produce cAMP concentration higher than ADCY10. A study from Zippin et al.

(2014) demonstrated that FSK induces cAMP production by 120% compared to basal control in whole cell lysate. In contrast, HCO_3^- induced an increase of cAMP production by 35% compared to basal control while FSK showed no significant different of cAMP production compared to control in nuclear lysate (Zippin et al., 2004). The current thesis suggests that ADCY1-9 and ADCY10 collaborate and contribute its proliferative to maintain tissue homeostasis certainly with the work from PDEs. Therefore, this evident support how ADCY10 knock out mouse model is not lethal and still living which might be due to the substitute source of cAMP provided from tmACs.

5.6 Perspective of further studies

A study by Flacke et al. (2013) reported that ADCY10 inhibition induces cytotoxicity in two different human prostate carcinoma cell lines (Flacke et al., 2013). This evidence indicates an essential role of ADCY10 for cell survival. From a different perspective, over expression of ADCY10 promotes radioresistance in non-tumor PNT2 cells by having ERK as a crucial downstream molecule (Appukuttan et al., 2014). Thus, these findings identified the protective effects of ADCY10.

Autophagy is a central recycling mechanism to maintain cellular homeostasis. Rahman et al. (2016) suggest a role of ADCY10 in endocytosis as well as autophagy, where ADCY10 is responsible for correct lysosomal acidification (Rahman et al., 2016). Moreover, the transcription factor p53 is essential for correct cell cycle progression. A pilot study extended from the current study suggests that inhibition of ADCY10 increases p53 level, which indicates high level of DNA damage (data not shown). It is known that p53 is an upstream of cyclin B1/CDK1 during G_2/M transition (Strasser-Wozak et al., 1998). Therefore, this observation is in accordance with arrest cells in G_2 via ADCY10 inhibition. In addition, preliminary results (data not shown) suggest that ADCY10 inhibition increases DNA double strand breaks. These findings raise more profound research questions regarding the role of ADCY10 on cell homeostasis. Further research will be needed to identify the exact role of ADCY10 in DNA protection.

6. Conclusions

The current study extends the knowledge of how ADCY10 promotes cell proliferation and regulates cell cycle control via HCO_3^-. Furthermore, all research questions as mentioned in the aim chapter (Chapter 2) have been addressed and elaborated. The conclusion for each research question is summarized as follows:

1. It has been shown that bicarbonate activates ADCY10 to induce cell proliferation. Inhibition of ADCY10 results in increased doubling time from 24 h to 48 h (Section 4.2).

2. ADCY10 maintains cell cycle progression, whereas ADCY10 inhibition delays cell cycle transitions of G_1/S as well as G_2/M (Section 4.2). In addition, ADCY10 inhibition using either KH7 or 0 mM HCO_3^- induces cell accumulation in G_2 phase (Section 4.2) indicating a decreased cyclin B1 levels (Section 4.2.3).

3. It has been proven that Epac controls cell cycle transition of G_1/S (Section 4.3.1), while PKA promotes cell cycle progression of G_2/M (Section 4.3.3). Therefore, it can be concluded that Epac and PKA collectively maintain cell cycle progression.

4. PP2A is a downstream signaling molecule of ADCY10. It has been shown experimentally that ADCY10 inhibition causes decreased PP2A activity (Section 4.4.2.3) and consequently leads to impairment of mitotic entry. Moreover, inhibition of PP2A itself shows similar results as ADCY10 inhibition regarding decreased cell proliferation and accumulation of cells in G_2 phase (Section 4.4.2). Taken together, lack of cAMP from ADCY10 causes decreased cyclin B1 and WEE1 content as well as decreased PP2A activity. These observations reflect the general “off” state of the cyclin B1/CDK1 auto-amplification loop.

5. It has been proven that ADCY10 and ADCY1-9 do not share the common signaling pathways GSK-3β and CREB for cell proliferation. Instead, ADCY10 induces cell proliferation via ERK1/2-MAPK pathway.

The results from this work gave further insights into the downstream pathways of ADCY10 regarding cell proliferation and cell cycle progression. Figure 30 provides a detail overview of these results.

Summary

The soluble form of ADCYs, ADCY10, is ubiquitously expressed in the cytoplasm and distinct organelles including cell nucleus. In contrast to its membrane-associated isoforms (ADCY1-9) which are stimulated by G-protein-coupled receptors, ADCY10 is activated by bicarbonate (HCO_3^-) and can form cAMP in nearly all cell compartments. ADCY10 is involved in a variety of physiological as well as pathological processes including cell cycle control in tumor cells. However, the underlying mechanism is still unclear. Here the role of ADCY10 in cell cycle control and cell proliferation is studied in endothelial cells from human umbilical veins (HUVECs).

The current study reveals that ADCY10 and α-Tubulin translocate and colocalize during mitosis suggesting a role of ADCY10 in cell division. In addition, FACS analysis demonstrated that ADCY10 plays a role in cell proliferation by modulating cell cycle control. Inhibition of ADCY10 by 0 mM HCO_3^- or 10 μM KH7 (specific ADCY10 inhibitor) induced cell accumulation in G_2 phase rather than M phase determined by decreased mitotic indicator cyclin B1 level. Thus, ADCY10 inhibition leads to decreased cell proliferation.

The known cAMP effectors, Epac and PKA, were assessed as possible downstream targets of ADCY10 in cell proliferation.

It was shown that ADCY10 and Epac induce cell proliferation via ERK1/2-MAPK pathway. Inhibition of Epac was associated with suppressed cell proliferation. However, an arrest of cell cycle after Epac inhibition was observed in G_0/G_1 phases rather than S or G_2/M phases. Thus, Epac inhibition causes a different arrest of cell cycle compared to ADCY10 inhibition.

Regarding PKA, it was demonstrated that deficiency of PKA might play a role in either activation or inhibition of cell proliferation. However, direct inhibition of PKA by PKI and H-89 did not lead to cell accumulation in G_2. This effect might be associated with broadened roles of PKA in different pathways. In contrast, direct stimulation of PKA under ADCY10 inhibition revealed that PKA is a downstream molecule of ADCY10 as a regulator of cell cycle transition from G_2 to mitotic phase. However, the underlying pathway remains to be investigated.

The cell cycle transition of G_2/M phase is regulated by an auto-amplification loop of cyclin B1/CDK1, which is controlled by the kinase WEE1 and the phosphatase PP2A. WEE1 content was regulated via ADCY10 but was independent of PKA or Epac.

Direct inhibition of PP2A showed a suppression of cell proliferation and induced cell cycle arrest in G_2. These results were in accordance with those observed after the ADCY10.

Furthermore, inhibition of ADCY10 had no effect on PP2A expression level but rather affected PP2A activity and was independent of Epac and PKA. Therefore, this data provides evidence that ADCY10 controls cell proliferation and cell cycle regulation via PP2A.

Taken together, ADCY10 coordinates the cell cycle progression in a complex framework. Downstream of ADCY10, Epac promotes G_1/S transition, whereas PKA mediates cell cycle transition of G_2/M. However, PP2A is the main signal molecule of ADCY10 in cell cycle progression (Figure 31).

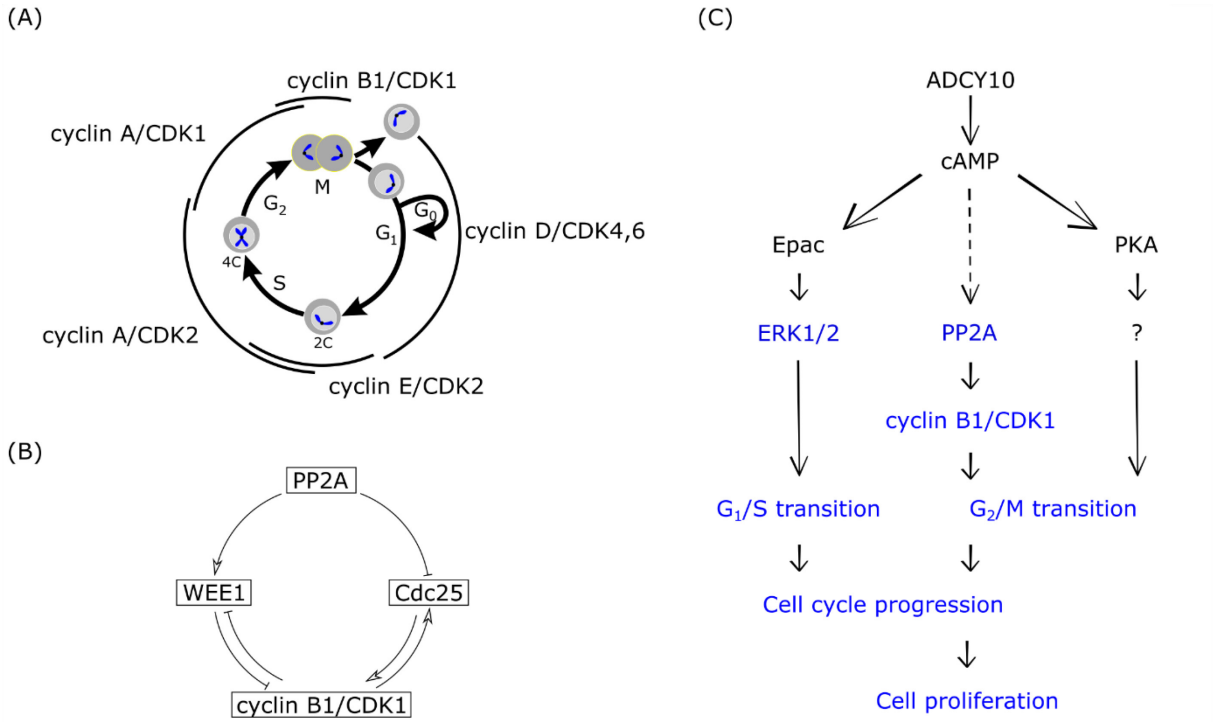

Figure 31. The roles of soluble adenylate cyclase in cell cycle control of endothelial cells. (A) Cell cycle stages of a somatic cell, which consist of two major phases: interphase (G1, S, G_2) and mitotic (M) phase as well as cyclins and CDKs present in each phase. **(B)** Cyclin B1/CDK1 auto-amplification loop, which contains PP2A, WEE1, Cdc25, and cyclin B1/CDK1 to regulate cell cycle transition from G_2 to M phase. **(C)** ADCY10 induces cell proliferation via Epac, PKA, and PP2A pathways. The blue texts represent the findings of the current study.

Zusammenfassung

Die lösliche Adenylatcyclase ADCY10 wird ubiquitär im Zytoplasma und in verschiedenen Zellorganellen einschließlich des Zellkerns exprimiert. Im Gegensatz zu den membranassoziierten Isoformen der Adenylatcyclase (ADCY1-9), die durch G-Protein-gekoppelte Rezeptoren stimuliert werden, wird ADCY10 durch Bicarbonat (HCO_3^-) aktiviert und bildet in fast allen Subkompartimenten der Zelle cAMP. ADCY10 ist an einer Vielzahl von physiologischen bzw. pathophysiologischen Prozessen beteiligt, wie auch an der Kontrolle des Zellzyklus in Tumorzellen. Allerdings ist der hier zugrundeliegende Mechanismus noch nicht vollständig aufgeklärt. In dieser Arbeit wird daher die Rolle von ADCY10 bei der Zellzykluskontrolle und der Zellproliferation am Modell der venösen Endothelzellen der humanen Nabelschnur (HUVECs) aufgeklärt.

In der vorliegenden Dissertation konnte gezeigt werden, dass ADCY10 und α-Tubulin sich während der Mitose räumlich umverteilen und sich dabei colokalisieren. Dies weist auf eine wesentliche Rolle von ADCY10 bei der Zellteilung hin. Darüber hinaus wurde mittels FACS-Analyse gezeigt, dass ADCY10 die Kontrolle des Zellzyklus verändert und damit an den Vorgängen der Zellproliferation beteiligt ist. Dies konnte anhand der folgenden Ergebnisse gezeigt werden. Eine Hemmung des Enzyms ADCY10 durch 0 mM HCO_3^- oder 10 µM KH7, einen spezifischen ADCY10 Inhibitor, führten zu einer Zellakkumulation in der G_2-Phase. Dabei bewirkte die Hemmung von ADCY10 eine verminderte Konzentration des Mitoseindikators Zyklin-B1, der dazu verwendet wurde die G_2-Phase von der M-Phase abzugrenzen. Damit konnte gezeigt werden, dass die Hemmung von ADCY10 zu einer verminderten Zellproliferation führt.

Weiter wurden die beiden Proteine Epac und PKA während der Zellproliferation untersucht, da die beiden im Signalweg der ADCY10 nachgeschaltet sind.

Es konnte gezeigt werden, dass ADCY10 und Epac die Zellproliferation über den ERK1/2-MAPK Signalweg stimulieren. Die Hemmung von Epac war mit einer verminderten Zellproliferation verbunden. Parallel wurde dabei ein Verharren der Zelle in den Phasen G_0/G_1, allerdings nicht in den Phasen S oder G_2/M, beobachtet. Dieses Ergebnis zeigt, dass die Hemmung von Epac die Zellen in einer anderen Phase des Zellzyklus verharren lässt als die Hemmung von ADCY10.

Für das Signalprotein PKA konnte gezeigt werden, dass ein Mangel an diesem sowohl eine Rolle bei der Aktivierung wie auch bei der Hemmung der Zellproliferation spielen könnte. Die direkte Hemmung von PKA durch die Inhibitoren PKI und H-89 führte jedoch wider Erwarten

nicht zu einer Zellakkumulation in der G_2-Phase. Dies könnte mit den unterschiedlichen Effekten von PKA auf verschiedene Stoffwechselwege erklärt werden. Im Gegensatz dazu zeigte die direkte Stimulation von PKA unter paralleler ADCY10-Hemmung, dass PKA ein nachgeschaltetes Signalmolekül von ADCY10 ist, welches den Zellzyklusübergang von der G_2-Phase zur mitotischen Phase reguliert. Der zugrundeliegende Signalweg muss jedoch noch genauer untersucht bzw. identifiziert werden.

Der Zellzyklusübergang der G_2/M-Phase wird durch eine selbstverstärkende Regulationsschleife von Cyclin B1/CDK1 geregelt, die wiederum von der Kinase WEE1 und der Phosphatase PP2A gesteuert wird. Der WEE1-Gehalt wurde über ADCY10 geregelt, war aber unabhängig von PKA oder Epac. Die direkte Hemmung von PP2A bewirkte eine verminderte Zellproliferation und eine direkte Anstauung der Zellen in der G_2-Phase. Dies war analog zu den Ergebnissen nach einer Inhibierung der ADCY10. Darüber hinaus hatte die Hemmung von ADCY10 keinen Einfluss auf die PP2A-Expression, allerdings auf die PP2A-Aktivität. Dabei war die PP2A-Aktivität unabhängig von Epac und PKA.

Schlussfolgernd liefern diese Daten den Nachweis, dass ADCY10 die Zellproliferation und die Regulation des Zellzyklus über PP2A steuert.

Zusammenfassend koordiniert ADCY10 den Verlauf des Zellzyklus in einem komplexen biologischen System. Dem Enzym ADCY10 nachgeschaltet fördert Epac den G_1/S-Übergang, während PKA den G_2/M-Übergang des Zellzyklus vermittelt. Dabei scheint PP2A das Hauptsignalmolekül der ADCY10 im Fortlauf des Zellzyklus zu sein (Abbildung 31).

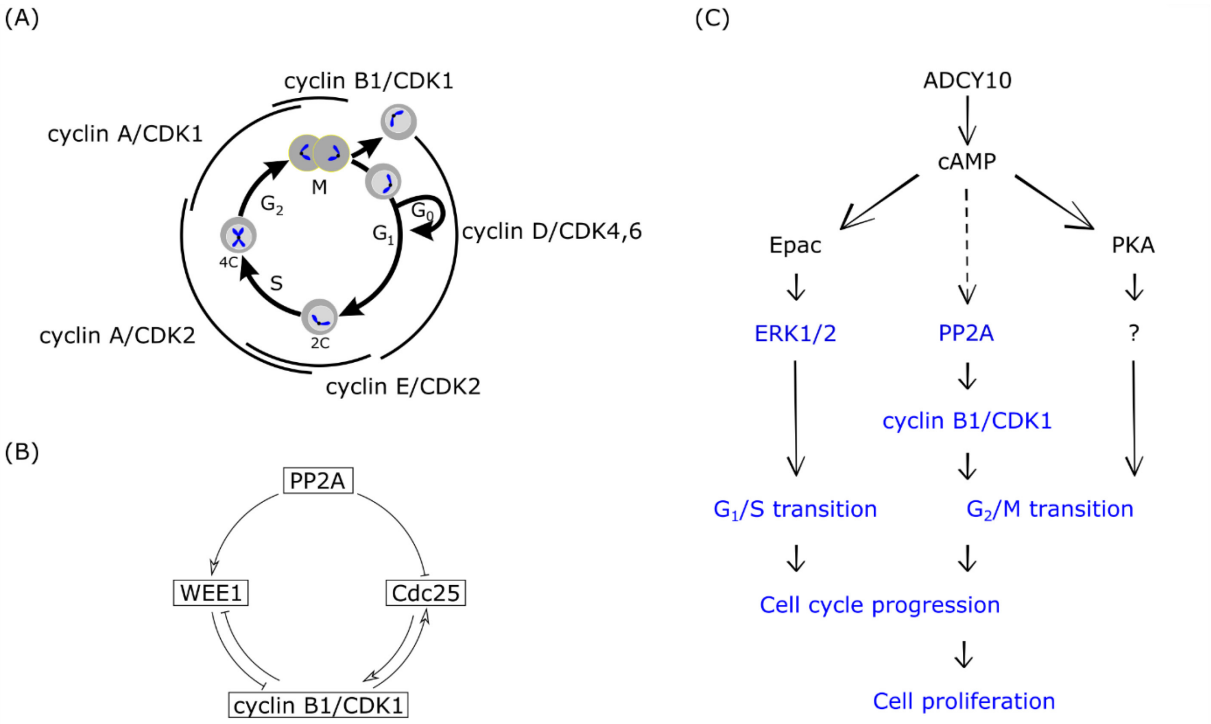

Abbildung 31. Die Signalwege der löslichen Adenylatcyclase während der Kontrolle des Zellzyklus von Endothelzellen. (A) Der Zellzyklus einer somatischen Zelle besteht aus zwei wesentlichen Phasen: Der Interphase (inklusive G_1-, S- und G_2-Phase) sowie der Mitose. Weiterhin zeigt die Grafik die entsprechenden Cycline und CDKs der einzelnen Phasen. **(B)** Die selbstverstärkende Regulationsschleife des Cyclin B1/CDK1 Komplexes beinhaltet PP2A, WEE1, Cdc25 und Cyclin B1/CDK1. Dieser Mechanismus spielt eine Rolle beim Übergang von der G_2- zur M-Phase. **(C)** ADCY10 bewirkt eine Steigerung der Zellproliferation über Epac, PKA und PP2A Signalwege. Die blaue Schriftfarbe kennzeichnet die Ergebnisse und Zusammenhänge, die im Rahmen der vorliegenden Arbeit gewonnen wurden.

References

Agarwal SR, Clancy CE, Harvey RD. 2016. Mechanisms Restricting Diffusion of Intracellular cAMP. Sci Rep, 6:19577 DOI: 10.1038/srep19577.

Ahn JH, McAvoy T, Rakhilin S V, Nishi A, Greengard P, Nairn AC. 2007. Protein kinase A activates protein phosphatase 2A by phosphorylation of the B56delta subunit. Proc Natl Acad Sci U S A, 104:2979–2984 DOI: 10.1073/pnas.0611532104.

Almahariq M, Mei FC, Cheng X. 2014. Cyclic AMP sensor EPAC proteins and energy homeostasis. Trends Endocrinol Metab, 25:60–71 DOI: 10.1016/j.tem.2013.10.004.

Appukuttan A, Flacke JP, Flacke H, Posadowsky A, Reusch HP, Ladilov Y. 2014. Inhibition of soluble adenylyl cyclase increases the radiosensitivity of prostate cancer cells. Biochim Biophys Acta, 1842:2656–2663 DOI: 10.1016/j.bbadis.2014.09.008.

Bar-Shavit R, Maoz M, Kancharla A, Nag JK, Agranovich D, Grisaru-Granovsky S, Uziely B. 2016. G Protein-Coupled Receptors in Cancer. Int J Mol Sci, 17 DOI: 10.3390/ijms17081320.

Bar HP, Hechter O. 1969. Adenyl cyclase and hormone action. I. Effects of adrenocorticotropic hormone, glucagon, and epinephrine on the plasma membrane of rat fat cells. Proc Natl Acad Sci U S A, 63:350–356 URL: http://www.ncbi.nlm.nih.gov/entrez/query.fcgi?cmd=Retrieve&db=PubMed&dopt=Citation&list_uids=4308273.

Belibi FA, Reif G, Wallace DP, Yamaguchi T, Olsen L, Li H, Helmkamp Jr. GM, Grantham JJ. 2004. Cyclic AMP promotes growth and secretion in human polycystic kidney epithelial cells. Kidney Int, 66:964–973 DOI: 10.1111/j.1523-1755.2004.00843.x.

Bergmann O, Zdunek S, Felker A, Salehpour M, Alkass K, Bernard S, Sjostrom SL, Szewczykowska M, Jackowska T, Dos Remedios C, Malm T, Andra M, Jashari R, Nyengaard JR, Possnert G, Jovinge S, Druid H, Frisen J. 2015. Dynamics of Cell Generation and Turnover in the Human Heart. Cell, 161:1566–1575 DOI: 10.1016/j.cell.2015.05.026.

Berridge MJ. 2014. Cell Cycle and Proliferation. Cell Signal Biol DOI: 10.1042/csb0001009.

Calebiro Davide, Nikolaev VO, Lohse MJ. 2010. Imaging of persistent cAMP signaling by internalized G protein-coupled receptors. J Mol Endocrinol, 45(1):1–8 DOI: 10.1677/JME-10-0014.

Calebiro D, Nikolaev VO, Persani L, Lohse MJ. 2010. Signaling by internalized G-protein-coupled receptors. Trends Pharmacol Sci, 31:221–228 DOI: 10.1016/j.tips.2010.02.002.

Cervone N, Monica RD, Serpico AF, Vetrei C, Scaraglio M, Visconti R, Grieco D. 2018. Evidence that PP2A activity is dispensable for spindle assembly checkpoint-dependent control of Cdk1. Oncotarget, 9:7312–7321 DOI: 10.18632/oncotarget.23329.

Chaloupka JA, Bullock SA, Iourgenko V, Levin LR, Buck J. 2006. Autoinhibitory regulation of soluble adenylyl cyclase. Mol Reprod Dev, 73:361–368 DOI: 10.1002/mrd.20409.

Chambard JC, Lefloch R, Pouyssegur J, Lenormand P. 2007. ERK implication in cell cycle regulation. Biochim Biophys Acta, 1773:1299–1310 DOI: 10.1016/j.bbamcr.2006.11.010.

Chen L, Marquardt ML, Tester DJ, Sampson KJ, Ackerman MJ, Kass RS. 2007. Mutation of an A-kinase-anchoring protein causes long-QT syndrome. Proc Natl Acad Sci U S A, 104:20990–20995 DOI: 10.1073/pnas.0710527105.

Chen TC, Hinton DR, Zidovetzki R, Hofman FM. 1998. Up-regulation of the cAMP/PKA pathway inhibits proliferation, induces differentiation, and leads to apoptosis in malignant gliomas. Lab Invest, 78:165–174 URL: https://www.ncbi.nlm.nih.gov/pubmed/9484714.

Chen Y, Cann MJ, Litvin TN, Iourgenko V, Sinclair ML, Levin LR, Buck J. 2000. Soluble adenylyl cyclase as an evolutionarily conserved bicarbonate sensor. Science (80-), 289:625–628 DOI: 10.1126/science.289.5479.625.

Cheng X, Ji Z, Tsalkova T, Mei F. 2008. Epac and PKA: a tale of two intracellular cAMP receptors. Acta Biochim Biophys Sin, 40:651–662 DOI: 10.1111/j.1745-

7270.2008.00438.x.
Clark AR, Ohlmeyer M. 2019. Protein phosphatase 2A as a therapeutic target in inflammation and neurodegeneration. Pharmacol Ther DOI: 10.1016/j.pharmthera.2019.05.016.
Conti M, Mika D, Richter W. 2014. Cyclic AMP compartments and signaling specificity: Role of cyclic nucleotide phosphodiesterases. J Gen Physiol, 143(1):29–38 DOI: 10.1085/jgp.201311083.
Cooper GM. 2000a. The Cell: A Molecular Approach. , 2nd [accessed: 08/22/2019] URL: https://www.ncbi.nlm.nih.gov/books/NBK9906/.
Cooper GM. 2000b. The Eukaryotic Cell Cycle. URL: https://www.ncbi.nlm.nih.gov/books/NBK9876/.
Das A. 2019. Role of soluble adenylyl cyclase on barrier function of human umbilical vein endothelial monolayers. TU Dresden, Dresden [Unpublished].
Defer N, Best-Belpomme M, Hanoune J. 2000. Tissue specificity and physiological relevance of various isoforms of adenylyl cyclase. Am J Physiol Ren Physiol, 279:F400-16 DOI: 10.1152/ajprenal.2000.279.3.F400.
Delghandi MP, Johannessen M, Moens U. 2005. The cAMP signalling pathway activates CREB through PKA, p38 and MSK1 in NIH 3T3 cells. Cell Signal, 17:1343–1351 DOI: 10.1016/j.cellsig.2005.02.003.
Dessauer CW, Scully TT, Gilman AG. 1997. Interactions of forskolin and ATP with the cytosolic domains of mammalian adenylyl cyclase. J Biol Chem, 272:22272–22277 DOI: 10.1074/jbc.272.35.22272.
DiPaola RS. 2002. To arrest or not to G(2)-M Cell-cycle arrest. Clin Cancer Res, 8:3311–3314 URL: https://www.ncbi.nlm.nih.gov/pubmed/12429616.
Dodge-Kafka KL, Bauman A, Mayer N, Henson E, Heredia L, Ahn J, McAvoy T, Nairn AC, Kapiloff MS. 2010. cAMP-stimulated protein phosphatase 2A activity associated with muscle A kinase-anchoring protein (mAKAP) signaling complexes inhibits the phosphorylation and activity of the cAMP-specific phosphodiesterase PDE4D3. J Biol Chem, 285:11078–11086 DOI: 10.1074/jbc.M109.034868.
Ehses JA, Casilla VR, Doty T, Pospisilik JA, Winter KD, Demuth HU, Pederson RA, McIntosh CH. 2003. Glucose-dependent insulinotropic polypeptide promotes beta-(INS-1) cell survival via cyclic adenosine monophosphate-mediated caspase-3 inhibition and regulation of p38 mitogen-activated protein kinase. Endocrinology, 144:4433–4445 DOI: 10.1210/en.2002-0068.
Della Fazia MA, Servillo G, Sassone-Corsi P. 1997. Cyclic AMP signalling and cellular proliferation: regulation of CREB and CREM. FEBS Lett, 410:22–24 DOI: 10.1016/s0014-5793(97)00445-6.
Feschenko MS, Stevenson E, Nairn AC, Sweadner KJ. 2002. A novel cAMP-stimulated pathway in protein phosphatase 2A activation. J Pharmacol Exp Ther, 302:111–118 DOI: 10.1124/jpet.302.1.111.
Finkel T, Hwang PM. 2009. The Krebs cycle meets the cell cycle: mitochondria and the G1-S transition. Proc Natl Acad Sci U S A, 106:11825–11826 DOI: 10.1073/pnas.0906430106.
Fischmeister R. 2006. Is cAMP good or bad? Depends on where it's made. Circ Res, 98:582–584 DOI: 10.1161/01.RES.0000215564.22445.7e.
Flacke JP, Flacke H, Appukuttan A, Palisaar RJ, Noldus J, Robinson BD, Reusch HP, Zippin JH, Ladilov Y. 2013. Type 10 soluble adenylyl cyclase is overexpressed in prostate carcinoma and controls proliferation of prostate cancer cells. J Biol Chem, 288:3126–3135 DOI: 10.1074/jbc.M112.403279.
Forester CM, Maddox J, Louis J V, Goris J, Virshup DM. 2007. Control of mitotic exit by PP2A regulation of Cdc25C and Cdk1. Proc Natl Acad Sci U S A, 104:19867–19872 DOI: 10.1073/pnas.0709879104.
Gold MG, Gonen T, Scott JD. 2013. Local cAMP signaling in disease at a glance. J Cell Sci, 126:4537–4543 DOI: 10.1242/jcs.133751.
Gong FR, Wu MY, Shen M, Zhi Q, Xu ZK, Wang R, Wang WJ, Zong Y, Li ZL, Wu Y, Zhou BP, Chen K, Tao M, Li W. 2015. PP2A inhibitors arrest G2/M transition through JNK/Sp1-

dependent down-regulation of CDK1 and autophagy-dependent up-regulation of p21. Oncotarget, 6:18469–18483 DOI: 10.18632/oncotarget.4063.
Gregory CY, Abrams TA, Hall MO. 1992. cAMP production via the adenylyl cyclase pathway is reduced in RCS rat RPE. Invest Ophthalmol Vis Sci, 33:3121–3124 URL: http://www.ncbi.nlm.nih.gov/entrez/query.fcgi?cmd=Retrieve&db=PubMed&dopt=Citation&list_uids=1328111.
Guyton A, Hall J. 2012. Textbook of medical physiology. Eleventh. Elsevier Inc.
Hanaoka K, Guggino WB. 2000. cAMP regulates cell proliferation and cyst formation in autosomal polycystic kidney disease cells. J Am Soc Nephrol, 11:1179–1187 URL: https://www.ncbi.nlm.nih.gov/pubmed/10864573.
Hanoune J, Defer N. 2001. Regulation and role of adenylyl cyclase isoforms. Annu Rev Pharmacol Toxicol, 41:145–174 DOI: 10.1146/annurev.pharmtox.41.1.145.
Hara M, Abe Y, Tanaka T, Yamamoto T, Okumura E, Kishimoto T. 2012. Greatwall kinase and cyclin B-Cdk1 are both critical constituents of M-phase-promoting factor. Nat Commun, 3:1059 DOI: 10.1038/ncomms2062.
Harry A, Chen Y, Magnusson R, Iyengar R, Weng G. 1997. Differential regulation of adenylyl cyclases by Galphas. J Biol Chem, 272:19017–19021 DOI: 10.1074/jbc.272.30.19017.
Heim A, Rymarczyk B, Mayer TU. 2017. Regulation of Cell Division. Adv Exp Med Biol, 953:83–116 DOI: 10.1007/978-3-319-46095-6_3.
Hess KC, Jones BH, Marquez B, Chen Y, Ord TS, Kamenetsky M, Miyamoto C, Zippin JH, Kopf GS, Suarez SS, Levin LR, Williams CJ, Buck J, Moss SB. 2005. The “soluble” adenylyl cyclase in sperm mediates multiple signaling events required for fertilization. Dev Cell, 9:249–259 DOI: 10.1016/j.devcel.2005.06.007.
Hewer RC, Sala-Newby GB, Wu YJ, Newby AC, Bond M. 2011. PKA and Epac synergistically inhibit smooth muscle cell proliferation. J Mol Cell Cardiol, 50:87–98 DOI: 10.1016/j.yjmcc.2010.10.010.
Horn V, Thelu J, Garcia A, Albiges-Rizo C, Block MR, Viallet J. 2007. Functional interaction of Aurora-A and PP2A during mitosis. Mol Biol Cell, 18:1233–1241 DOI: 10.1091/mbc.e06-12-1152.
Howe AK. 2004. Regulation of actin-based cell migration by cAMP/PKA. Biochim Biophys Acta, 1692:159–174 DOI: 10.1016/j.bbamcr.2004.03.005.
Ichiki T. 2006. Role of cAMP response element binding protein in cardiovascular remodeling: good, bad, or both? Arter Thromb Vasc Biol, 26:449–455 DOI: 10.1161/01.ATV.0000196747.79349.d1.
Jackman J, O’Connor PM. 2001. Methods for synchronizing cells at specific stages of the cell cycle. Curr Protoc Cell Biol, Chapter 8:Unit 8 3 DOI: 10.1002/0471143030.cb0803s00.
Jaffe EA, Nachman RL, Becker CG, Minick CR. 1973. Culture of human endothelial cells derived from umbilical veins. Identification by morphologic and immunologic criteria. J Clin Invest, 52:2745–2756 DOI: 10.1172/JCI107470.
Jang MW, Yun SP, Park JH, Ryu JM, Lee JH, Han HJ. 2012. Cooperation of Epac1/Rap1/Akt and PKA in prostaglandin E(2) -induced proliferation of human umbilical cord blood derived mesenchymal stem cells: involvement of c-Myc and VEGF expression. J Cell Physiol, 227:3756–3767 DOI: 10.1002/jcp.24084.
Jeong AL, Yang Y. 2013. PP2A function toward mitotic kinases and substrates during the cell cycle. BMB Rep, 46:289–294 DOI: 10.5483/BMBRep.2013.46.6.041.
Jiang Y. 2006. Regulation of the cell cycle by protein phosphatase 2A in Saccharomyces cerevisiae. Microbiol Mol Biol Rev, 70:440–449 DOI: 10.1128/MMBR.00049-05.
Kalucka J, Missiaen R, Georgiadou M, Schoors S, Lange C, De Bock K, Dewerchin M, Carmeliet P. 2015. Metabolic control of the cell cycle. Cell Cycle, 14:3379–3388 DOI: 10.1080/15384101.2015.1090068.
Kamenetsky M, Middelhaufe S, Bank EM, Levin LR, Buck J, Steegborn C. 2006. Molecular details of cAMP generation in mammalian cells: a tale of two systems. J Mol Biol, 362:623–639 DOI: 10.1016/j.jmb.2006.07.045.
Kaplon J, van Dam L, Peeper D. 2015. Two-way communication between the metabolic and

cell cycle machineries: the molecular basis. Cell Cycle, 14:2022–2032 DOI: 10.1080/15384101.2015.1044172.
Kim KH, Sederstrom JM. 2015. Assaying Cell Cycle Status Using Flow Cytometry. Curr Protoc Mol Biol, 111:28 6 1–11 DOI: 10.1002/0471142727.mb2806s111.
Kleinboelting S, Diaz A, Moniot S, van den Heuvel J, Weyand M, Levin LR, Buck J, Steegborn C. 2014. Crystal structures of human soluble adenylyl cyclase reveal mechanisms of catalysis and of its activation through bicarbonate. Proc Natl Acad Sci U S A, 111:3727–3732 DOI: 10.1073/pnas.1322778111.
Knapp J, Bokník P, Lüss I, Huke S, Linck B, Lüss H, Müller FU, Müller T, Nacke P, Noll T, Piper HM, Schmitz W, Vahlensieck U, Neumann J. 1999. The protein phosphatase inhibitor cantharidin alters vascular endothelial cell permeability. J Pharmacol Exp Ther, 289(3):1480–1486.
Ladilov Y, Appukuttan A. 2014. Role of soluble adenylyl cyclase in cell death and growth. Biochim Biophys Acta, 1842:2646–2655 DOI: 10.1016/j.bbadis.2014.06.034.
Lechward K, Awotunde OS, Swiatek W, Muszynska G. 2001. Protein phosphatase 2A: variety of forms and diversity of functions. Acta Biochim Pol, 48:921–933 URL: http://www.ncbi.nlm.nih.gov/entrez/query.fcgi?cmd=Retrieve&db=PubMed&dopt=Citation&list_uids=11996003.
Leslie SN, Nairn AC. 2019. cAMP regulation of protein phosphatases PP1 and PP2A in brain. Biochim Biophys Acta Mol Cell Res, 1866:64–73 DOI: 10.1016/j.bbamcr.2018.09.006.
Lin FC, Arndt KT. 1995. The role of Saccharomyces cerevisiae type 2A phosphatase in the actin cytoskeleton and in entry into mitosis. EMBO J, 14:2745–2759 URL: http://www.ncbi.nlm.nih.gov/entrez/query.fcgi?cmd=Retrieve&db=PubMed&dopt=Citation&list_uids=7796803.
Litvin TN, Kamenetsky M, Zarifyan A, Buck J, Levin LR. 2003. Kinetic properties of “soluble” adenylyl cyclase. Synergism between calcium and bicarbonate. J Biol Chem, 278:15922–15926 DOI: 10.1074/jbc.M212475200.
Liu Y, An S, Ward R, Yang Y, Guo XX, Li W, Xu TR. 2016. G protein-coupled receptors as promising cancer targets. Cancer Lett, 376:226–239 DOI: 10.1016/j.canlet.2016.03.031.
Lodish H. 2012. Molecular Cell Biology. Regulating the Eukaryotic Cell Cycle. Fifth Edit. DOI: 10.1016/S1470-8175(01)00023-6.
Loffler I, Grun M, Bohmer FD, Rubio I. 2008. Role of cAMP in the promotion of colorectal cancer cell growth by prostaglandin E2. BMC Cancer, 8:380 DOI: 10.1186/1471-2407-8-380.
Ludwig MG, Seuwen K. 2002. Characterization of the human adenylyl cyclase gene family: cDNA, gene structure, and tissue distribution of the nine isoforms. J Recept Signal Transduct Res, 22:79–110 DOI: 10.1081/RRS-120014589.
Lv P, Wang W, Cao Z, Zhao D, Zhao G, Li D, Qi L, Xu J. 2018. Fsk and IBMX inhibit proliferation and proapoptotic of glioma stem cells via activation of cAMP signaling pathway. J Cell Biochem DOI: 10.1002/jcb.27364.
MacCorkle RA, Tan T-H. 2005. Mitogen-Activated Protein Kinases in Cell-Cycle Control. Cell Biochem Biophys, 43(3):451–462 DOI: 10.1385/CBB:43:3:451.
Madamanchi A. 2007. Beta-adrenergic receptor signaling in cardiac function and heart failure. Mcgill J Med, 10:99–104 URL: http://www.ncbi.nlm.nih.gov/entrez/query.fcgi?cmd=Retrieve&db=PubMed&dopt=Citation&list_uids=18523538.
Manic G, Corradi F, Sistigu A, Siteni S, Vitale I. 2017. Molecular Regulation of the Spindle Assembly Checkpoint by Kinases and Phosphatases. Int Rev Cell Mol Biol, 328:105–161 DOI: 10.1016/bs.ircmb.2016.08.004.
Manolopoulos VG, Liu J, Unsworth BR, Lelkes PI. 1995. Adenylyl cyclase isoforms are differentially expressed in primary cultures of endothelial cells and whole tissue homogenates from various rat tissues. Biochem Biophys Res Commun, 208:323–331 DOI: 10.1006/bbrc.1995.1341.
Mebratu Y, Tesfaigzi Y. 2009. How ERK1/2 activation controls cell proliferation and cell death:

Is subcellular localization the answer? Cell Cycle, 8:1168–1175 DOI: 10.4161/cc.8.8.8147.
Murray AJ. 2008. Pharmacological PKA inhibition: all may not be what it seems. Sci Signal, 1:re4 DOI: 10.1126/scisignal.122re4.
O'Connor CM, Perl A, Leonard D, Sangodkar J, Narla G. 2018. Therapeutic targeting of PP2A. Int J Biochem Cell Biol, 96:182–193 DOI: 10.1016/j.biocel.2017.10.008.
Obiako B, Calchary W, Xu N, Kunstadt R, Richardson B, Nix J, Sayner SL. 2013. Bicarbonate disruption of the pulmonary endothelial barrier via activation of endogenous soluble adenylyl cyclase, isoform 10. Am J Physiol Lung Cell Mol Physiol, 305:L185-92 DOI: 10.1152/ajplung.00392.2012.
Pastor-Soler N, Beaulieu V, Litvin TN, Da Silva N, Chen Y, Brown D, Buck J, Levin LR, Breton S. 2003. Bicarbonate-regulated adenylyl cyclase (sAC) is a sensor that regulates pH-dependent V-ATPase recycling. J Biol Chem, 278:49523–49529 DOI: 10.1074/jbc.M309543200.
Perry JA, Kornbluth S. 2007. Cdc25 and Wee1: analogous opposites? Cell Div, 2:12 DOI: 10.1186/1747-1028-2-12.
Pozdniakova S, Ladilov Y. 2018. Functional Significance of the Adcy10-Dependent Intracellular cAMP Compartments. J Cardiovasc Dev Dis, 5 DOI: 10.3390/jcdd5020029.
Qiao J, Mei FC, Popov VL, Vergara LA, Cheng X. 2002. Cell cycle-dependent subcellular localization of exchange factor directly activated by cAMP. J Biol Chem, 277:26581–26586 DOI: 10.1074/jbc.M203571200.
Rahman N, Ramos-Espiritu L, Milner TA, Buck J, Levin LR. 2016. Soluble adenylyl cyclase is essential for proper lysosomal acidification. J Gen Physiol, 148:325–339 DOI: 10.1085/jgp.201611606.
Raju DN, Hansen JN, Rassmann S, Stuven B, Jikeli JF, Strunker T, Korschen HG, Moglich A, Wachten D. 2019. Cyclic Nucleotide-Specific Optogenetics Highlights Compartmentalization of the Sperm Flagellum into cAMP Microdomains. Cells, 8 DOI: 10.3390/cells8070648.
Remmerie M, Janssens V. 2019. PP2A: A Promising Biomarker and Therapeutic Target in Endometrial Cancer. Front Oncol, 9:462 DOI: 10.3389/fonc.2019.00462.
Richardson RB, Allan DS, Le Y. 2014. Greater organ involution in highly proliferative tissues associated with the early onset and acceleration of ageing in humans. Exp Gerontol, 55:80–91 DOI: 10.1016/j.exger.2014.03.015.
Roa JN, Tresguerres M. 2017. Bicarbonate-sensing soluble adenylyl cyclase is present in the cell cytoplasm and nucleus of multiple shark tissues. Physiol Rep, 5 DOI: 10.14814/phy2.13090.
Rodriguez G, Ross JA, Nagy ZS, Kirken RA. 2013. Forskolin-inducible cAMP pathway negatively regulates T-cell proliferation by uncoupling the interleukin-2 receptor complex. J Biol Chem, 288:7137–7146 DOI: 10.1074/jbc.M112.408765.
Rowley R, Hudson J, Young PG. 1992. The wee1 protein kinase is required for radiation-induced mitotic delay. Nature, 356:353–355 DOI: 10.1038/356353a0.
Sadana R, Dessauer CW. 2009. Physiological roles for G protein-regulated adenylyl cyclase isoforms: insights from knockout and overexpression studies. Neurosignals, 17:5–22 DOI: 10.1159/000166277.
Sassone-Corsi P. 2012. The cyclic AMP pathway. Cold Spring Harb Perspect Biol, 4 DOI: 10.1101/cshperspect.a011148.
Sayner SL. 2011. Emerging themes of cAMP regulation of the pulmonary endothelial barrier. Am J Physiol Lung Cell Mol Physiol, 300:L667-78 DOI: 10.1152/ajplung.00433.2010.
Sayner SL, Alexeyev M, Dessauer CW, Stevens T. 2006. Soluble adenylyl cyclase reveals the significance of cAMP compartmentation on pulmonary microvascular endothelial cell barrier. Circ Res, 98:675–681 DOI: 10.1161/01.RES.0000209516.84815.3e.
Schafer KA. 1998. The cell cycle: a review. Vet Pathol, 35:461–478 DOI: 10.1177/030098589803500601.
Schmidt Robert F., Thews G. 1987. Human Physiology. 2nd ed. Schmidt R.F., Thews G (eds)

Springer-Verlag, Berlin.
Schmitt JM, Stork PJ. 2001. Cyclic AMP-mediated inhibition of cell growth requires the small G protein Rap1. Mol Cell Biol, 21:3671–3683 DOI: 10.1128/MCB.21.11.3671-3683.2001.
Sinha SC, Sprang SR. 2006. Structures, mechanism, regulation and evolution of class III nucleotidyl cyclases. Rev Physiol Biochem Pharmacol DOI: 10.1007/112_0603.
Sontag E, Nunbhakdi-Craig V, Bloom GS, Mumby MC. 1995. A novel pool of protein phosphatase 2A is associated with microtubules and is regulated during the cell cycle. J Cell Biol, 128:1131–1144 DOI: 10.1083/jcb.128.6.1131.
Steer ML. 1975. Adenyl cyclase. Ann Surg, 182:603–609 URL: https://www.ncbi.nlm.nih.gov/pubmed/172034.
Strasser-Wozak EM, Hartmann BL, Geley S, Sgonc R, Bock G, Santos AJ, Hattmannstorfer R, Wolf H, Pavelka M, Kofler R. 1998. Irradiation induces G2/M cell cycle arrest and apoptosis in p53-deficient lymphoblastic leukemia cells without affecting Bcl-2 and Bax expression. Cell Death Differ, 5:687–693 DOI: 10.1038/sj.cdd.4400402.
Sun H, Jiang YJ, Yu QS, Luo CC, Zou JW. 2008. Effect of mutation K85R on GSK-3beta: Molecular dynamics simulation. Biochem Biophys Res Commun, 377:962–965 DOI: 10.1016/j.bbrc.2008.10.096.
Sun Y, Liu WZ, Liu T, Feng X, Yang N, Zhou HF. 2015. Signaling pathway of MAPK/ERK in cell proliferation, differentiation, migration, senescence and apoptosis. J Recept Signal Transduct Res, 35:600–604 DOI: 10.3109/10799893.2015.1030412.
Sunahara AJKRK. 2010. Adenylyl Cyclases. 2nd ed. Bradshaw RA, Dennis EA (eds) Elsevier Inc., Amsterdam DOI: 10.1016/B978-0-12-374145-5.00171-6.
Sutherland EW, Rall TW. 1958. Fractionation and characterization of a cyclic adenine ribonucleotide formed by tissue particles. J Biol Chem, 232:1077–1091 URL: https://www.ncbi.nlm.nih.gov/pubmed/13549488.
Torres VE, Harris PC. 2014. Strategies targeting cAMP signaling in the treatment of polycystic kidney disease. J Am Soc Nephrol, 25:18–32 DOI: 10.1681/ASN.2013040398.
Tresguerres M, Barott KL, Barron ME, Roa JN. 2014. Established and potential physiological roles of bicarbonate-sensing soluble adenylyl cyclase (sAC) in aquatic animals. J Exp Biol, 217:663–672 DOI: 10.1242/jeb.086157.
Tresguerres M, Levin LR, Buck J. 2011. Intracellular cAMP signaling by soluble adenylyl cyclase. Kidney Int, 79:1277–1288 DOI: 10.1038/ki.2011.95.
Tresguerres M, Parks SK, Salazar E, Levin LR, Goss GG, Buck J. 2010. Bicarbonate-sensing soluble adenylyl cyclase is an essential sensor for acid/base homeostasis. Proc Natl Acad Sci U S A, 107:442–447 DOI: 10.1073/pnas.0911790107.
Valsecchi F, Ramos-Espiritu LS, Buck J, Levin LR, Manfredi G. 2013. cAMP and mitochondria. Physiol, 28:199–209 DOI: 10.1152/physiol.00004.2013.
Vandame P, Spriet C, Trinel D, Gelaude A, Caillau K, Bompard C, Biondi E, Bodart JF. 2014. The spatio-temporal dynamics of PKA activity profile during mitosis and its correlation to chromosome segregation. Cell Cycle, 13:3232–3240 DOI: 10.4161/15384101.2014.950907.
Wallace DP. 2011. Cyclic AMP-mediated cyst expansion. Biochim Biophys Acta, 1812:1291–1300 DOI: 10.1016/j.bbadis.2010.11.005.
Warfel JM, D'Agnillo F. 2009. Anthrax lethal toxin enhances IkappaB kinase activation and differentially regulates pro-inflammatory genes in human endothelium. J Biol Chem, 284:25761–25771 DOI: 10.1074/jbc.M109.036970.
Wiggins S V, Steegborn C, Levin LR, Buck J. 2018. Pharmacological modulation of the CO2/HCO3(-)/pH-, calcium-, and ATP-sensing soluble adenylyl cyclase. Pharmacol Ther, 190:173–186 DOI: 10.1016/j.pharmthera.2018.05.008.
Wlodarchak N, Xing Y. 2016. PP2A as a master regulator of the cell cycle. Crit Rev Biochem Mol Biol, 51:162–184 DOI: 10.3109/10409238.2016.1143913.
Yamaguchi T, Pelling JC, Ramaswamy NT, Eppler JW, Wallace DP, Nagao S, Rome LA, Sullivan LP, Grantham JJ. 2000. cAMP stimulates the in vitro proliferation of renal cyst epithelial cells by activating the extracellular signal-regulated kinase pathway11See

Editorial by Grande, p. 1770. Kidney Int, 57(4):1460–1471 DOI: 10.1046/j.1523-1755.2000.00991.x.
Yang LM, Rinke R, Korbmacher C. 2006. Stimulation of the epithelial sodium channel (ENaC) by cAMP involves putative ERK phosphorylation sites in the C termini of the channel's beta- and gamma-subunit. J Biol Chem, 281:9859–9868 DOI: 10.1074/jbc.M512046200.
Zhang W, Liu HT. 2002. MAPK signal pathways in the regulation of cell proliferation in mammalian cells. Cell Res, 12:9–18 DOI: 10.1038/sj.cr.7290105.
Zippin JH, Chen Y, Nahirney P, Kamenetsky M, Wuttke MS, Fischman DA, Levin LR, Buck J. 2003. Compartmentalization of bicarbonate-sensitive adenylyl cyclase in distinct signaling microdomains. FASEB J, 17(1):82–84.
Zippin JH, Farrell J, Huron D, Kamenetsky M, Hess KC, Fischman DA, Levin LR, Buck J. 2004. Bicarbonate-responsive "soluble" adenylyl cyclase defines a nuclear cAMP microdomain. J Cell Biol, 164(4):527–534 DOI: 10.1083/jcb.200311119.

Supplementary data for materials

No.	Materials	Manufacturer	Catalog number
1	Phosphate-buffered saline (PBS)		
	a. KCl, 2.7 mM	VWR International, Monroeville, Pennsylvania, USA	26764.298
	b. KH_2PO_4, 1.5 mM	Sigma-Aldrich Merck, St. Louis, Missouri, USA	1.04873
	c. Na_2HPO_4, 8 mM	Sigma-Aldrich Merck, St. Louis, Missouri, USA	S7907
	d. NaCl, 137 mM	VWR International, Monroeville, Pennsylvania, USA	27810.295
2	Trypsin-ethylenediaminetetraacetic acid (EDTA), 0.05%	Thermo Fisher Scientific, Waltham, Massachusetts, USA	25300-054
3	Medium M199	Sigma-Aldrich Merck, St. Louis, Missouri, USA	M2520-10X1L
4	Endothelial cell supplement	PromoCell GmbH, Heidelberg, Germany	C-39210
	Fetal bovine serum	Sigma-Aldrich Merck, St. Louis, Missouri, USA	F 7524
	L-glutamine	Sigma-Aldrich Merck, St. Louis, Missouri, USA	G 7513
	Sodium Pyruvate	Thermo Fisher Scientific, Waltham, Massachusetts, USA	11360-039
	Pennisilin/streptomysin	Thermo Fisher Scientific, Waltham, Massachusetts, USA	15140-122
5	Culture-Insert 2 Well in µ-Dish 35 mm	Ibidi GmbH, Martinsried, Germany	81176
	8 well slide for fluorescence	Corning™ Falcon™, Steuben County, New York, USA	354108
6	Sample buffer		
	a. Tris, 62.5 mM, pH 6.8	Carl Roth Gmbh & Co. Kg, Karlsruhe, Germany	5429.3
	b. Sodium dodecyl sulfate (SDS), 2%	Carl Roth Gmbh & Co. Kg, Karlsruhe, Germany	CN30.3
	c. Glycerol, 10%	Carl Roth Gmbh & Co. Kg, Karlsruhe, Germany	3783.1
	d. Bromophenol blue, 0.0025%	Carl Roth Gmbh & Co. Kg, Karlsruhe, Germany	A512.1
	e. HCl, 37%	VWR International, Monroeville, Pennsylvania, USA	20252.244
7	Benzonase solution		
	a. Benzonase	Sigma-Aldrich Merck, St. Louis, Missouri, USA	1.01654.0001
	b. $MgCl_2$	Sigma-Aldrich Merck, St. Louis, Missouri, USA	M-8266
8	Dithiothreitol (DTT)	GE Healthcare, Chicago, Illinois, USA	17-1318-02

9	RIPA buffer	Sigma-Aldrich Merck, St. Louis, Missouri, USA	R0278
10	Pierce BCA Protein Assay Kit	Thermo Fisher Scientific, Waltham, Massachusetts, USA	23225
11	SDS-polyacrylamide gel		
	1. Tris	Carl Roth Gmbh & Co. Kg, Karlsruhe, Germany	5429.3
	2. 30% Acrylamide	Serva Electrophoresis GmbH, Heidelberg, Germany	10688.03
	3. SDS, 10%	Carl Roth Gmbh & Co. Kg, Karlsruhe, Germany	CN30.3
	4. Tetramethylethylenediamine (TEMED)	Carl Roth Gmbh & Co. Kg, Karlsruhe, Germany	2367.3
	5. Ammonium persulfate (APS), 10%	Sigma-Aldrich Merck, St. Louis, Missouri, USA	1.01201.0500
12	Triton X-100	Serva Electrophoresis GmbH, Heidelberg, Germany	374240.01
13	4',6-diamidino-2-phenylindole (DAPI)	Sigma-Aldrich Merck, St. Louis, Missouri, USA	D9542
14	Ethylenediaminetetraacetic acid (EDTA)	Sigma-Aldrich Merck, St. Louis, Missouri, USA	324503-100GM
15	PVDF membrane	Merck Millipore, Danvers, Massachusetts, USA	IPVH00010
16	Multiblot 2020-E semi dry blotter	BIOTEC-FISCHER, Berlin, Germany	BIOFI_4041
17	Tris-bufered saline-Tween (TBS-T)		
	a. Tris, 10 mM, pH 7.4	Carl Roth Gmbh & Co. Kg, Karlsruhe, Germany	5429.3
	b. NaCl, 150 mM	VWR International, Monroeville, Pennsylvania, USA	27810.295
	c. Tween, 0.1%	Serva Electrophoresis GmbH, Heidelberg, Germany	37470.01
18	Primary antibodies		
	a. Anti-MEK1/2~p	Sigma-Aldrich Merck, St. Louis, Missouri, USA	M-7683
	b. Anti-ERK1/2~p	Cell Signaling Technology, Inc., Massachusetts, USA	4370
	c. Anti-GAPDH	Abcam, Cambridge, United Kingdom	P04406
	d. Anti-CREB~p	Merck Millipore, Danvers, Massachusetts, USA	06-519
	e. Anti-GSK-3β~p	Cell Signaling Technology, Inc., Danvers, Massachusetts, USA	9336
	f. Anti-cyclin B1	Cell Signaling Technology, Inc., Danvers, Massachusetts, USA	4138
	g. Anti-PP2A	Sigma-Aldrich Merck, St. Louis, Missouri, USA	05-421
	h. Anti-vinculin	Sigma-Aldrich Merck, St. Louis, Missouri, USA	V-9131
	i. Anti-WEE1	Santa Cruz Biotechnology, Inc., Dallas, Texas, USA	sc-5285
	j. Anti-α-Tubulin	Sigma-Aldrich Merck, St. Louis, Missouri, USA	CP06
	k. Anti-DAPI	Sigma-Aldrich Merck, St. Louis, Missouri, USA	Sigma D9542
19	Secondary antibodies		

	a. Anti-Mouse	VWR International, Monroeville, Pennsylvania, USA	NA931
	b. Anti-Rabbit	VWR International, Monroeville, Pennsylvania, USA	NA 934
	c. Anti-Mouse, TRITC-conjugate	Sigma-Aldrich Merck, St. Louis, Missouri, USA	T-5393
	d. Anti-Rabbit, FITC-conjugate	Sigma-Aldrich Merck, St. Louis, Missouri, USA	F-0382
20	ECL Western blotting substrate	Thermo Fisher Scientific, Waltham, Massachusetts, USA	32106
21	MACSQuant Analyzer 10	Miltenyi Biotec GmbH, Bergisch Gladbach, Germany	
22	FlowJo™ Software	FlowJo LLC, Ashland, Oregon, USA	
23	Axio Observer.Z1 microscope	Carl Zeiss Jena GmbH; Jena, Germany	
24	Microplate reader	Clariostar, BMG Labtech, Ortenberg, Germany	
25	Fusion® FX7	Peqlab Biotechnologie GbmH, Erlangen, Germany	
26	Bioprofil Bio1D (version 15.06a)	Vilber Lourmat Sté, Collégien, France	
27	RediPlate™ 96 EnzChek® Serine/Threonine Phosphatase Assay Kit	Thermo Fisher Scientific, Waltham, Massachusetts, USA	R33700
28	GraphPad Prism	GraphPad Software, Inc., San Diego, CA, USA	
29	Chemical Inhibitors		
	a. KH7	CAYMAN chemical, Ann Arbor, Michigan	330676-02-3
	b. ESI-09	Sigma-Aldrich Merck, St. Louis, Missouri, USA	SML0814
	c. H-89	Enzo Biochem, Inc., Farmingdale, New York, USA	BML-EI196-0005
	d. PKI	Enzo Biochem, Inc., Farmingdale, New York, USA	BML-P204-0001
	e. Okadaic Acid (OA)	Merck Millipore, Danvers, Massachusetts, USA	459620
30	cAMP agonist		
	a. Epac agonist cAMP (8-pcpt-2'-o-me-cAMP)	Biolog Life Science Institute GmbH & Co. KG, Bremen, Germany	C 041-05
	b. PKA agonist cAMP (6-Bnz)	Biolog Life Science Institute GmbH & Co. KG, Bremen, Germany	B 009-10

Acknowledgements

I would like to express my deep gratitude appreciation to my advisor, Prof. Thomas Noll, who gave guidance, support and patience throughout my study. Because of his kindness and understanding, I was free to express my ideas during this thesis. Above all, without his empathy, this work would have never been accomplished.

My sincere appreciation is also expressed to Dr. Mats Moskopp, one of the major contributors to my work. Thank you for taking the time to go through all the obstacles during the writing process. This includes your valuable time, thoughts, and suggestions that you invested in my thesis as well as your advice on how to structure and organize matters in my thesis. Furthermore, thank you for being my best friend. I value your patience, loyalty, and honesty. Because of you, being far from home is not that miserable.

Many thanks to Anupam Das, who supported me and introduced me to the cell culture lab. His guidance, support, and kindness towards me helped my laboratory work.

I especially want to mention Dr. Melanie Martin, Dr. Peter Dieterich, Dr. Frauke Härtel, Dr. Caroline Jahn-Carta, Dr. Treewut Rassamegevanon, and Dr. Sara Sofia Deville for their kindness and valuable time that they invested in correcting my thesis.

I would like to thank my colleague Dr. Karolina Ihle for her kindness and the effective research discussions.

Many thanks to Antje Messer and Sandra Tuchscheerer-Hoffmeister for their kind cooperation in the laboratory that greatly speeded up the progress of my work.

Finally, I would like to thank my family, especially my mom and my twin sister, for their support and for always standing by my side during all situations.

Anlage 1

Technische Universität Dresden
Medizinische Fakultät Carl Gustav Carus
Promotionsordnung vom 24. Juli 2011

Erklärungen zur Eröffnung des Promotionsverfahrens

1. Hiermit versichere ich, dass ich die vorliegende Arbeit ohne unzulässige Hilfe Dritter und ohne Benutzung anderer als der angegebenen Hilfsmittel angefertigt habe; die aus fremden Quellen direkt oder indirekt übernommenen Gedanken sind als solche kenntlich gemacht.

2. Bei der Auswahl und Auswertung des Materials sowie bei der Herstellung des Manuskripts habe ich Unterstützungsleistungen von folgenden Personen erhalten:

Wissenschaftliche Anleitung: Prof. Dr. Thomas Noll

Lektorat: Dr. Mats Leif Moskopp, Dr. Caroline Jahn-Carta, Dr. Melanie Martin, Dr. Peter Dieterich, Dr. Frauke Härtel, Anupam Das.

3. Weitere Personen waren an der geistigen Herstellung der vorliegenden Arbeit nicht beteiligt. Insbesondere habe ich nicht die Hilfe eines kommerziellen Promotionsberaters in Anspruch genommen. Dritte haben von mir weder unmittelbar noch mittelbar geldwerte Leistungen für Arbeiten erhalten, die im Zusammenhang mit dem Inhalt der vorgelegten Dissertation stehen.

4. Die Arbeit wurde bisher weder im Inland noch im Ausland in gleicher oder ähnlicher Form einer anderen Prüfungsbehörde vorgelegt.

5. Die Inhalte dieser Dissertation wurden in folgender Form veröffentlicht:

Nicht zutreffend.

6. Ich bestätige, dass es keine zurückliegenden erfolglosen Promotionsverfahren gab.

Nicht zutreffend.

7. Ich bestätige, dass ich die Promotionsordnung der Medizinischen Fakultät der Technischen Universität Dresden anerkenne.

8. Ich habe die Zitierrichtlinien für Dissertationen an der Medizinischen Fakultät der Technischen Universität Dresden zur Kenntnis genommen und befolgt.

Ort, Datum

Unterschrift des Doktoranden

(Diese Erklärungen sind an das Ende der Arbeit einzubinden) Formblatt 1.2.1, Seite 1-1, erstellt 18.10.2013

Anlage 2

Hiermit bestätige ich die Einhaltung der folgenden aktuellen gesetzlichen Vorgaben im Rahmen meiner Dissertation

☐ das zustimmende Votum der Ethikkommission bei Klinischen Studien, epidemiologischen Untersuchungen mit Personenbezug oder Sachverhalten, die das Medizinproduktegesetz betreffen
Aktenzeichen der zuständigen Ethikkommission

……Nicht zutreffend.…… ……

☐ die Einhaltung der Bestimmungen des Tierschutzgesetzes
Aktenzeichen der Genehmigungsbehörde zum Vorhaben/zur Mitwirkung

……Nicht zutreffend.……..

☐ die Einhaltung des Gentechnikgesetzes

Projektnummer ……Nicht zutreffend.……

☒ die Einhaltung von Datenschutzbestimmungen der Medizinischen Fakultät und des Universitätsklinikums Carl Gustav Carus.

Dresden, den

Unterschrift des Doktoranden